uOttawa

L'Université canadienne
Canada's university

FACULTÉ DES ÉTUDES SUPÉRIEURES ET POSTOCTORALES

uOttawa

L'Université canadienne
Canada's university

FACULTY OF GRADUATE AND POSDOCTORAL STUDIES

Emilie Boudreau
AUTEUR DE LA THÈSE / AUTHOR OF THESIS

M.Sc. (Biochemistry)
GRADE / DEGREE

Department of Biochemistry, Microbiology and Immunology
FACULTÉ, ÉCOLE, DÉPARTEMENT / FACULTY, SCHOOL, DEPARTMENT

Lamin A/C and Sumoylation: Implication of Laminopathic Mutant Lamin A/C Expression on the Dybamics of Sumo 1

TITRE DE LA THÈSE / TITLE OF THESIS

Frédérique Tesson
DIRECTEUR (DIRECTRICE) DE LA THÈSE / THESIS SUPERVISOR

CO-DIRECTEUR (CO-DIRECTRICE) DE LA THÈSE / THESIS CO-SUPERVISOR

Alexandre Stewart

Erik Suuronen

Gary W. Slater
Le Doyen de la Faculté des études supérieures et postdoctorales / Dean of the Faculty of Graduate and Postdoctoral Studies

Lamin A/C and sumoylation: Implications of laminopathic mutant lamin A/C expression on the dynamics of sumo1

Emilie Boudreau

A thesis submitted to the Faculty of Graduate and Postdoctoral studies in partial fulfillment of the requirements for the degree of Masters of Science in Biochemistry specializing in Human and Molecular Genetics

Department of Biochemistry, Microbiology, and Immunology
University of Ottawa
Ottawa, ON, Canada

Your file Votre référence
ISBN: 978-0-494-73797-2
Our file Notre référence
ISBN: 978-0-494-73797-2

Abstract

Laminopathies are a collection of over ten distinct and overlapping disease phenotypes resulting from over 340 known mutations in the LMNA gene. This gene encodes the alternatively spliced nuclear intermediate filament proteins, lamins A and C, that localize to the nuclear envelope and the nucleoplasm. These proteins are part of the nuclear lamina which is a complex meshwork of over 80 proteins underlying the inner nuclear membrane. Lamins have proposed roles in nuclear structural support and in multiple cell processes that include gene regulation, chromatin organization, and protein localization/scaffolding. Previous research has shown that *in vitro* expression of a laminopathic mutant lamin C resulted in nuclear aggregation of lamin C and subsequently sequestration of a co-expressed post-translational modification protein, sumo1. Sumoylation is the attachment of the small ubiquitin-like modifier 1 (sumo1) to a target lysine(s) on substrate proteins which serves to regulate various protein characteristics such as transcriptional activity, localization, protein interaction, and stability.

In this thesis, I investigated the sumolyation of lamin A/C and the effect of laminopathic mutant lamin A/C on sumoylation and sumo1 localization. It was demonstrated that although not modified by sumo1, mutant lamin A/C elicits a mutation-dependent alteration of sumo1 localization *in vitro* in cultured mouse myoblasts overexpressing lamin A/C and primary mouse myoblasts expressing endogenous mutant lamins, as well as *in vivo* in affected muscle tissue from a laminopathy knock-in mouse model. Furthermore, in cultured myoblasts, this correlated with a mutation-dependent significant increase in the steady-state level of protein sumoylation by sumo1. Taken together, these results suggest that the alteration of sumo1 localization and sumoylation may be contributing factors in the pathophysiological mechanisms underlying the development of laminopathies.

Acknowledgements

I would first like to sincerely thank my supervisor, Dr. Frédérique Tesson, for giving me the opportunity to pursue my Master's degree in her laboratory. I am grateful for all her support, wisdom, and encouragement. I highly appreciate the experience I have gained and the skills I have developed throughout my time with her and her wonderful team. I also would like to thank my thesis advisory committee for their support and guidance throughout my degree.

To my labmate, Sarah Labib, I extend a huge thank you for her unending support, understanding, help, and friendship. I could not have done it without her. We have shared many triumphs and defeats, problems and solutions, as well as laughs and frustrations that I will never forget. I will also cherish my time with the other past and present members of the lab including Pierrette Bolongo, Tracy Jackson, Pallavi Gupta, Siham Yasari, Nicolas Sylvius, Akil Hamza, and Nicole Mikhael. They have all made my time enjoyable and full of fond memories. We always made each other laugh and got along so well. I will miss you all.

Futhermore, I could not have completed this degree without the support of my amazing friends and family. They are the foundation upon which I have built my life and have been with me every step of the way. Words cannot express how much they mean to me.

I am also grateful for Dr, Gisèle Bonne and the Government of France for the France Foreign Government Award I received that allowed me to study in Dr. Bonne's laboratory in Paris. It was a fantastic experience that allowed me to broaden my scientific as well as cultural horizons. I learned so much with her and her extraordinary lab.

List of Abbreviations

ANP:	Atrial natriuretic peptide
AP1:	Activating protein-1
BAF:	Barrier-to-autointegration factor
bFGF:	basic fibroblast growth factor
BNP:	B-type natriuretic peptide
BSA:	Bovine serum albumin
CD:	Conduction defects
CFP:	Cyan fluorescent protein
CMT:	Charcot-Marie Tooth syndrome
CO_2:	Carbon dioxide
DAPI:	4'6-diamidino-2-phenylindole
DCM:	Dilated cardiomyopathy
DMEM:	Dulbecco's modified eagle medium
DNA:	Deoxyribonucleic acid
DTT:	Dithiothreitol
EDMD:	Emery-Dreifuss muscular dystrophy
ERK:	Extracellular signal-regulated kinase
FBS:	Fetal bovine serum
FPLD:	Familial partial lipodystrophy
GTP:	Guanosine triphosphate
H:	Histone
HA:	Hemaglutinin
HDAC:	Histone deacetylase
HGPS:	Hutchison-Gilford progeria syndrome
INM:	Inner nuclear membrane
kDa:	Kilo Daltons
LGMD:	Limb-girdle muscular dystrophy
LMNA:	Lamin A/C gene
MAD:	Mandibuloacral dysplasia
Mef2:	Myocyte enhancing factor 2
MHC:	Major histocompatibility complex
MAPK:	Mitogen-activated protein kinase
mRNA:	Messenger ribonucleic acid
NB:	Nuclear body
NE:	Nuclear envelope
NEM:	N-Ethylmaleimide
NLS:	Nuclear localization sequence
NPC:	Nuclear pore complex
PBS:	Phosphate buffered saline
PcG2:	Polycomb group protein 2
PIAS:	Protein inhibitor of activated STATs
RD:	Restricitive dermopathy
PKCα:	Protein kinase C alpha
PML:	Promyelocytic leukaemia protein
pRB:	Phosphorylated retinoblastoma
RanGAP1:	Ran GTPase-activating protein 1
RanBP2:	Ran binding protein 2
RD:	Restrictive dermopathy
Red:	Red fluorescent protein
RNA:	Ribonucleic acid
SDS:	Sodium dodecyl sulfate
SENP:	Sentrin(sumo)-specific protease
SIM:	Sumo-interacting-motif
SREBP:	Sterol regulatory element binding protein
SRF:	Serum response factor
STAT:	Signal transducers and activators of transcription
Sumo:	Small ubiquitin-like modifier
T:	Tween 20
TβRI:	TGFβ receptor I
TGFβ:	Transforming growth factor beta
TOP1:	Topoisomerase I
Ubc9:	Ubiquitin-conjugating enzyme 9
UNT:	Untransfected
WB:	Western Blot
WT:	Wild-type
YFP:	Yellow fluorescent protein

List of Figures

Chapter 1: Introduction

1.1 LMNA gene and its products: Lamins A and C

1.1.1 General information and post-translational processing

The human LMNA gene is found at 1q21.2 and spans 21kb with 12 exons. The gene product is alternatively spliced in exon 10 to produce the A-type lamins A and C which are type V nuclear intermediate filament proteins (OMIM #150330). They are expressed in all terminally differentiated tissues with the exception of erythrocytes. There are also two other minor A-type lamin isoforms denoted AΔ10 which is very lowly expressed and C2 that is expressed in spermatocytes (Furukawa et al., 1994; Machiels et al., 1996). The lamin A and C proteins are identical for the first 566 amino acids but differ at the C-terminus where lamin A has 98 and lamin C has 6 unique amino acids. Lamin A has a protein molecular weight of approximately 74kDa and lamin C of approximately 65kDa. Human lamin A/C shares 86% similarity to mouse lamin A/C at the mRNA level and 95% similarity at the protein level which demonstrates that it is highly conserved. The LMNA gene is also conserved in chimpanzee, dog, cow, rat, zebrafish, and mosquito (NCBI ENTREZ Gene, LMNA).

Lamin A is synthesized as a precursor that is modified to become the mature protein. Its unique sequence contains a tetrapeptide motif that signals for isoprenylation of a cysteine residue followed by cleavage of the last 3 amino acids, then carboxymethylation and finally cleavage of the last 18 residues including the modified cysteine. Isoprenylation is known to increase a proteins membrane affinity and the subsequent cleavage allows lamin A to localize to the inner nuclear membrane and also in the nucleoplasm (Goldberg et al., 2008; OMIM #150330). Both lamin A and C are post-translationally modified by phosphorylation which occurs primarily on the assembled filaments (Ottaviano and Gerace, 1985). This modification regulates filament

assembly/disassembly during mitosis and nuclear localization (Heald and McKeon, 1990; Ward and Kirschner, 1990; Haas and Jost, 1993).

1.1.2 Protein characteristics

Both isoforms consist of an N-terminal globular head domain followed by a central alpha helical rod domain containing heptad repeats and end with a larger C-terminal globular tail domain (Figure 1: Top panel). They contain a DNA binding site, an Ig-fold, and together with the B-type lamins, are the only intermediate filaments that have a nuclear localization sequence (NLS) which is found in the tail domain (Holtz et al., 1989; Stierle et al., 2003; Goldberg et al., 2008; Marmiroli et al., 2009). As type V intermediate filaments, lamins form the basic parallel unstaggered coiled-coil dimer units which then associate in a head-to-tail manner to form tetramers and then further associate to form ~15nm unit-length intermediate-like filaments (Strelkov et al., 2003; Strelkov et al., 2004). In the end, they are thought to form stable paracrystal structures (Furukawa et al., 2009). A-type lamin filament arrays have recently been shown to have the ability to form 3-dimensional bundles of filaments instead of only 2-dimensional sheets (Goldberg et al., 2008).

Lamins A and C are a major component of the nuclear lamina which is a complex meshwork of over 80 proteins that underlie the inner nuclear membrane (INM) of all nucleated cells. They are also found throughout the nucleoplasm as small foci or a diffuse skeletal network (Bridger et al., 1993; Hozak et al., 1995). The other nuclear intermediate filaments are the B-type lamins (B1 and B2 encoded by LMNB1 and LMNB2 genes, respectively) which are ubiquitously expressed at all developmental stages in all cell types and are essential for survival. They interact with A-type lamins and are also major components of the inner nuclear lamina. However, due to experimental constraints, most studies on lamina assembly are performed either *in vitro* or in

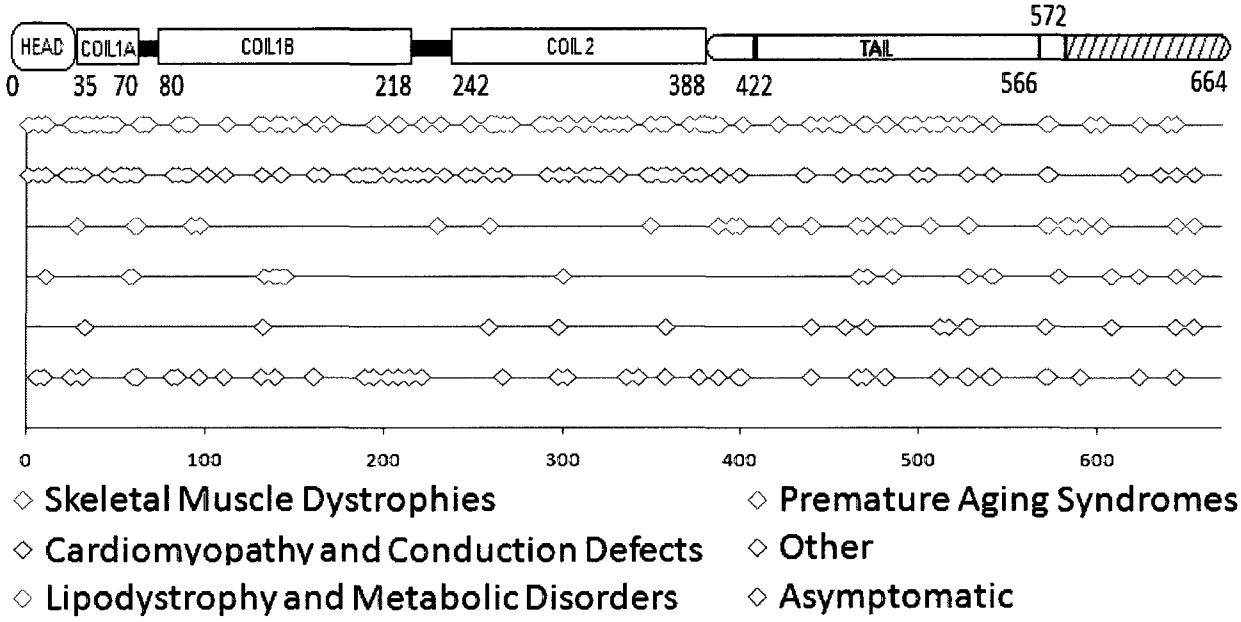

Figure 1 Schematic of lamin A/C protein and location of currently known mutations associated with different types of laminopathies. Top panel: Lamin A/C protein denoting amino acid positions of protein domain boundaries. Note: amino acid position 422 signifies the lamin A/C nuclear localization signal and residue 566 signifies the end of residues identical to both lamin A and C. Amino acid positions 566-572 denote lamin C-specific residues and 566-664 denote Lamin A-specific residues. Bottom panel: Locations of mutations reported in the Universal Mutation Database (www.umd.be) along the lamin A/C gene (LMNA) associated with different types of laminopathies and asymptomatic mutation carriers.

Figure 1

invertebrate organisms and thus vertebrate lamina assembly in vivo remains poorly understood (Goldberg et al., 2008).

1.2 Lamin A/C functions and interactions

1.2.1 Structural roles

Lamins A and C have been implicated in many important nuclear functions and have been found to have numerous interacting partners. They have been shown as a key determinant of nuclear shape and strength as lamin deficient cells show smaller nuclei, altered nuclear morphology with increased nuclear deformation under strain as well as impaired mechanotransduction (Hutchison et al., 2002; Lammerding et al., 2004; Lammerding et al., 2006). Lamins also regulate nuclear envelope (NE) organization by anchoring and spacing nuclear pore complexes (NPCs) as they interact with NPCs in the early stages of lamina assembly and are involved in proper NPC localization (Furukawa et al., 2009). Lamins are often considered as scaffolds for proteins and protein complexes. They have been found to be responsible for protein recruitment to the INM as studies have shown that mutant lamins mediate a mislocalization of certain proteins into nuclear foci (Hubner et al., 2006, Dreuillet et al., 2008). Lamins are also implicated in anchoring heterochromatin at the NE (Verstraeten et al., 2007). Through their interaction with other structural proteins such as Nesprin, they form a link between the nucleoskeleton/lamina and the actin cytoskeleton in cells (Padmakumar et al., 2005). They also interact with emerin and function to anchor it at the NE as some mutant lamin expression resulted in misassembly of lamin filaments into aggregates with the co-localization of emerin (Holt et al., 2003).

1.2.2 Regulatory roles

Lamin filaments are disassembled and reassembled during cell division which is mediated by hyper- and hypo-phosphorylation, respectively, and their disassembly is necessary for nuclear envelope dissociation (Gerace et al., 1984; Nigg, 1992). Lamins also have important regulatory roles in various cell processes. They have been shown to maintain efficient DNA replication speed and expression of mutant lamin A resulted in the inhibition of the elongation phase (Moir et al., 2000; Prokocimer et al., 2009). Lamins interact with DNA, chromatin, and chromatin-associated proteins such as histone deacetylases (HDACs) in both direct binding and indirect scaffolding manners. The lamin protein contains a chromatin binding site in the alpha helical rod domain and another in the C-terminal globular domain (Dechat et al., 2009). It is reported that chromatin regions that interact with lamins are transcriptionally silent (i.e. heterochromatin) and that when in proximity of promoters, lamins transcriptional repressors (Verstraeten et al., 2007; Prokocimer et al., 2009; Lee et al., 2009). They also interact with multiple histone (H) proteins/complexes such as H2A and H2B dimers as well as H3 and H4 tetramers (Taniura et al., 1995; Goldberg et al., 1999). Through their interaction with Lap2α, lamin A/C functions to anchor the hypophosphorylated retinoblastoma protein (pRb) at the NE to inhibit it from preventing cell cycle progression (Markiewicz et al., 2002; Pekovic et al., 2007). Furthermore, PP2 is a protein phosphatase that interacts with lamins and when lamins are absent in fibroblasts, PP2 cannot dephosphorylate pRb, and thus fibroblast proliferation is accelerated (van Berlo et al., 2005).

Lamins are also implicated in anchoring transcription factors such as c-Fos of the activating protein -1 (AP1) complex thus inhibiting its transcriptional activation activity and the transcriptional regulator MOK2 by sequestering it at the nuclear periphery (Dreuillet et al., 2002; Ivorra et al., 2006). Lamins also interact with barrier-to-autointegration factor (BAF) in the

organization of chromatin and sterol regulatory element binding protein -1c (SREBP-1c) interacts with pre-lamin A in regulating cholesterol synthesis and adipogenesis (Markiewicz et al., 2002; Lloyd et al., 2002; Capanni et al., 2005; Verstraeten et al., 2007). Furthermore, a study found that disrupting normal lamin organization resulted in the displacement of the TATA-binding protein and thus inhibited RNA polymerase II activity which highlights the role of intranuclear lamins as a scaffold in regulating transcription directly (Spann et al., 2002). Lamin A/C also has functions in DNA repair as research has shown that the accumulation of pre-lamin A causes genomic DNA to be more sensitive to genotoxic stress and impaired DNA repair foci (Varela et al., 2005; Liu et al., 2005; Manju et al., 2006).

Additionally, lamins have been proposed as participants in several other signalling pathways. Lamin A/C is known to bind protein kinase C-alpha (PKCα) and thus may have a role in the regulation of PKCα signalling possibly modulating cell proliferation and apoptosis (Martelli et al., 2002; Parnaik, 2008). Lamins are also implicated in the mitogen-activated protein kinase (MAPK) and extracellular signal-regulated kinase (ERK) signalling cascades. An increase in MAPK signalling was found at disease onset and through disease progression in the $LMNA^{H222P/H222P}$ mouse model that expresses mutant lamins (discussed in chapter 1.9.3) (Muchir et al., 2009). Lamins have been shown to interact with the E2 conjugating enzyme, Ubc9, of the post-translational modification pathway known as sumoylation. Our laboratory has since demonstrated the sequestration of the effector protein, sumo1, inside mutant lamin aggregates (discussed in chapter 1.4) (Zhong et al., 2005; Sylvius et al., 2005).

1.2.3 Roles in muscle

Lamin A/C filaments are known to undergo disassembly and reassembly during the cell cycle yet they also undergo regulated reorganization during myoblast differentiation (Muralikrishna et al., 2001). It is also known that myoblasts lacking lamin A/C show lower

expression of important differentiation proteins such as MyoD and pRb (Frock et al., 2006). Furthermore, disease-associated mutant lamin A/C expression resulted in the inhibition of differentiation of myoblasts into myotubes (Favreau et al., 2004) that our laboratory has also observed (unpublished observations). This highlights lamins as important in proper myogenesis. Also, as discussed earlier, cells lacking lamins are more sensitive to mechanical stress, especially in tissues that are subject to mechanical forces such as cardiac and skeletal muscles (Lammerding et al., 2004; Mittlebronn et al., 2008). This implicates a properly functioning nuclear lamina in structural integrity.

1.3 Laminopathies

1.3.1 Disease phenotypes resulting from mutations in LMNA

Laminopathies are a collection of over 10 distinct and overlapping human disease phenotypes associated with over 340 known mutations in the LMNA gene (Figure 1: Bottom panel) (OMIM#150330 and UMD database). They comprise a wide-range of tissue-specific and overlapping phenotypes that include dilated cardiomyopathy 1A (DCM) with or without conduction defects, autosomal dominant Emery Dreifuss muscular dystrophy (EDMD), limb-girdle muscular dystrophy type 1B (LGMD1B), restrictive dermopathy (RD), familial partial lipodystrophy type 2 (FPLD), Charcot-Marie Tooth syndrome type 2B1 (CMT2B1), mandibuloacral dysplasia (MAD), heart hand syndrome Slovenian type, atypical Werner syndrome, Seip Syndrome, and Hutchinson-Gilford progeria syndrome (HGPS) as well as a syndrome of lipoatrophy with diabetes, hepatic steatosis, hypertrophic cardiomyopathy and leukomelanodermic papules (OMIM #150330). So far, there is no definitive genotype/phenotype relationship for mutations in this gene. Moreover, asymptomatic carriers have mutations along the full length of the gene. In Figure 1, the top panel shows a schematic of the lamin A/C protein

domains corresponding to the amino acid residues while the bottom panel demonstrates the location of known mutations along the LMNA gene and the disease phenotype that presents.

In particular, DCM is characterized as dilatation of the left or both heart ventricles and impaired myocardial contractility (Richardson et al., 1996). As the heart chambers become enlarged and the chamber walls thin, contraction is compromised resulting in decreased ejection fraction. Age of onset is variable but commonly occurs in the 4^{th} or 5^{th} decades of life (Mestroni et al., 1999). In the United States, the incidence of DCM accounts for approximately 40 cases per 100,000 population and 10,000 deaths per year (Dec and Fuster, 1994; Karkkainen and Peuhkurinen, 2007). It is estimated that up to 50% of idiopathic DCM cases are familial and our laboratory has determined that approximately 5% of genotyped DCM probands from 1999 to 2006 had LMNA mutations (Sylvius and Tesson, 2006; Malhotra and Mason, 2009). This implicates LMNA as a major causative gene for familial DCM. This disease has an autosomal dominant transmission and it is associated with a worse prognosis that other forms of DCM (Arbustini et al., 2002; Taylor et al., 2003).

EDMD is characterized by early onset contractures of the elbows, spinal extensor muscles, and Achilles tendon followed by slowly progressive muscle wasting/weakness and cardiac conduction defects that often present before the age of 30 (Emery, 2000). It can be caused by X-linked mutations in the EMD gene (encoding emerin) but more commonly by autosomal dominant mutations in LMNA. Mutations in LMNA are often responsible for an earlier onset and more severe form of EDMD (Vytopil et al., 2003). Furthermore, DCM and cardiac complications are often found with EDMD and other muscular dystrophy laminopathies, and are responsible for an increased risk of sudden death and heart failure requiring transplantation (Bonne et al., 1999; Wessely et al., 2005).

1.3.2 Molecular characteristics of laminopathies

At the molecular level, DCM cardiomyocytes undergo events such as cellular hypertrophy, myocyte degeneration, and myocardial fibrosis (Dec and Fuster, 1994). Also, nuclear abnormalities are commonly found in DCM cardiomyocytes and include oddly shaped nuclei, irregular chromatin deposition, and the disruption of nuclear membranes leading to invasion of cytoplasmic organelles into the nucleoplasm (Sylvius et al., 2005; Fidzianska et al., 2008, Gupta et al., 2010 - Appendix I). Our lab reported one LMNA mutation carrier (p.D192G) to have a completely disrupted nuclear membrane in 30% of cardiomyocytes (Sylvius et al., 2005). We have also shown that a lamin A/C gene deletion encompassing exons 3-12 in a DCM patient resulted in diminished lamin A/C staining in an endomyocardial biopsy, discontinuous nuclear envelopes and invasion of mitochondria in the nuclear space (Gupta et al., 2010).

Apart from DCM, aggregations and altered localization of lamin A/C is reported in patient tissues from other laminopathies. Fibroblasts from an FPLD patient with the p.R482L mutation have shown intranuclear aggregations with decreased staining of lamin A/C at the nuclear rim and altered chromatin distribution (Capanni et al., 2003). The aggregates were not bound to DNA or splicing factors and there was also a decreased rate of transcription leading to the hypothesis that this mutation may be eliciting its effects through disrupted interaction with chromatin and other interacting partners (Capanni et al., 2003). A study by Muchir et al. (2004) examined fibroblasts from 13 patients with various laminopathies. In eight of the patients they found intranuclear aggregations (foci), dysmorphic nuclei, blebbing (protrusions of lamin A/C outside the NE), and honeycomb-like appearance of lamin A/C in an average of 10% of nuclei compared to about 1% in controls. These eight patients represented EDMD, FPLD, LGMD and DCM disease phenotypes. The remaining patients, which included EDMD and LGMD phenotypes, did not show significant differences from controls. This study showed that lamin

A/C localization is perturbed in patient fibroblasts but highlights the lack of correlation between laminopathies and their molecular phenotype (Muchir et al., 2004). Moreover, this study as well as a study by Favreau et al. (2003) aided to demonstrate that different mutations causing different diseases can elicit similar molecular alterations of lamin A/C. They also helped validate *in vitro* results by showing that patient fibroblasts show comparable characteristics to exogenously expressed mutant lamin A/C in cell culture (Favreau et al., 2003).

Furthermore, the failing DCM heart undergoes structural re-modelling and altered gene expression. Multiple micro-array analyses have reported hundreds of genes that have shown up- or down-regulation from various cellular pathways. The main limitation is that the different studies do not often replicate the same gene sets. Several targets that have been identified in at least two studies are LMNA, cardiac troponin, Atrial natriuretic peptide (ANP), and B-type natriuretic peptide (BNP) (reviewed in Asakura and Kitakaze, 2009). The latter two represent part of a re-employment of a fetal cardiac gene expression program that may occur either as an attempt to compensate for the malfunctioning muscle or as a defective mechanism due to gene regulation dysfunction (Gerdes and Capasso, 1995; Kuwahara et al., 2003; Barton et al., 2004; Oka et al., 2007).

1.4 Mutant lamin A/C overexpression alters lamin dynamics

Our laboratory has shown that expression of p.D192G (DCM) and p.R386K (DCM) mutant lamin A results in nuclear aggregates that appear to retain the ability to target the NE. Wild-type lamin A expression shows the normal veil-like distribution. Wild-type lamin C formed small aggregates that contacted the NE. Conversely, the expression of p.D192G and p.R386K mutant lamin C formed large aggregates that were unable to target the NE and instead remained in the nucleoplasm (Sylvius et al., 2008 – Appendix II). It is important to note that aggregate

formation is not due to an excess of transfected DNA or different transfection efficiencies. We demonstrated that similar lamin C aggregates were formed at varying transfection concentrations and that transfection efficiency is comparable between samples (Sylvius et al., 2008). Furthermore, p.D192G and p.R386K mutant lamin C molecules in aggregates from transfected COS7 cells show an increased mobility which indicates a lower stability of the lamin complexes. This also suggests that these mutant lamin C aggregates do not target the NE and may preferably interact with each other (Sylvius et al., 2008).

Co-expression of p.D192G and p.R386K mutant lamin A and C together resulted in co-localized aggregates that target to the NE. This suggests that lamin A has a role in the correct localization or tethering of lamin C at the NE. Interestingly, one DCM-associated LMNA mutation, p.L85R, did not show any significant differences from the wild-type in the above mentioned experiments except for expression of only mutant lamin C. We found that this mutation shows large intranuclear aggregates like the other mutation but re-introducing lamin A, even though it is also p.L85R mutated, rescues the wild-type phenotype. This suggests that the ratio of lamin A to lamin C is important for lamin C incorporation into the lamina. In addition, one FPLD-associated mutation, p.R482W, does not show any differences in protein localization or lamina appearance compared to the wild-type which demonstrates that not all mutations affect lamina assembly (Sylvius et al., 2008 and unpublished observations).

It is important to note that some of the results may be weakened by the fact that these cells endogenously express wild-type lamin A/C and although the expression vectors cause over-expression, this does not negate the presence of some endogenous lamins. However, these models aid to mimic the heterozygous mutation state found in virtually all laminopathy patients.

In 2005, our laboratory used COS7 cells to co-express p.D192G mutant lamin C with the post-translational modification protein, sumo1 (small ubiquitin-like modifier 1) (Sylvius et al., 2005). This resulted in sumo1 being targeted to and sequestered inside the aggregates (Figure 2 from Sylvius et al., 2005). When the sumo1 vector was mutated to abolish the c-terminal di-glycine motif required for sumo1 to be covalently linked to target proteins, the sequestration in mutant aggregates was abolished and there was a diffuse nuclear distribution of sumo1 lacking the normal punctate aspect. Normal sumo1 localization usually appears diffuse with small nuclear bodies in the nucleus and diffuse in the cytoplasm. Expression of wild-type lamin C did not alter normal sumo1 localization. This suggests that there is recruitment of sumo1 and/or proteins modified by sumo1 within mutant lamin C aggregates and that this phenomenon is dependent on the sumoylation competency of sumo1 (Sylvius et al., 2005).

1.5 Sumoylation and sumo1

1.5.1 The sumoylation process

Sumoylation is the covalent yet reversible post-translational attachment of the small ubiquitin-like modifier (sumo or sentrin) protein to a target lysine on a substrate protein in a process that is similar to ubiquitination yet with different enzymes. Figure 3 shows a schematic representation of the sumoylation process. The sumo protein (~11kDa) is first synthesized as an inactive precursor protein that has 4 residues cleaved at the C-terminus to reveal the di-glycine motif required for conjugation. This is accomplished by sumo-specific isopeptidases (SENPs – sentrin(sumo)-specific proteases). Next, Aos1 and Uba2 form a heterodimer that functions as the E1 activating enzyme through an ATP-dependent reaction. First, a thioester bond is formed between the C-terminal carboxy group of sumo and a catalytic cysteine on Uba2. Second, sumo

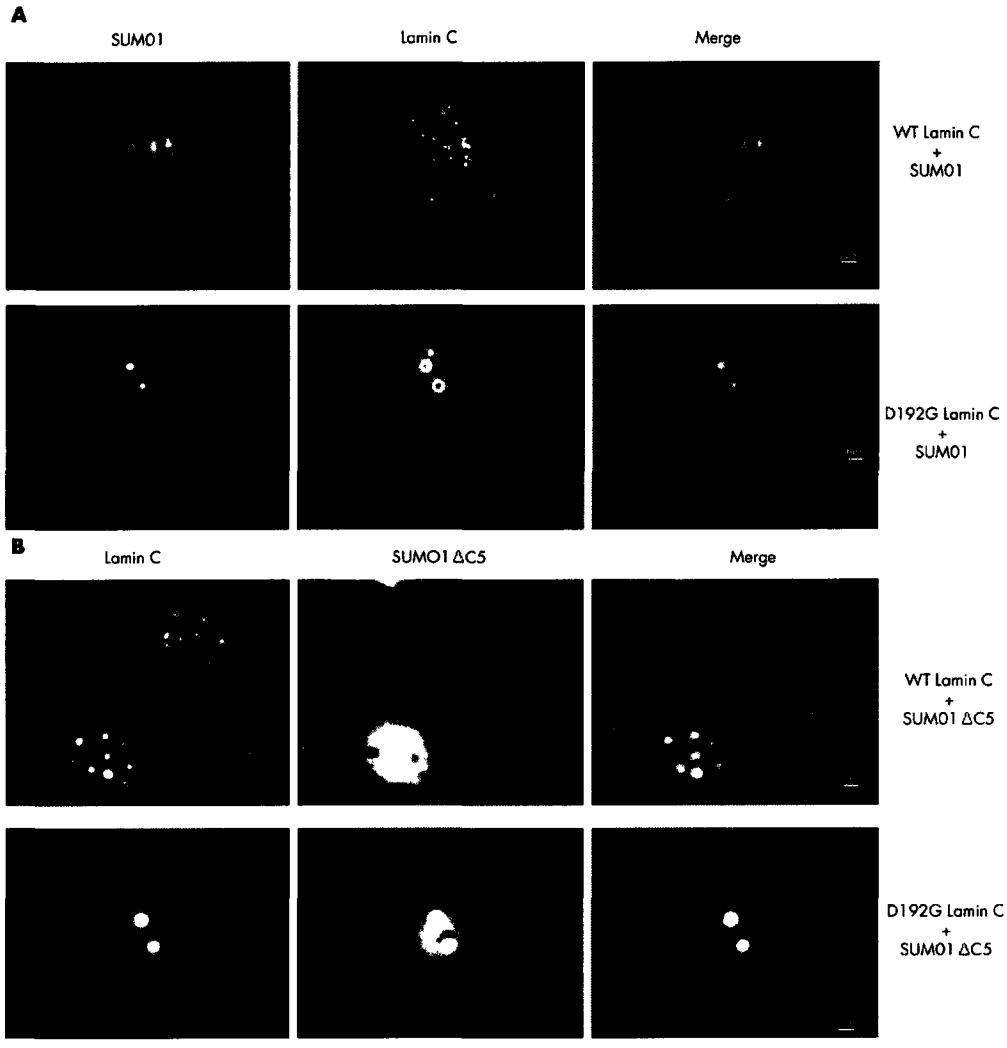

Figure 2: Sumo1 is sequestered in mutant lamin C aggregates in a sumoylation-dependent manner. Obtained from Sylvius et al. J Med Genet 2005;42:639-47. COS7 Cells co-transfected with fluorescently tagged lamin C (red) and (A) SUMO1 or (B) SUMO1DC5 (yellow green). (A) Presence of wild type lamin C did not alter SUMO1 distribution (small dots within and nearby the nucleus), while co-transfection with D192G lamin C shows recruitment of SUMO1 within the lamin C spots. (B) No difference is observed in the localisation of SUMO1DC5 in cell transfected with wild type lamin C or D192G lamin.

Figure 2

is transferred to the E2 conjugating enzyme, Ubc9, and a thioester is formed between the C-terminal carboxy group of sumo and the catalytic cysteine of Ubc9. Subsequently, Ubc9 interacts with the substrate protein and transfers sumo to the substrate by forming an isopeptide bond between the C-terminal glycine and the target lysine, thereby covalently attaching sumo to its target protein. This last reaction may be catalyzed by specific E3 ligase enzymes that are unique to certain targets and with varying specificities but are not absolutely required for sumoylation (reviewed in Johnson, 2004). E3 ligases act by promoting the interaction of Ubc9 with the target or the transfer of sumo to the target and are proposed to aid in activating Ubc9. The major examples of E3s include the PIAS family (protein inhibitors of activated STATs), the nuclear pore protein RanBP2, and the polycomb group protein 2 (PcG2) and appear to have mostly distinct target sets. Finally, sumo can be removed from the substrate protein by the same family of enzymes that cleave the immature precursor sumo protein, the SENPs. SENPs 1, 2, 3, 5, 6 and 7 have varying specificities for maturation, isopeptidase activity, and to the different sumo proteins as well as at different intracellular locations (Johnson, 2004; Geiss-Friedlander and Melchior, 2007; Mukhopadhyay and Dasso, 2007). Major sites of sumoylation in the cell include the nuclear rim, nucleolus, and PML nuclear bodies (Saitoh et al., 2006).

1.5.2 The sumo protein family

In mammals, there are 4 proposed sumo proteins (sumo1 to sumo4) that share a 3D conformation with ubiquitin but only about 20% sequence identity. They are ubiquitously expressed except for sumo4 which appears to be expressed mainly in the kidney, lymph node, and spleen. They all contain N-terminal unstructured sequences for sumo chain formation yet there are conflicting reports that sumo1 is able to form chains as its extension lacks a sumoylation consensus sequence (Vertegaal, 2007; Yang et al., 2006; Hammer et al., 2007). The most common sumoylation consensus sequence is Ψ-K-X-E/D where Ψ is a large hydrophob

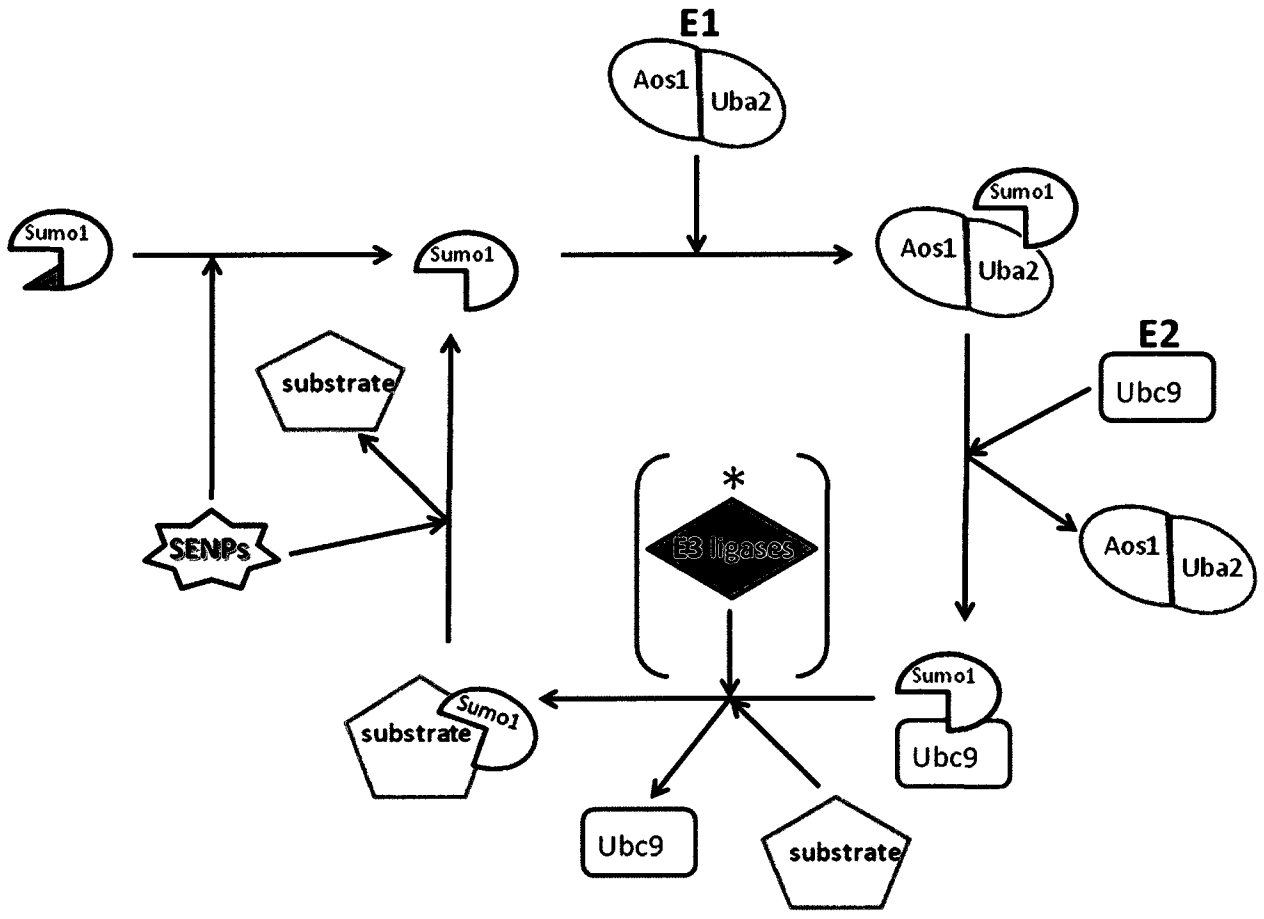

Figure 3 Schematic of sumoylation pathway. Sumo1 is synthesized as an inactive precursor and cleaved by sumo-specific proteases (SENPs) then is transferred to the E1 activating complex where it is activated in an ATP-dependent reaction. Sumo1 is then transferred to the E2 conjugating enzyme, Ubc9, which interacts with the substrate protein and covalently attaches sumo1 to the target lysine in the substrate. This step can be catalyzed by substrate-specific E3 ligase enzymes but is not necessary for sumoylation to occur. As the process is reversible, the substrate may undergo de-sumoylation by SENPs to release the protein and sumo1 from their covalent attachment.

Figure 3

amino acid, K is the modified lysine, X is any amino acid, and E/D is aspartic or glutamic acid. Sumoylation is not limited to these sites but appears to preferentially occur there. Sumo2 and sumo3 are almost identical in sequence yet only share ~50% identity to sumo1. Sumo4 was formerly thought to lack the ability to undergo sumoylation and therefore lack functionality. It was recently shown to be degraded during normal cellular conditions but reported to undergo maturation by a stress-activated hydrolase and can then modify target proteins (Wei et al., 2008). Sumo2/3 is also generally linked to acute stress response and is mostly found in a free/unconjugated form although there is growing evidence to suggest it has roles in cellular processes (Flick and Kaiser, 2009; Yang and Paschen, 2009). Sumo1 is mostly found conjugated to target proteins and has roles in many tightly regulated cell processes (Saitoh and Hinchey, 2000). It was shown that sumo1 and sumo2/3 share modification of certain targets but also have separate substrates (Vertegaal et al., 2006).

1.6 Functions of sumoylation by sumo1

Sumoylation by sumo1 has been found to have roles in a growing number of integral cell processes and elicits a wide range of different effects on substrate proteins. Sumoylation can interfere with other post-translational modifications (ex. Ubiquitination), provide or mask protein interaction sites, alter protein localization/trafficking, alter chromatin regulation, as well as activate or repress transcription factors.

Ubc9, the sumoylation conjugation enzyme, has been shown to be essential for survival in mice as knock-out mice die at an early embryonic stage. They display nuclear envelope abnormalities, mislocalized RanGAP1 (a sumoylation target discussed later), chromosome segregation defects and chromosome condensation (Nacerddine et al., 2005). This implicates sumoylation in viability, cell cycle, chromosome regulation, and proper nuclear functioning

(Kuehn, 2005; Nacerddine et al., 2005). Below are a number of specific examples to highlight the diversity of sumo1 modification targets and pathways:

1.6.1 Sumoylation in chromatin regulation

Sumoylation is implicated as part of the "histone code" in the regulation of chromatin. Both core histones as well as histone deacetylases are sumo1 targets. The core H4 histone protein was found to be sumoylated which recruits histone deacetylase 1 (HDAC1) and heterochromatin protein 1 which mediate transcriptional repression (Shiio and Eisenman, 2003). Moreover, HDAC-1, -4, and -6 were found to be sumoylated. HDAC4 is modified at the NPC appearing important for its nuclear import and like H4, sumoylation increased repression ability (Kirsh et al., 2002). The modification of HDAC4 is catalyzed in the presence of the E3 ligase, RanBP2. At nuclear pores, RanBP2 interacts with the irreversibly sumoylated RanGAP1 protein as well as Ubc9 and this complex is required for proper nuclear import (Mahajan et al., 1997). Sumoylation of RanGAP1 is also important for the proper association of RanGAP1 with the mitotic spindles during mitosis again in complex with RanBP2 (Joseph et al., 2002).

1.6.2 Sumoylation and PML

PML nuclear bodies (NBs) represent another major meeting point of sumo1 and its targets, especially in the goal of transcriptional repression. These dynamic nuclear bodies are named as such due to the tumour suppressor promyelocytic leukaemia protein that specifically localizes to them. Sumoylation of PML is required for the formation of PML-NBs which themselves have been implicated in many nuclear processes and their loss is observed in leukaemia and tumours (Salomoni and Pandolfi, 2002). They are also generally thought to be a storage site for repressed transcription factors, appear to be a site of active sumoylation, and are responsive to cellular stress and DNA damage (Dellaire and Bazett-Jones, 2004; Saitoh et al., 2006; Bernardi and Pandolfi, 2007; Heun, 2007). Still, they are known to interact tightly with

certain areas of chromatin that are transcriptionally active and that contain many genes including the MHC class I and p53 loci (Sun et al., 2003; Wang et al., 2004; Kumar et al., 2007). Interestingly, some PML-NBs have been observed to co-localize with over-expressed proteins and protein aggregates, as well as mutant proteins and are suggested to promote their degradation (Dino Rockel and von Mikecz, 2002; Fu et al., 2005). It is not currently known if mutant lamin aggregates co-localize with PML-bodies.

1.6.3 Sumoylation and TGFβ-mediated fibrosis

Another pathway linked to sumoylation is the TGFβ-mediated fibrosis pathway. The TGFβ receptor I (TβRI) and an intracellular effector of the TGFβ pathway (smad4) are known to be sumoylated. When the TGFβ ligand binds, TβRII trans-phosphorylates TβRI and this induces the intracellular phosphorylation and thus activation of smad proteins -2 and -3 that then interact with smad-4 and translocate to the nucleus where they activate gene expression (Kang et al., 2008; Miyazono et al., 2008). Sumoylation of TβRI enhances this activation and it is hypothesized that sumoylated TβRI increases the affinity of smads-2 and -3 to TβRI to outcompete the inhibitory smad7 protein (Miyazono et al., 2008). Smad4 is also sumoylated however there are differing reports on the functional result of its sumoylation. Also, a point mutation in the TβRI gene near the sumoylation site was found in humans with several types of cancers and although there was no observed change in the phosphorylation ability of TβRI, its sumoylation was reduced. This correlated with a lower activation of the TGFβ signal (Kang et al., 2008). Therefore although not completely elucidated, sumoylation is still implicated in the regulation of the TGFβ pathway.

1.6.4 Sumoylation roles in muscle

Sumoylation has been implicated in myogenesis and adult cardiac tissue homeostasis. Ubc9 was shown to be important for myoblast differentiation in C2C12 cells (Riquelme et al.,

2006). This occurred independently of MyoD and myogenin which are early myogenic factors. This suggests that the role of ubc9 in myogenesis may be related with more downstream myogenic factors (Riquelme et al., 2006). Also, there are several important muscle factors that are known to be sumoylated: Interacting partners GATA4, serum response factor (SRF), and myocardin are transcriptional activators important in cardiogenesis and their activities are all enhanced or activated by sumo-1 modification (Molkentin et al., 1994; Wang et al., 2004; Wang et al., 2007; Wang, 2009). Conversely, myocyte enhancing factor 2 proteins (Mef2s) are positively acting myogenic and cardiogenic transcription factors yet there is a negative effect of sumoylation to inhibit transcriptional activation ability (Zhao et al., 2005).

1.7 Linking lamin A/C and sumo1

It has been shown that lamin A/C interacts with the only conjugating enzyme of the sumoylation process, ubc9, which is known to interact directly with proteins that are sumoylated (Zhong et al., 2005). The lamin A/C protein sequence harbours 4 common sumoylation consensus sequences (Figure 4A) which lead us to hypothesize that wild-type lamins may be sumoylated by sumo1. In addition, if mutations in lamins alter the folding of the protein, this may mask the sumoylation site or reveal an otherwise concealed modification site and thus may alter lamin A/C function and localization. During the course of this thesis, Zhang and Sarge (2008) found lamin A to be sumoylated by sumo2/3 in HeLa cells and mouse cardiomyocytes. However, they did not demonstrate sumoylation of lamins by sumo1. They also showed that a DCM-linked mutation (p.E203G) in one of the consensus sequences resulted in abolishment of sumoylation and mislocalization of lamin A into nuclear aggregates. Although it is possible that sumoylation affects lamin A localization as they suggested, it is also plausible that the point

mutation altered filament assembly for proper localization as we and other groups have shown with other lamin A/C point mutations (discussed in chapters 1.3.2 and 1.4).

Furthermore, sumo1 has been found sequestered in mutant lamin C aggregates in a sumoylation-dependent manner (discussed in chapter 1.4). Lamins are also known to scaffold and/or interact with multiple proteins that are sumoylated such as core histones, HDACs, c-Fos, SREBP1/2, and ubc9 (discussed above). Therefore, mutant lamins may be mediating a disturbance in protein sumoylation/de-sumoylation, sumo1 turnover, and protein function. More specifically, multiple myogenic and cardiogenic factors interact with lamins and are sumoylated, thus mutant lamins may be contributing to the tissue specificity of laminopathies especially those which affect striated muscle.

1.8 Selected striated muscle laminopathy mutations

There were five mutations which were investigated in this thesis (Figure 4B). They were chosen as they are specifically related to two myopathic laminopathies in humans: Dilated cardiomyopathy and Emery-Dreifuss muscular dystrophy. They also represented mutations that when expressed in cell culture resulted in different effects on lamin A/C localization. The p.L85R mutation, located at the beginning of coil domain 1B, was found in a family with severe autosomal dominant DCM and conduction system disease (without skeletal myopathy) with incidences of sudden death and heart transplantation (Fatkin et al., 1999). Coil 1B is a region important for lamin A/C dimerization and interaction with lamin B (Perrot et al., 2009). Interestingly, despite the major change of a leucine to an arginine amino acid and its important location, research has shown that p.L85R mutant lamin A/C retains either slightly aberrant but predominantly normal localization (Raharjo et al., 2001; Holt et al., 2003; Sylvius et al., 2008). The p.D192G mutation is also located in coil 1B and has a particularly severe disease phenotype.

It was found by our laboratory in a family with suspected autosomal dominant DCM with atrioventricular block and without skeletal myopathy. Cardiac tissue sections displayed dramatic nuclear membrane abnormalities such as complete loss of the nuclear membrane with invasion of cytoplasmic organelles in the nucleoplasm and chromatin disorganization. *In vitro* expression results in large intranuclear aggregations of co-localized lamins A and C as well as large intranuclear aggregations of lamin C with sequestration of sumo1 inside the aggregates (Sylvius et al., 2005; Sylvius et al., 2008). The p.H222P mutation is located in the flexible linker region (L12) of the rod domain between coil 1B and coil 2 and may function to provide flexibility between the coiled coils (Strelkov et al., 2003). It was found in a family with classic autosomal dominant Emery-Dreifuss muscular dystrophy with DCM and conduction defects (Bonne et al., 2000). In 2005, a mouse laminopathy model was generated with this mutation (discussed in chapter 1.9) and lamins are reported to retain normal localization (Arimura et al., 2005). The p.Q353K mutation is located in the rod domain in coil 2 which is also a region important for dimerization (Strelkov et al., 2003). This mutation was discovered by our laboratory in a DCM patient that required a heart transplant and had a skeletal myopathy but interestingly showed no major cardiomyocyte ultrastructural abnormalitites (Gupta et al., 2010 – Appendix I). The p.R386K mutation is found at the distal end of coil 2 at a highly conserved position. Although this mutation is not thought to disrupt coiled-coil formation, this region could be important for later filament assembly and protein-protein interactions (Strelkov et al., 2004). It was originally discovered in a family with autosomal dominant EDMD with cardiac involvement (Bonne et al., 2000). Our laboratory has shown that expression of this mutation in COS7 cells shows aggregations of lamins at and outside the NE (Sylvius et al., 2008).

1.9 Mouse models of laminopathies

1.9.1 Lamin A/C knock-out mouse model LMNA$^{-/-}$

The LMNA$^{-/-}$ mice were generated by Sullivan et al. (1999) by truncating the 3' end of the LMNA gene encompassing exon 8 to the middle of exon 11. This deleted 152 codons from lamin A and 114 codons including the polyadenylation signal from lamin C. Although the mutated genes were still lowly expressed, there was complete loss of lamin A/C protein expression. The homozygous knock-out mice were undistinguishable from heterozygotes and wild-type mice at birth. Yet, after 2-3 weeks, they displayed reduced growth rate and after 3-4 weeks, they began to show symptoms of a severe EDMD-like phenotype. All homozygous mice died by 8 weeks and were found to have cardiac and skeletal myopathy. They also display nuclear abnormalities such as elongated shape, blebbing, mislocalization of emerin into the endoplasmic reticulum, some NPC clustering, as well as the exclusion of LAP2 and Lamin B from one pole (Sullivan et al., 1999). LMNA$^{-/-}$ mice have recently been shown to have shorter telomeres and impaired telomere processing, implicating lamins in the DNA damage response (Gonzalez-Suarez et al., 2009). Heterozygous mice were normal at 8 weeks but later develop atrioventricular conduction defects (Stewart et al., 2007). Both hetero- and homo-zygote LMNA knock-out mice are free of metabolic and adiposity defects associated with FPLD (Cutler et al., 2002). This is a very informative mouse model for lamin insufficiency but does not represent a true laminopathy as no patients have ever been found to completely lack lamins A and C. One case where a newborn died at birth was carrying a homozygous mutation introducing a premature stop codon at position 259 (p.Y259X). There was no lamin A/C found in immunostained quadriceps. The heterozygous family members showed 50% lamin A/C expression and a LGMD1B phenotype (van Engelen et al., 2005).

A

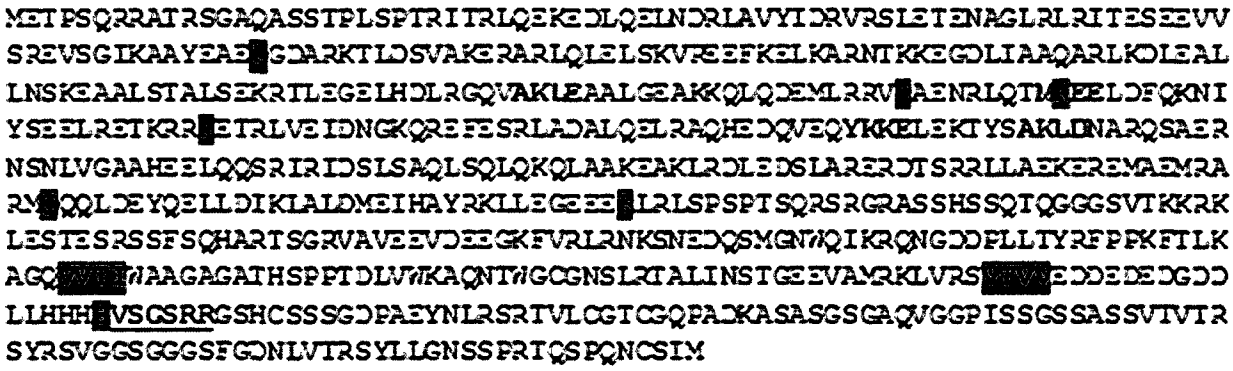

B

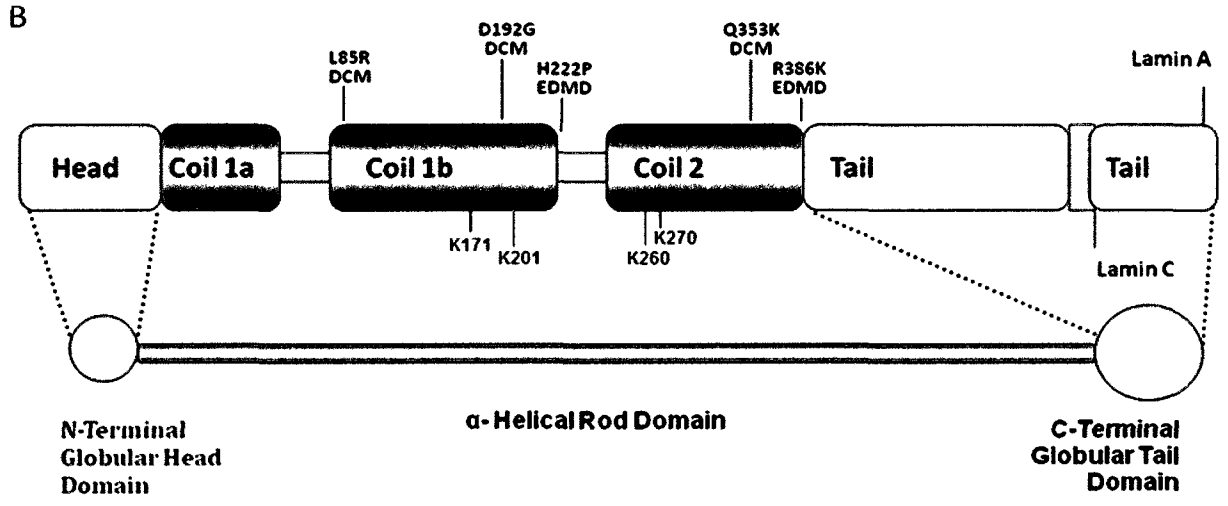

Figure 4 A) Lamin A/C protein sequence denoting residues of interest. Residues are representedby highlight colours of red for mutation sites included in this project, yellow for sumo1 sumoylation consensus sequences, pink for known sumo2/3 sumoylation site, blue for possible sumo interacting motifs, and green for the point at which lamin A and lamin C are no longer identical. Underlining represents lamin C specific resiudes and all residues following are lamin A specific residues. B) Locations of laminopathic mutations investigated. Point mutations examined (top) and potential lysine sumoylation residues (bottom) are indicated. White bars represent linker regions and checkered bar represents lamin C specific amino acids.

Figure 4

1.4.2 Other laminopathy mouse models

The $LMNA^{N195K/N195K}$ mouse model was produced to model a laminopathy of autosomal dominant dilated cardiomyopathy with conduction defects found in humans (DCM-CD1) (Mounkes et al., 2005). Homozygous mice develop DCM, fibrosis, arrythmias, cardiomyocyte nuclear membrane defects and die at 3 months of age. This mutation also results in the up-regulation of the fetal expression program genes atrial natriuretic peptide (ANP) and B-type natriuretic peptide (BNP) (Mounkes et al., 2005) that is also observed in humans with DCM (Hwang et al., 2002). Heterozygous mice were indistinguishable from WT mice (Mounkes et al., 2005).

The $LMNA^{M371K/M371K}$ mouse model was produced to investigate the cardiac effects of this mutation that was found to cause EDMD in humans. The transgene was made to only be expressed in heart tissue. Homozygous mice showed high prenatal mortality and died by 8 weeks of age. Interestingly, they do not develop DCM but show cardiomyocyte abnormalities and nuclear deformities (Wang et al., 2006).

The $LMNA^{L530P/L530P}$ mouse model was originally generated to elucidate the mechanisms of EDMD yet heterozygous mice have no obvious phenotype and homozygous mice developed a strong progeria phenotype of premature aging and died by 5 weeks of age. (Mounkes et al., 2003). Homozygous mice showed nuclear abnormalities including discontinuities of the nuclear envelope, less lamin A in the lamina, and localization of lamin C in the cytoplasm. They found the mutant protein and mRNA to be unstable most likely due to aberrant splicing. Also, they observed abnormal differentiation of myoblasts and fibroblasts into adipocytes suggesting that a defective nuclear lamina mediates an inability to maintain terminal differentiation (Mounkes et al., 2003).

1.4.5 EDMD knock-in mouse model LMNA$^{H222P/H222P}$

The LMNA$^{H222P/H222P}$ knock-in mouse model for the EDMD laminopathy was made by Dr. Gisele Bonne's laboratory in Paris, France (Arimura et al., 2005). This mutation was found in a human family to cause autosomal dominant EDMD. The hetero- and homo-zygous p.H222P mice are undistinguishable from wild-type mice at birth and develop normally through sexual maturity. At 2-3 months of age, adult male homozygous mice develop progressive dilated cardiomyopathy with conduction defects, reduced growth rate, hunched position, stiff walking posture, and abnormal shallow breathing. Female mice show the same trend but with a later onset and slower progression starting at 4-6 months of age. At the end stage of disease, homozygous mice displayed dramatic atria/chamber dilation as well as a striking increase in fibrosis. Skeletal muscle at this stage exhibited some regenerative fibres and an increase in the numbers of atrophic fibres, hypertrophic fibres, and nuclei internalization. All homozygous male mice die by 9 months of age and homozygous females by 13 months of age. They do not show any characteristics of lipodystrophy or metabolic disorders. They exhibit normal lamin A/C and emerin localization yet display nuclear abnormalities in cardiac and skeletal muscle with convoluted membranes and irregular heterochromatin deposition in 10% of nuclei. Furthermore, there was an increase in the nuclear accumulation of Smad proteins in cardiac and skeletal muscles. Smads 2, 3, and 4 are the intracellular effectors of the transforming growth factor beta (TGF-β) signalling pathway of fibrosis. The heterozygous LMNA$^{H222P/+}$ mice show no abnormalities for the majority of their normal lifespan but have been observed to develop signs of cardiomyopathy at 24 months of age (unpublished observation by G. Bonne, Arimura et al., 2005). Muchir et al. (2007) assayed heart tissue from this mouse model for changes in global gene expression during disease development in comparison with wild-type mice. Interestingly, they found that there was an up-regulation of the mitogen-activated protein kinase (MAPK)

pathway and a group of its target genes that include c-Jun, Elk1, JunD and Elk4. Transfections of cell lines with the p.H222P and other EDMD and DCM associated mutant lamins A and C resulted in the same activation of the MAPK pathway and showed increased phosphorylation of its protein targets including ERK1/2 and JNK. Lamin A/C is also known to interact with c-Fos, another player in the MAPK pathway and thus implicates lamin A/C in MAPK signalling (Muchir et al., 2007). They also found an up-regulation of fetal cardiac genes, supporting the finding in human heart tissue on the re-expression of the fetal gene program as well as an up-regulation of genes involved in fibrosis (Muchir et al., 2007).

1.10 Laminopathy Cell Models

1.10.1 Mouse skeletal myoblasts: C2C12 cell line

The C2C12 myoblast cell line is a sub-clone originally derived from skeletal muscle of wild-type normal C3H mice by Yaffe and Saxel (1977). To isolate myogenic cells, they first injured the muscle in 2 month old mice by crushing it with forceps. They then harvested the myoblast cells from muscle preparations 3 days later. This cell line has a doubling time of 24 hours and retains the ability to proliferate as mononucleated (undifferentiated) cells. If they are cultured in horse serum or become confluent, they can rapidly differentiate into myotubes that are contractile and express many muscle-specific genes/proteins such as MyoD, myogenin, myosins and troponins (Tomczak et al., 2004; Kislinger et al., 2005). They are also easily transfected to express proteins of interest. This makes them a good model of mammalian myoblast dynamics and is validated by the hundreds of published peer-reviewed articles that have used them.

1.10.2 COS7 monkey kidney and H9c2 rat cardiomyocyte cell lines

The COS7 cell line was originally derived from African green monkey kidney cells (CV-1 cell line) and transformed by an origin-defective SV40 virus (Gluzman, 1981). They have the morphology of fibroblast cells and are easily cultured and transfected. This cell line has been used extensively in molecular biology research.

The H9c2 cell line is a subclone of a rat embryonic heart tissue clonal cell line. Yet phenotypically they exhibit many characteristics of skeletal muscle cells and upon differentiation produce multinucleated myotubes (Kimes and Brandt, 1976). This cell line has been used by many research groups as a model of mammalian cardiomyoblasts.

1.10.3 Primary mouse myoblasts

Primary mouse skeletal myoblasts were derived from C57 Black 6 $LMNA^{+/+}$, $LMNA^{+/H222P}$, and $LMNA^{H222P/H222P}$ mice that were described in chapter 1.9.3 (Arimura et al., 2005). Although there are no articles published specifically with myoblasts from this model, the homozygous mutant mice have been show to recapitulate the human disease phenotype (Arimura et al., 2005). This provides a very informative mammalian skeletal muscle cell model where mutant lamins are expressed endogenously. These myoblasts are also transfection competent.

1.11 Hypotheses

1. Lamin A/C is sumoylated by sumo1. Certain disease-associated LMNA mutations will cause altered sumoylation of lamin A/C.
2. *In vitro* expression of mutant lamin A/C will alter the localization of sumo1 and will perturb the sumoylation process.
3. *In vivo* expression of mutant lamin A/C will perturb the localization of sumo1 and will perturb the sumoylation process in a laminopathy mouse model ($LMNA^{H222P/H222P}$).

1.12 Objectives

1. A) Determine if lamin A and/or lamin C is sumoylated by sumo1 *in vitro* in C2C12 myoblasts. B) Delineate the target lysine(s) of lamin A/C at which sumoylation occurs by systematically mutating lysines to arginines that lie within sumoylation consensus sequences. C) Investigate if expressing disease-associated mutant lamin A/C results in increased or decreased sumoylation of lamin A/C in C2C12 myoblasts.
2. A) Determine if mutant lamin A and lamin C expression alters sumo1 localization in C2C12 myoblasts. B) Investigate the effect of mutant lamin A/C expression on total steady-state sumoylation levels in C2C12 myoblasts.
3. A) Determine if sumo1 localization is altered in cultured primary myoblasts from $LMNA^{H222P/H222P}$ mice. B) Investigate the effect of mutant lamin A/C expression on total steady-state sumoylation levels in the primary myoblasts. C) Determine if sumo1 localization is altered *in vivo* in skeletal muscle tissue sections from affected mice.

Chapter 2: Materials and Methods

2.1 Expression plasmid preparation

Full length lamin A, lamin C, and sumo1 cDNA was previously cloned into fluorescent expression vectors that express C-terminally fused cyan, red or yellow fluorescent proteins (pECFP-C1, pDsRed2-C1, and pEYFP-N1, respectively from Clonetech laboratories) as described in Sylvius et al., 2005. The ubc9-HA vector was a kind gift from Peter Howley as seen in Yasugi and Howley (1996). The p.L85R, p.D192G, and p.R386K point mutations were previously introduced into the lamin A and C cDNA by site-directed mutagenesis as described in

Sylvius et al., 2005 (Clonetech laboratories). The p.H222P point mutation corresponds to the cDNA A>C transversion at position 665. The p.Q353K point mutation corresponds to the cDNA C>A transversion at position 1057. These mutations were introduced into the lamin A and lamin C expression vectors using the QuikChange XL Site-Directed Mutagenesis Kit from Stratagene according to the manufacturer's protocol except for extending the transformation time to 45 seconds and using LB broth to grow and dilute the competent cells. Primers used for the p.H222P mutation included forward primer 5'-TCTCCACCAGTCGGGTCTCAGGAC GGCGCTTGGTCTCACGC-3' and reverse primer 5'-GCGTGAGACCAAGCGCCGTCCT GAGACCCGACTGGTGGAGA-3'. Primers used for the p.Q353K mutation included forward primer 5'-CCGAGATGCGGGCAAGGATGAAGCAGCAGCTGGACGAGTAC-3' and reverse primer 5'-GTACTCGTCCAGCTGCTGCTTCATCCTTGCCCGCATCTCGG-3'. Plasmid DNA was extracted from transformed clones using the Mini-Prep kit from Invitrogen and was subsequently sequenced at the mutation site to ensure introduction of appropriate point mutation. Mutation positive clones were then grown up and vector DNA extracted to make stock solutions using the Maxi-Prep kit from Invitrogen. All stock vector preparations were then subjected to sequencing of the entire coding sequence to ensure that the proper point mutation is present as well as to ensure that no other point mutations or coding sequence changes were introduced during manipulation.

2.2 Cell culture, transfection, and protein extraction

2.2.1 Immortalized cell lines

C2C12 mouse skeletal myoblasts (ATCC), H9C2 rat cardiomyoblasts (ATCC), and COS7 African green monkey kidney cells (ATCC) were cultured in 60mm tissue culture plates with Dulbecco's Modified Eagle Medium (DMEM) supplemented with 1% L-Glutamine and

20% FBS and incubated at 37°C with 5% CO_2. Selected plates also contained a glass coverslip for microscopy evaluation. Cells were grown to a visual confluency of 60-80% prior to transfection. One hour prior to transfection cells were given fresh, supplemented media. C2C12 cells were transiently transfected with Metafectene Pro (Biontex) according to manufacturer's protocol optimized to 9µg total DNA and 30µl of transfection reagent in serum-free DMEM. Cos7 and H9c2 cells were transiently transfected with Lipofectamine (Invitrogen) according to manufacturer's protocol and optimized for a 3:1 Lipofectamine to DNA ratio and 9µg total DNA. Media was changed 4-6 hours post-transfection. Glass coverslips were processed immediately prior to or during protein extraction. Coverslips were transferred to 24-well plates and washed twice with 1X PBS. Cells were fixed using 400µl of ice-cold methanol and incubated at -20°C for 5 minutes. Cells were then washed three times with 1x PBS and mounted on glass slides using aqueous mounting medium (DakoCytomation #S3023). Slides were stored in the dark at 4°C. Total protein was harvested with 100µl of RIPA buffer with protease inhibitors and nuclear protein was harvested using a nuclear protein extraction kit (Active Motif) following manufacturer's protocol 20-22 hours post-transfection. Selected protein samples were harvested in the presence of 20mmol N-Ethylmaleimide (NEM) (Invitrogen) to inhibit sumo isopeptidases.

2.2.2 Primary mouse myoblasts

All experimentation with $LMNA^{H222P/H222P}$ mice was performed in the laboratory of Gisele Bonne PhD in Paris, France (Inserm U582). Primary mouse myoblasts were harvested from $LMNA^{H222P/H222P}$ mice (Arimura et al., 2005) as described in Rosenblatt et al., 1995 by Anne Bertrand PhD. I cultured the cells in Myo-1 culture medium with 20% FBS and 1:1000 gentamicin and supplemented with 6µl of dexa and 10µl bFGF per 50ml of medium. Cells were grown in 100mm culture plates coated with Matrigel diluted 1:10 in Myo-1 complete media and

incubated at 37°C with 5% CO_2. Cells were transiently transfected using an electroporation kit (Amaxa) according to the manufacturer's protocol optimized for $5x10^5$ cells and 3μg of vector used per transfection. Cells were grown for 24hours post-transfection and harvested in a total protein extraction buffer containing 2% SDS, 250mM sucrose, 75mM urea, 1mM DTT and 50mM Tris-HCl, pH7.5 with 1:100 dilution of the protease inhibitors aprotinin, leupeptin, and sodium orthovanadate.

2.2.3 Western blotting and analysis

Western blot analysis was performed on primary mouse myoblasts, COS7 and H9c2 total protein or C2C12 nuclear protein. In France, primary mouse myoblast protein samples were resolved by size using denaturing 10% acrylamide gels run for 2 hours at 20mA and in Canada, C2C12 nuclear protein and COS7/H9c2 total protein samples were resolved using 4-20% pre-cast Tris-Glycine gels (Invitrogen) run at 180V for 1.5hours. Proteins were then transferred to a nitrocellulose membrane for 2 hours at 300mA. Membranes were blocked in 1X phosphate buffered saline with 0.5% Tween20 (PBS-T) with 5-7.5% non-fat milk powder for 30 minutes and incubated in primary antibody overnight at 4°C. Primary antibodies used were goat anti-lamin A/C, rabbit anti-SP3, mouse anti-SUMO1, mouse anti-β-Actin, (Santa Cruz Biotechnology 6215, 644, 5308, and 47778), mouse anti-GapDH (ABM G041), mouse anti-vinculin (Sigma-Aldrich 4505). The following day, membranes were washed 3 times for 5 minutes in 1X PBS-T with 7.5% non-fat milk powder then incubated with secondary antibody for 1 hour at room temperature. Secondary antibodies used were goat anti-mouse, rabbit anti-goat, and goat anti-rabbit conjugated to the horseradish peroxidase enzyme (Santa Cruz 2005, 2768, 2004). Membranes were then washed 2 times for 10 minutes and once for 5 minutes in 1X PBS-T and incubated with detection reagent for 2 minutes following manufacturer's protocol (Amersham) and subsequently exposed in the Fluorchem chemiluminescent imager (Alpha Innotech).

Western blots were analyzed using the AlphaEase program corresponding to the Alpha Imager. Selected Western blost were then stripped and re-probed with Re-Blot Plus Strong antibody stripping solution (Millipore 2504) to normalize for protein loading differences. Densitometry analyses were presented graphically as normalized means (± standard deviation) while statistical significance was calculated using a non-parametric Wilcoxon rank test.

2.3 Immunostaining and fluorescent microscopy

2.3.1 Immortalized cell lines

Transfected C2C12 cells grown on glass coverslips were transferred to a 24-well plate, washed 3 times with 1X PBS then fixed by incubation in 100% methanol for 5 minutes at -20°C. They were washed 3 times in 1X PBS and mounted on glass slides with Faramount aqueous mounting medium (DakoCytomation). Images were captured on an Olympus Fluoview FV1000 confocal microscope with a 100X 1.4 NA oil immersion objective and using the Olympus FV-10 acquisition software, version 5.0. Excitation wavelengths of the fluorescent proteins were 434nm for cyan, 558nm for red, and 514nm for yellow.

2.3.2 Primary mouse myoblasts

Untransfected and transfected primary mouse myoblasts for immunostaining and microscopy were plated on 8-well Labtek slides and processed 24 hours post-transfection. At this time, the cells were washed 3 times in 1X PBS, fixed with 100% ice-cold methanol for 5 minutes at -20°C, washed 3 times in 1X PBS, then blocked for 20 minutes in 5% BSA in PBS. The cells were incubated with 1:50 mouse anti-SUMO1 (Santa Cruz Biotechnology 6215) primary antibody overnight at 4 degrees Celcius, washed 3 times with 1X PBS, incubated with 1:200 Alexa Fluor 568 goat anti-mouse (Invitrogen A-21124) secondary antibody for 30 minutes in the dark, washed 3 times in 1X PBS, and then mounted on glass slides with Vectashield mounting

media with DAPI. Slides were stored at 4°C. Images were captured on CarlZeiss Axiophot2 or Z1 Imager fluorescent microscopes.

2.3.3 Soleus muscle tissue cross sections

Cryostat soleus muscle cross sections 6μm thick from frozen soleus muscle of C57 Black 6 mice $LMNA^{+/+}$ and $LMNA^{H222P/H222P}$ were mounted on glass slides by Valerie Decostre PhD. I fixed the soleus muscle cross sections in paraformaldehyde for 5 minutes at room temperature. Sections were then rinsed once with 1X PBS with 0.1M Glycine for 2 min and twice with 1X PBS for 5 minutes. Sections were permeabilized with ice cold methanol for 6 minutes at -20°C then washed twice with 1X PBS. Slides were immersed in 90°C preheated 0.01M citric acid (pH 6.0) and micro waved at minimum power without boiling for 5 minutes then covered and cooled at room temperature for 5-10 minutes. Slides were transferred to a dark and humid incubation tray and divided into single sections using a hydrophobic barrier pen (Vector laboratories) then washed twice with 1X PBS for 2 minutes. Sections were blocked in 5% BSA in 1X PBS for 1 hour at room temperature then washed twice with 1X PBS for 2 minutes. They were incubated with 0.05 mg/ml mouse Fab in 1X PBS for 30 minutes at room temperature and washed twice in 1X PBS for 2 minutes. Selected sections were incubated with a 1:50 diltion of mouse anti-SUMO1 (Santa Cruz Biotechnology 6215) primary antibody overnight at 4°C. The following day, slides were washed once for 2 minutes and 3 times for 10 minutes in 1X PBS then incubated with a 1:200 dilution of Alexa Fluor 568 goat anti-mouse (Invitrogen A-21124) secondary antibody for 1 hour at room temperature in the dark. Slides were washed once for 2 minutes and 3 times for 10 minutes in 1X PBS and then covered with a glass coverslip mounted with Vectashield mounting media with DAPI and stored at 4°C. Images were captured on a CarlZeiss Axiophot2 fluorescent microscope.

Chapter 3: Results

3.1 Lamin A/C is not sumoylated by sumo1

Our laboratory had previously observed a disruption of sumo1 in the COS7 cell line overexpressing p.D192G mutant lamin C. The sumo1 protein was found sequestered within mutant lamin C aggregates in a sumoylation-dependent manner (Sylvius et al., 2005 and discussed in chapter 1.4). This observation and the presence of 4 sumoylation consensus sequences in the lamin A/C protein, led to the hypothesis that lamin A/C was sumoylated by sumo1. Since it was published during the course of this research that lamin A/C is sumoylated by sumo2/3 and presumably not sumo1 in Hela cells and mouse cardiomyocytes (Zhang and Sarge, 2008), we sought to confirm that result in C2C12 cells. I further investigated if mutant lamins are sumoylated by sumo1 which could occur if an otherwise hidden modification site was revealed as protein folding or filament assembly may be disrupted by a mutation. Total protein was harvested from cells and western blotting was performed probing for endogenous and exogenous lamins A and C. Cells were transfected with lamin A and lamin C tagged with cyan fluorescent protein (pECFP-C1) and red fluorescent protein (pdsRed2), respectively. Due to the transient nature of sumoylation and the low steady-state levels of sumoylated proteins (Pichler, 2008), cells were also transfected with sumo1 tagged with yellow fluorescent protein (pEYFP-N1). N-ethylmaleimide was added to preserve sumo conjugation by inhibiting de-sumoylation enzymes (isopeptidases) during protein extraction (Sacher et al., 2005). As sumoylation is a covalent bond, modified proteins can be visualized on western blots as more slowly migrating bands that migrate roughly to the combined size of the protein of interest plus sumo1 (~11kDa).

3.1.1 Testing lamin A/C and sumo1 expression/sumoylation

To determine the optimal cell model to assess sumoylation, I tested the functionality of three cell lines (COS7, H9c2, and C2C12) for transfection efficiency and sumoylation detection (Figure 5). Protein underwent western blotting for lamin A/C (panel A), sumo1 (panel B), and the endogenous irreversibly sumoylated protein, ranGAP1 (panel C). The COS7 cells showed high transfection efficiency (~80%) and this correlated with easily detectable transfected lamins and sumo1/sumoylated proteins. Although H9c2 cells are derived from cardiomyoblasts and are the closest cell type to cardiac tissue, transfection efficiency was only ~10% and consistent detection of transfected lamins and sumoylation was difficult. The C2C12 cells showed moderate transfection efficiency (~40%) and easily detectable expressed proteins. As they are skeletal myoblasts, they more closely represent muscle tissue that is affected by myopathic laminopathies while COS7 cells are kidney cells and not as applicable to laminopathies. RanGAP1 was observed to be sumoylated by both endogenous sumo1 and exogenous sumo1-YFP in all three cell lines. Further investigations were performed in C2C12 cells.

3.1.2 Assaying sumoylation of lamin A/C in C2C12 cells

Cells were untransfected or transfected with either 1: wild-type sumo1-YFP (Figure 6 panels A and B); 2: wild-type lamin A-CFP, lamin C-Red and sumo1-YFP (Figure 6 panels A and B) or 3: wild-type and mutant lamin C-Red, wild-type sumo1-YFP, and ubc9-HA (Figure 6 panel C). The sumoylation conjugating enzyme, ubc9, was co-transfected to further promote sumoylation. Protein was assayed by Western blot for lamin A/C, however, no slower migrating bands corresponding to sumoylated lamin A or lamin C by either endogenous or exogenous sumo1 were observed (Figure 6: panel A). As a positive control of our protocol and of the sumoylation process in the C2C12 cell line, the blot was stripped and re-probed for the

endogenously expressed reversibly sumoylated protein, SP3. I observed bands for SP3 sumoylated by both endogenously and exogenously expressed sumo1 (Figure 6: panel B). The previous western blots from the COS7 and H9c2 cells confirms that the C2C12 cells result was not cell type specific as there was no detection of any bands corresponding to sumoylated lamin A or C (Figure 5).

Previously, our lab demonstrated that p.D192G mutated lamin C sequesters sumo1 inside the lamin C aggregates in a sumoylation-dependent manner (Sylvius et al., 2005). I therefore investigated whether the expression of disease-associated mutant lamin C result in sumoylation by revealing masked lamin C modification sites. I transfected lamin C, sumo1, and ubc9 tagged with pECFP-C1, pdsRed2 and hemagglutinin (HA), respectively. No bands corresponding to sumoylated lamin C were observed (Figure 6: panel C). Fellow M.Sc. student Sarah Labib performed co-immunoprecipitations of lamin A/C and sumo1 to confirm the absence of lamin A/C sumoylation (Boudreau et al., in preparation - Appendix III). As neither wild-type nor mutant lamin A/C was found to be sumoylated by sumo1, I did not mutate the possible consensus sequences and could not examine if sumoylation was significantly altered by mutations and so objectives 1B and 1C were not investigated further (Chapter 1.12).

3.2 Mutant lamin A/C alters localization of sumo1 and sumoylation

3.2.1 Expression of mutant lamin A/C results in mislocalization of sumo1

I next investigated the effect of disease-associated LMNA point mutations on the localization of sumo1 in the C2C12 myoblast cell line. C2C12 cells were transiently transfected with wild-type and mutant lamin A-CFP, lamin C-Red and sumo1-YFP expression vectors and visualized using confocal microscopy (Figure 7). Wild-type lamin A, lamin C, and sumo1 show a relatively even distribution in the nucleus. In agreement with previously published results in other cell lines, the

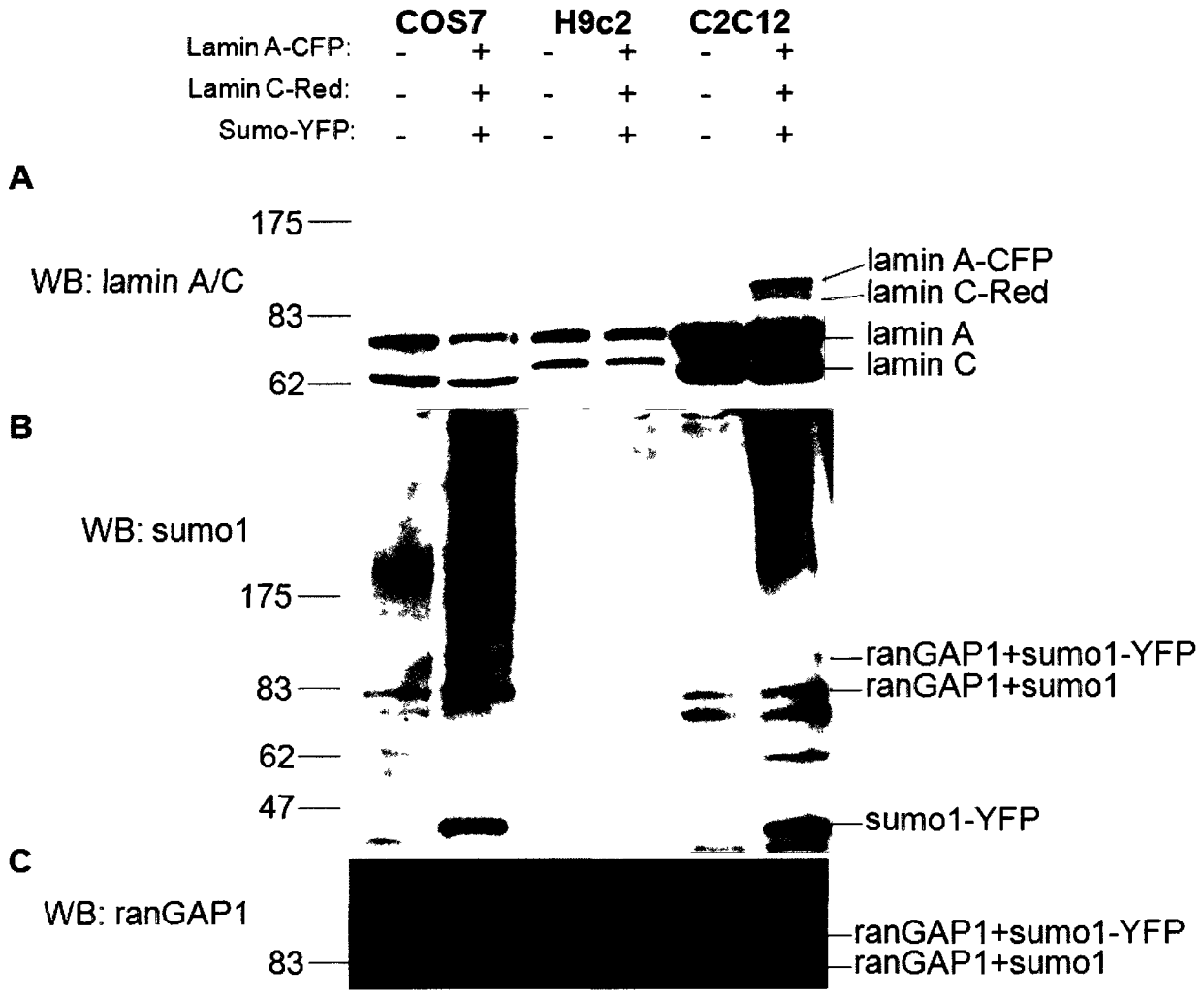

Figure 5 Optimization of fluorescent vector expression and sumoylation. Western blots of total protein from COS7 (14μg), H9c2 (5μg), and C2C12 (14μg) cells untransfected or transiently transfected with lamin A-CFP, lamin C-Red, and sumo-YFP. A) Probing for endogenous and exogenously expressed lamins A and C. B) Blot A stripped and re-probed for sumo1. C) Blot B stripped and re-probed for sumoylated protein RanGAP1.

Figure 5

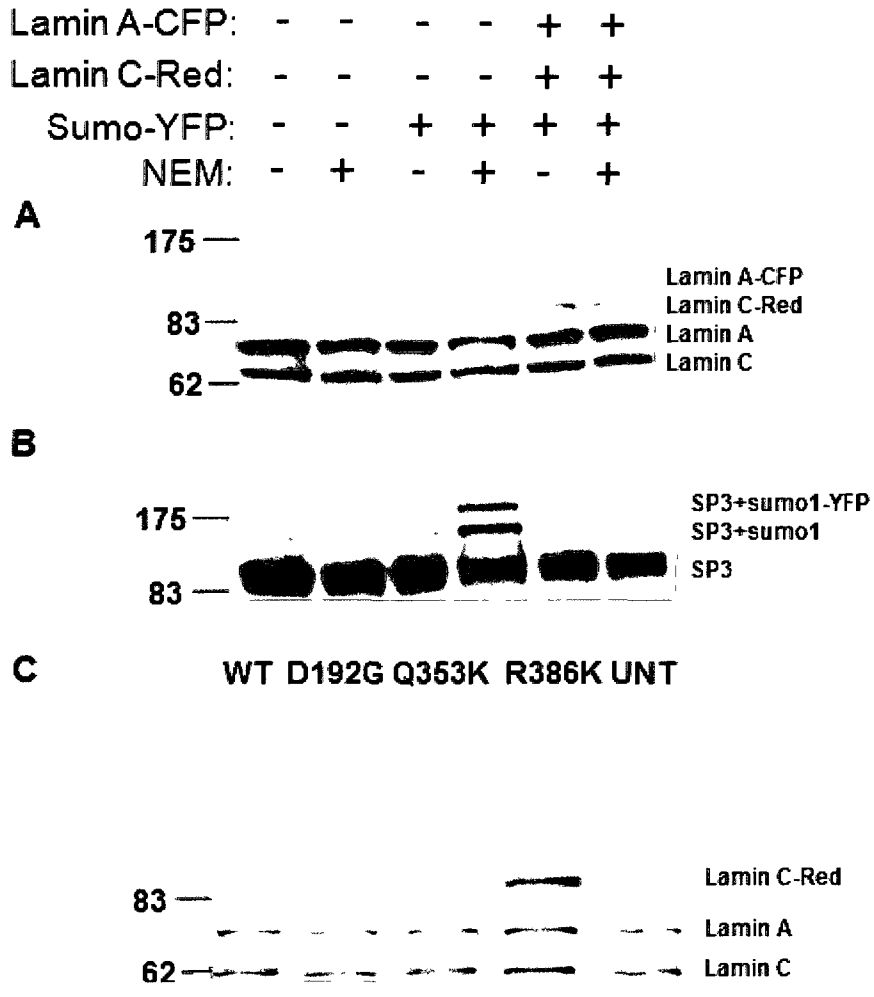

Figure 6 Lamin A/C is not sumoylated by sumo1 in C2C12 cells. Western blots of C2C12 nuclear protein: A) Untransfected (UNT) or sumo1-YFP transfected, or triple transfected wild-type lamin A-CFP, lamin C-Red and sumo1-YFP probed for lamin A/C. N-ethylmaleimide (NEM) was added to selected samples to stabilize sumo conjugation. B) Western blot A stripped and reprobed for SP3. C) UNT or triple transfected wild-type and mutant lamin C-Red, wild-type sumo1-YFP and wild-type Ubc9-HA probed for lamin A/C.

Figure 6

p.L85R mutant lamin A/C shows a comparable phenotype to the wild-type samples, and the p.D192G mutant lamin A/C results in nuclear aggregation of co-localized lamin A and C. Shown previously with only p.D192G lamin C (Sylvius et al., 2005), here it is shown that co-expression of both p.D192G lamin A and C result in aggregates that also disturb the localization of sumo1 by sequestering it within the aggregates. Here, the localization of tagged p.Q353K mutant lamin A and C *in vitro* is reported for the first time. This mutation results in variable sizes and distributions of aggregated lamins A and C within the nucleus as well as at the nuclear periphery. This mutant also sequesters sumo1 within some of the formed aggregates. As previously reported, the p.R386K mutation also results in the formation of lamin A/C aggregates and here we demonstrate the trapping of a substantial amount of the sumo1 protein. The p.H222P mutant lamin A/C retains the ability to localize to the nuclear lamina but also develops aggregates with some sumo1 sequestration. In the H222P mouse model, lamin A/C is reported to retain normal localization in both cardiac and skeletal muscle (Arimura et al., 2005).

3.2.2 Mutant lamin A/C alters cellular sumoylation

3.2.2.1 Western blotting for sumo1 and sumoylation

Even though lamins were not found to be sumoylated, expression of mutants still mediated an alteration of sumo1 intranuclear localization. This led to next investigate a correlation between the mislocalization of sumo1 and an alteration of the cellular sumoylation process with the presence of mutant lamin A/C. We harvested nuclear protein from C2C12 cells transfected with equal amounts of vectors encoding lamin A-CFP, lamin C-Red, and sumo1-YFP then performed Western blot analysis for sumo1. Interestingly, it was observed that the expression of mutant lamin A/C that trapped sumo1 in aggregates paralleled with an increase in both non-conjugated sumo1-YFP and sumo1 conjugated to other proteins (Figure 8 – top panel). The Western blot and

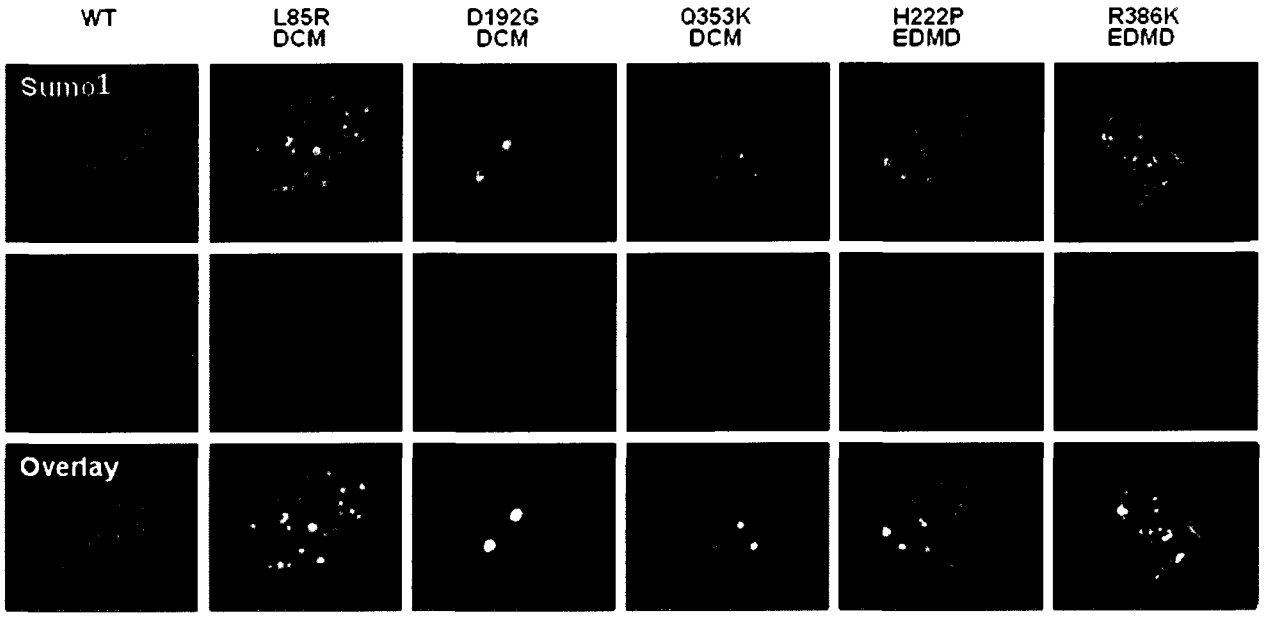

Figure 7 Sumo1 localization is disturbed by mutant lamin A/C in a mutation-dependent manner in C2C12 cells. Confocal microscopy images of nuclei of C2C12 cells expressing wild-type and mutant lamin A-CFP, lamin C-Red and wild-type sumo1-YFP. Lamin A and lamin C images are represented in one panel as they co-localize in all cells.

Figure 7

densitometry analysis in Figure 8 is representative of 7 blots each performed as independent experiments.

3.2.2.2 Densitometry analysis of western blots

Densitometry analysis was performed on the bands corresponding to all the conjugated sumo1 and also on the band of non-conjugated sumo1 tagged with YFP. Each western blot was stripped and re-probed for GapDH or β-actin to account for protein loading differences and to which all densitometry values were first normalized. As densitometry values were greatly variable between blots, the values were converted to ratios so comparisons between blots could be made. The wild-type value was set at 100% and mutant values were compared against the wild-type. Standard error on the mean (SEM) was calculated after normalization. Values are presented graphically in Figure 8 – bottom panel as mean ± SEM comparing the change of the steady-state levels of conjugated and non-conjugated sumo1 from C2C12 cells expressing mutant lamin A/C to those of the wild-type. As these calculations have not been previously shown to follow a normal distribution, I could not assume that the values would be appropriate for parametric analysis. Therefore, statistical significance was determined using a non-parametric Wilcoxon rank test with significance set at $p<0.01$.

Expression of the p.D192G mutant, which showed sequestration of sumo1 within lamin A/C aggregates, resulted in an average (SEM) significant increase of 55% (17%) with a significance of $p<0.002$ for conjugated sumo1. There was also an increase of 44% (16%) in the level of non-conjugated sumo1-YFP however this change fell below statistical significance ($p<0.025$). Expression of the p.Q353K mutation which also showed trapping the sumo1 protein within the aggregates resulted in a significant increase in sumoylated proteins of 41% (8%) $p<0.002$. There was no significant increase in non-conjugated sumo1 with an average increase of

24% (14%) and p<0.025. Expression of the p.R386K mutant that also perturbed sumo1 resulted in significant increases of 65% (23%) p<0.002 and 35% (8%) p<0.002 for conjugated and non-conjugated sumo1 levels, respectively. I found that expression of the p.L85R mutant which did not appear to significantly affect sumo1 localization, also did not significantly affect the level of either conjugated (increase of 22% (18%) p<0.25) or non-conjugated (21% (15%) p<0.055) sumo1 yet followed the same trend as the other mutants investigated.

3.3 Sumo1 localization and sumoylation are altered in LMNA$^{H222P/H222P}$ mouse model

3.3.1 Sumo1 localization is altered in LMNA$^{H222P/H222P}$ mouse myoblasts

In order to confirm my results in a more physiologically relevant model, I cultured primary skeletal myoblasts harvested from LMNA$^{+/+}$ and LMNA$^{H222P/H222P}$ mice and immunostained for sumo1 (Figure 9 - left panel WT). In LMNA$^{+/+}$ myoblasts, sumo1 shows homogenous nuclear and cytoplasmic distribution (Figure 9). In homozygous myoblasts that solely express p.H222P mutated lamin A/C, approximately 75% of cells show sumo1 localizing into nuclear foci and approximately 20% display a pronounced appearance at the nuclear envelope (Figure 9 - left panel H222P). In agreement with published results from striated muscles (Arimura et al., 2005), I found lamin A/C localization to be normal with no sumo1 sequestration (data not shown). The myoblasts were then transfected to express YFP-tagged sumo1 which resulted in exacerbation of the nuclear foci localization observed in the endogenously sumo1 expressing myoblasts to approximately 87% but abolished the nuclear envelope localization (Figure 9 - right panel). It is important to note that sumo1 localization in primary myoblasts was more variable than that observed in the C2C12 cells and that the images in Figure 9 represent the most common phenotype.

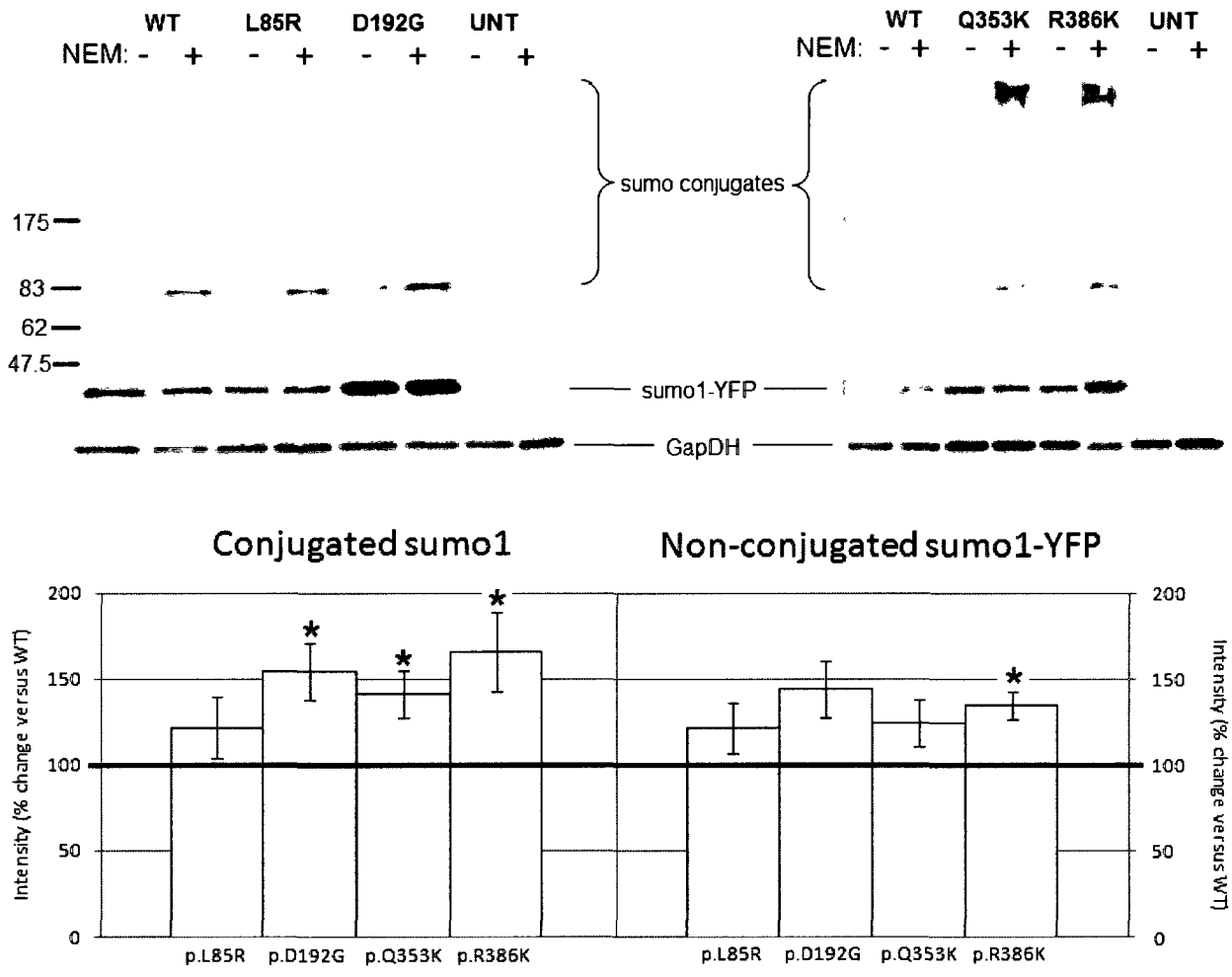

Figure 8 Expression of mutant lamin A/C results in increased levels of steady-state sumoylation and non-conjugated sumo1 in a mutation-dependent manner. Top panel: Western blot analysis of sumo1 from C2C12 nuclear protein untransfected and transfected with wild-type and mutant lamin A-CFP, lamin C-Red and sumo1-YFP harvested in the presence or absence of NEM. Bottom panels: sumo1 blots stripped and reprobed for GapDH as a loading control. Bottom panel: Densitometry performed on western blots of C2C12 nuclear protein probed for sumo1 (n=7 independent experiments). Left graph represents the collection of higher molecular weight sumo1 conjugates (encompassing bands from 85kDa to top of blot). Right graph represents non-conjugated sumo1-YFP band at 41kDa. Samples were normalized to GapDH or β-actin

housekeeping protein to account for protein loading differences. Values were subsequently converted to ratios so comparisons between blots could be made. The wild-type value was set at 100% and mutant values are changes compared against the wild-type. P-values refer to statistically significant changes versus wild-type levels where * represents a significant difference $p<0.01$ of a non-parametric Wilcoxon rank test.

Figure 8

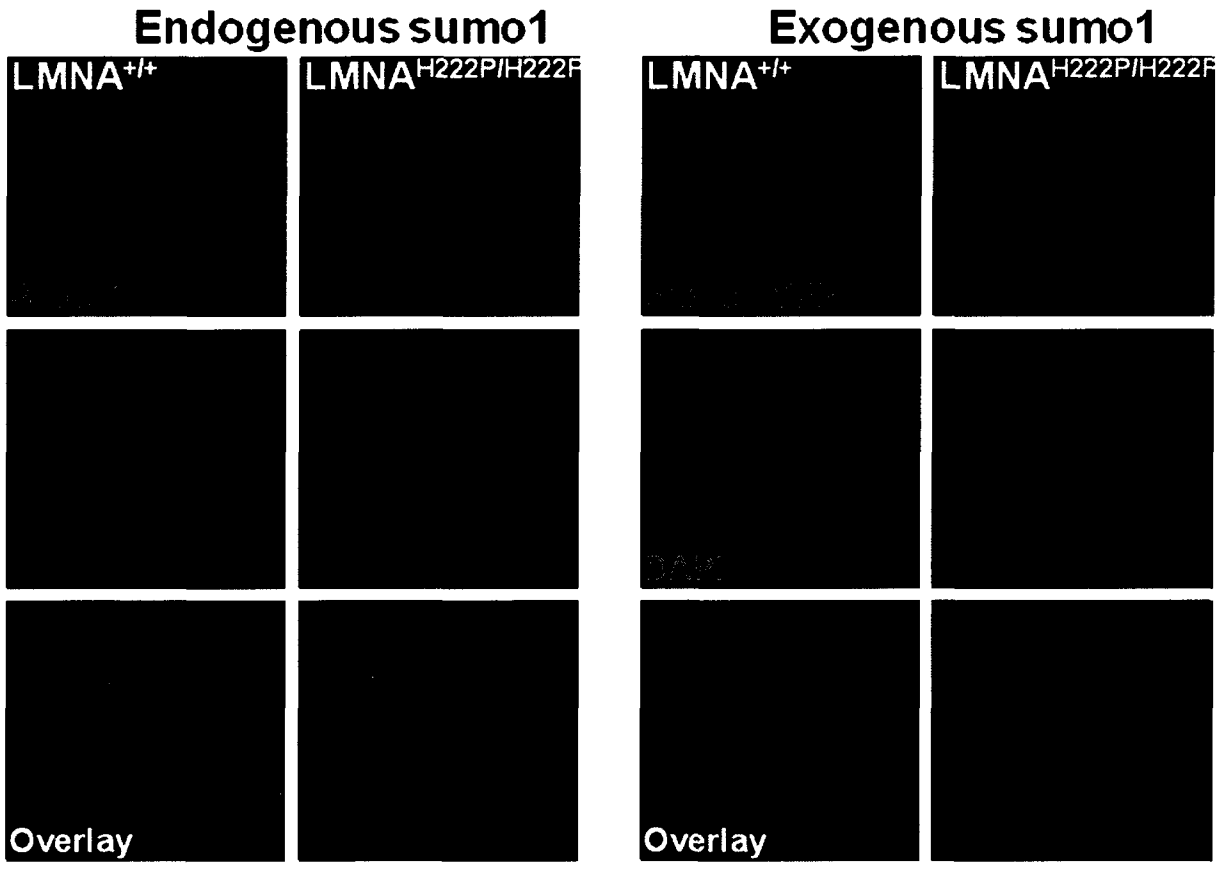

Figure 9 Endogenous and exogenous sumo1 localization is disturbed in homozygous $LMNA^{H222P/H222P}$ primary mouse myoblasts. Fluorescent microscopy images of non-transfected and sumo1-YFP transfected $LMNA^{+/+}$ (WT) and $LMNA^{H222P/H222P}$ (H222P) primary myoblast nuclei. Left panel: Untransfected myoblasts immunostained for endogenous sumo-1 (green). Right panel: Sumo1-YFP transfected myoblasts expressing YFP-tagged sumo1 (green). All myoblasts were counterstained for DAPI (blue).

Figure 9

3.3.2 Expression of endogenous p.H222P mutant lamin A/C disrupts sumoylation

To determine if the sumoylation profile is disturbed in $LMNA^{H222P/H222P}$ mice as it was determined in C2C12 cells exongenously expressing mutant lamin A/C, western blotting analysis was performed on total protein harvested from sumo1-YFP transfected $LMNA^{+/+}$, $LMNA^{+/H222P}$, and $LMNA^{H222P/H222P}$ primary myoblasts. In three western blots representing two independent experiments, I did not detect a significant change in the levels of sumo1 conjugated proteins yet I observed an increase in the amount of non-conjugated sumo1-YFP in p.H222P homozygous myoblasts (Figure 10). I also noticed an increase in sumoylation of one unknown sumo1 conjugated protein in $LMNA^{H222P/H222P}$ myoblasts (Figure 10 - asterisk). This sumoylated protein migrates to approximately 60kDa and as such indicates a sumo1-YFP (41kDa) modified protein about 10-20kDa in size.

3.3.3 Altered localization of endogenous sumo1 in $LMNA^{H222P/H222P}$ mouse muscle tissue

As endogenous sumo1 was found mislocalized in myoblasts cultured from $LMNA^{H222P/H222P}$ mice, I wanted to determine if this occurred *in vivo* in dystrophic muscle tissue. Therefore I examined its localization directly by immunostaining for sumo1 in cross-sections of soleus muscle tissue from $LMNA^{+/+}$ and symptomatic $LMNA^{H222P/H222P}$ mice (Figure 11). Soleus skeletal muscle is known to be dystrophic in this mouse model (Arimura et al., 2005). As expected, normal myocyte architecture is found in wild-type mice. Sumo1 staining in wild-type muscle tissue shows consistent punctate myocyte staining and homogenous punctate nuclear localization (Figure 11 - left panel) that is comparable to endogenous myoblast sumo1 staining (Figure 11 - left panel). Conversely, in the H222P mutant muscle tissue, I observed abnormalities in the myocyte architecture with variable fibre size, appearance of degeneration, and some internal nuclei as was previously shown (Arimura et al., 2005). Interestingly, I also observed a

prominent nuclear envelope localization of sumo1 in approximately 25% of nuclei (Figure 11 - right panel). Alternatively, the wild-type muscle showed this phenotype in approximately 3% of nuclei. The cytoplasmic localization appears conserved in this tissue. A small proportion of nuclei from both wild-type (~4%) and mutant mice (~6%) showed intranuclear aggregation of sumo1.

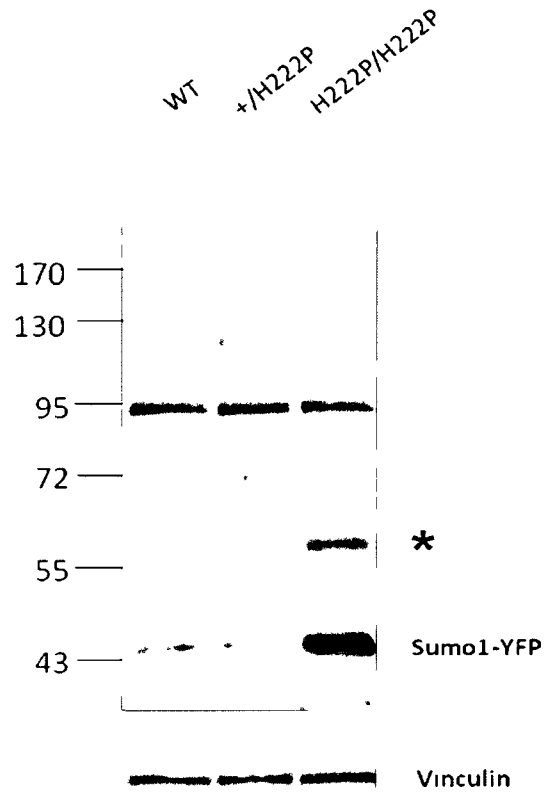

Figure 10 Increased level of non-conjugated sumo1 and an unknown substrate in homozygous $LMNA^{H222P/H222P}$ primary mouse myoblasts. Western blot analysis for sumo1 of whole cell extracts from $LMNA^{+/+}$ and $LMNA^{H222P/H222P}$ myoblasts transfected with wild-type sumo1-YFP harvested with NEM. Bottom panel: sumo1 blot reprobed for vinculin as a loading control. The asterisk (*) marks an unknown sumoylated protein whose sumoylation is increased only in the $LMNA^{H222P/H222P}$ myoblasts.

Figure 10

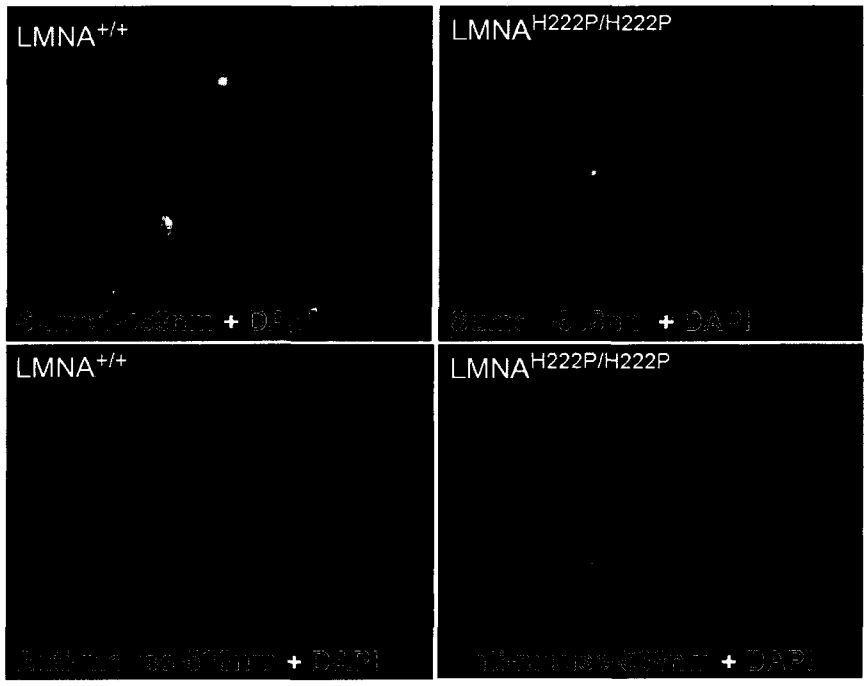

Figure 11 Sumo1 localization is disturbed in soleus muscle sections from $LMNA^{H222P/H222P}$ mice. Fluorescent microscopy images taken at 63X magnification of cross sections of soleus muscle from $LMNA^{+/+}$ and $LMNA^{H222P/H222P}$ mice. Top row sections were stained for sumo1 (green). Bottom row sections were stained with only secondary antibody to show background signal of anti-mouse-568nm antibody (green). All sections were counterstained for DAPI (blue).

Figure 11

Chapter 4: Discussion and future directions

4.1 Neither wild-type lamin A/C nor mutant lamin C is sumoylated by sumo1 in C2C12 myoblasts

After observing the sequestration of sumo1 inside mutant lamin C aggregates, I hypothesized that lamin C and/or lamin A was post-translationally modified by sumo1 and that mutations will alter its level of sumoylation and possibly its functions and interaction(s). I also hypothesized that the co-expression of p.D192G and other disease-associated mutant lamin A and C together would disrupt sumo1 localization. This would subsequently result in alteration of the sumoylation of certain cellular targets. These effects in turn may modulate the roles of lamin A/C and other proteins which could contribute to the pathophysiological development of laminopathies. The intranuclear intermediate filament proteins lamins A and C have proposed roles in numerous cell processes that range from structural support to protein scaffolding, to signalling, to gene expression as well as interact with many other nuclear lamina and intranuclear proteins. Sumoylation is a dynamic, transient and reversible modification regulates many similar cell processes (Makhnevych et al., 2009). As the functions of lamins and sumo1 vary between cell and tissue types, laminopathic mutant lamins may be exerting their tissue-specific phenotypes through perturbation of sumo1 and sumoylation.

Through the presence of 4 common sumoylation consensus sequences in the lamin A/C protein, its interaction with the sumoylation E2 conjugating enzyme, ubc9 (Zhong et al., 2005), and our observation of sumo1 sequestration in mutant lamin C aggregates, I first hypothesized that lamins A and C would be modified by sumo1. However, I did not observe sumoylation of lamin A or C by either endogenously or exogenously expressed sumo1. This outcome might be explained by the structural motifs in the lamin A/C protein and subsequent filament conformation that conceal sumo1 sumoylation sites from modification (Anckar and Sistonen,

2007) or these sites are not conducive to sumo1 attachment. Research published during this thesis supported the results we obtained and found lamin A to be sumoylated at lysine 201 by sumo2/3 and apparently not sumo1 (Zhang and Sarge, 2008). They further demonstrated that two DCM-associated lamin A/C mutations at position 203 (the glutamic acid (E) within one consensus sequence) display lower lamin A sumoylation, mislocalization of lamin A, and increased cell death. The authors suggest that the sumo2/3 modification of lamin A is important for the proper localization and functioning of the protein (Zhang and Sarge, 2008). However, lamins are structural proteins whose coiled coil regions, including coil 1B, are crucial for filament assembly and amino acid 203 lies within coil 1B (Perrot et al., 2009). Thus mutating the glutamic acid at that position to a glycine (p.E203G) or a lysine (p.E203K) would result in the change of a negatively charged hydrophilic amino acid to a nonpolar neutral or a positively charged hydrophilic residue, respectively. This may then have disastrous consequences on filament assembly/structure (Fatkin et al., 1999) and lead to the observed mislocalization of lamins into aggregates as we and many other groups have shown when expressing mutated lamins. So it does not appear conclusive that sumo2/3 regulates lamin A/C localization. Still, it is interesting to consider if sumo2/3 sumoylation of lamin A regulates its interaction with other lamina proteins that affect cell viability or as a stress compensation as sumoylation was reduced with a DCM-associated mutation (Zhang and Sarge, 2008) and is linked to stress response (Flick and Kaiser, 2009).

Although wild-type lamin C is not sumoylated by sumo1, it was shown in our previous study that DCM-associated p.D192G mutant lamin C formed intranuclear aggregates that sequestered sumo1 and that the trapping of sumo1 within the aggregates was dependent upon sumoylation competency (Sylvius et al., 2005). This led us to investigate whether this and other

mutations in lamin C would produce a misfolding of the protein that might reveal an otherwise masked sumoylation site. I did not observe any sumoylation of exogenous mutant lamin C even with the co-overexpression of the conjugating enzyme, ubc9, to further promote sumoylation. This implies that mutant lamin C was mediating a mislocalization of sumo1 through indirect mechanisms possibly by its interaction or scaffolding with other proteins that are sumoylated and not through its own increased sumoylation.

4.2 Sumo1 localization and steady-state sumoylation levels are altered in C2C12 myoblasts in a mutation-dependent manner

Despite the lack of lamin A/C sumoylation by sumo1, I demonstrated that the expression of disease-associated mutant lamin A/C results in the mislocalization and misregulation of sumoylation and/or sumo1 turnover *in vitro*. The mutations I included were located in the α-helical coiled coil rod domains and are present in both lamin A and lamin C isoforms. These domains are essential for both filament assembly and protein-protein interactions (Dechat et al., 2008). *In vitro* in C2C12 cells, I observed mislocalization of lamins from a normal veil-like phenotype in the wild-type to various sizes of intranuclear aggregates that appeared to target the nuclear envelope or nucleoplasm or both. In the cells expressing p.D192G (DCM), p.Q353K (DCM), p.H222P (EDMD), and p.R386K (EDMD) mutated lamin A/C, these aggregates were observed to trap sumo1 within them. Following this observation, in the cells expressing p.R386K (EDMD) mutant lamins, we detected a significant increase in the amount of non-conjugated transfected sumo1. This implies that the sequestration of monomeric sumo1 within aggregates may offer a means of protection from normal sumo1 degradation by SENPs and/or prevents its conjugation to target proteins possibly by excluding ubc9 or E3 ligases.

As sumo1 is mostly found conjugated to target proteins in vertebrate cells and less in monomeric form (Saitoh and Hinchey, 2000), I suggest that the trapped sumo1 may likely be not only non-conjugated sumo1 but also other proteins that are sumoylated. Supporting this hypothesis, I detected a significant increase in the steady-state levels of sumoylated nuclear proteins in the cells expressing aggregating p.D192G (DCM), p.Q353K (DCM), and p.R386K (EDMD) mutant lamin A/C that were observed to sequester sumo1. Unfortunately, I was unable to detect if the sumoylation of any single protein was particularly increased. Research by our laboratory has examined the localization of RanGAP1 which is an irreversibly sumoylated nuclear pore complex (NPC) protein found on the cytosolic side of the NE. We found that the localization of RanGAP was not affected by the expression of certain lamin A/C mutants and does not co-localize with lamin aggregates (Sylvius et al., 2008). A fellow M.Sc. student, Pallavi Gupta, investigated the localization of a sumoylated nuclear myogenic protein, GATA4, and found that it was not one of the possible proteins recruited into the lamin aggregates (Boudreau et al., in preparation). Expression of the p.L85R (DCM) mutant lamin A/C did not produce lamin aggregates and also did not have a significant effect on sumo1 localization, sumoylation, or on the level of non-conjugated sumo1 when expressed in C2C12 cells. However, it was interesting that this mutant had slightly increased non-conjugated sumo1 and sumoylation following the same trend that was observed with the other mutants which may suggest a possible non-specific response to a defective lamina.

The increased steady-state sumoylation level results suggest the mutant lamin A/C may recruit sumoylated proteins into the aggregates and conceal them from interacting with and undergoing normal regulation of de-conjugation by SENPs. Conversely, these results could also represent an independent function of mutant lamin A/C in mediating an increased level of protein

sumoylation. In fact, fellow M.Sc. student, Sarah Labib, has demonstrated that co-expression of lamin A/C with ubc9 results in co-localization of the proteins. When co-expressing p.D192G (DCM), p.Q353K (DCM), and p.R386K (EDMD) mutant lamin A/C with wild-type ubc9, the ubc9 remains co-localized with but is not trapped by the lamin A/C aggregates (Boudreau et al., in preparation). Still, it remains inconclusive whether the sequestered sumo1 is in monomeric form or conjugated to target proteins. We propose that it is likely a mutation-dependent combination of both forms as our results from nuclear protein extracts indicate variable increases in levels of both non-conjugated and conjugated sumo1. I was unable to determine if there was an increase or decrease in cytoplasmic sumo1 or sumoylated proteins due to low sumo1 detection, yet preliminary experiments showed no detectable change.

It remains uncertain whether altered sumo1 localization and increased nuclear sumoylation is an attempt at a compensatory mechanism in response to a weakened nuclear lamina or a pathological mechanism by which it, and proteins it has modified, are recruited into the mutant lamin aggregates. Reviewed in Dorval and Fraser (2007), it has been demonstrated that in several neurodegenerative disorders, sumo1 was found to target protein inclusions/aggregates. Researchers have found multiple implicated proteins to be sumoylated yet there are conflicting reports whether sumo1 and/or sumoylation have a positive or negative effect on neurodegeneration. They implicated sumoylation to have proposed roles in cell survival, aggregate deposition, and disease pathogenesis. It was also suggested that increased sumoylation may out-compete ubiquitination as both modifications target lysine residues which may then reduce mutant protein degradation and thus promote aggregate formation (Dorval and Fraser, 2007).

4.3 Sumo1 mislocalization may be mediated by lamin A/C interacting proteins

One plausible mechanism of disrupting the sumoylation process may be through the disturbance of sumoylated lamin A/C interacting proteins. Although lamin A/C itself is not sumoylated, it interacts both directly and indirectly with several sumoylated proteins, including ubc9 that may recruit sumo1. Also, other research groups have reported a co-localization/mislocalization of other nuclear proteins with lamin A/C aggregates which suggests that this sequestration effect may be, in part, a secondary effect of lamin scaffolding networks. In fact, fellow M.Sc. student Sarah Labib performed immunoprecipitation of lamins A and C that were co-expressed with sumo1 and observed four bands that did not correspond to lamin interacting partners known to be sumoylated (unpublished observations). Known sumoylated lamin interacting proteins were excluded due to molecular weight inconsistencies and lack of expression within the cell system used. Thus the identities of these protein bands remain unknown and so may represent possibly novel sumoylated lamin A/C interacting proteins. If lamins are sequestering these sumoylated targets within aggregates, then the function of these proteins may be compromised. Future work in characterizing these proteins may give insight toward laminopathy pathogenesis and may uncover previously unknown proteins whose interaction with lamin A/C is only apparent and/or enriched when sumoylated. A possible method to determine the identity of these unknown proteins would be to compare mass spectrometry profiles on the smear of sumoylated proteins between wild-type and mutant lamin A/C expressing cells. This would implicate the specific targets that may be recruited into the aggregates and thus implicate certain up- or down- regulated processes.

4.4 Mutant lamin A/C in muscle may affect myogenic targets of sumoylation

Laminopathies are known to elicit various tissue-specific effects with a wide-range of ages of disease onset. As there are hundreds of proteins known to undergo sumoylation, the consequences of sumo1 mislocalization could have disastrous consequences on the regulation of different cell processes in different tissues. Our results highlight the possible effects of mutant lamin A/C in myoblasts due to the alteration of sumo1 localization, turnover, and sumoylation in the model systems that were used in this research.

The processes of myogenesis and cardiogenesis have been linked to sumoylation. Introduced earlier yet explained in more detail here, this occurs via sumo1 modification of crucial components of these pathways as well as the importance of ubc9 in myoblast differentiation (Riquelme et al., 2006). GATA4 is a transcriptional activator of early cardiac gene expression whose nuclear localization and thus activity is enhanced by sumo-1 modification which is supported by its increased activation in the presence of ubc9 (Molkentin et al., 1994; Wang et al., 2004). Transgenic mice engineered to produce 70 or 95% less GATA4 in myocytes were viable, yet developed cardiac dilatation and heart failure (Oka et al., 2006). Serum response factor (SRF) is promoter activation factor, a GATA4 interacting partner, and critical for cardiogenesis. SRF also undergoes sumoylation which increases its activation ability (Wang, 2009). Furthermore, transgenic mice expressing a less functional mutant SRF developed DCM and died of premature death (Zhang et al., 2001). As a coactivator of SRF and interactor with GATA4, myocardin is another cardiac gene expression modulator known to be activated by sumoylation (Wang et al., 2007). The myocyte enhancing factor family (Mef2s) are transcription factors involved in early myogenic and cardiogenic gene expression programs. Unlike the above mentioned sumo1 substrates, the sumoylation of Mef2s negatively regulates their transcriptional activation (Zhao et al., 2005). If one or more of these sumoylated proteins were recruited into

lamin A/C aggregates or if their sumoylation was altered, this could be a contributing factor for the development of DCM with certain laminopathic mutations. The manuscript (Boudreau et al., in preparation) includes the investigation by Pallavi Gupta of whether mutant lamin A/C mediated a mislocalization of GATA4 and thus altered the expression of a GATA4 target gene, troponin C. An alteration of the intranuclear localization of GATA4 was not observed. There was a trend towards decreased expression of troponin C; however this change was not statistically significant. These results suggest that mutant lamin A/C may then be eliciting its effects via other myogenic factors. It would be interesting to pursue future work to investigate the localization and target gene expression of the other aforementioned sumoylated myogenic factors.

4.5 Increased sumoylation may be a stress response

The first group to demonstrate a similar increase in total sumoylation as I have shown was for cytoprotection and tolerance to *in vitro* ischemia (Lee et al., 2007; Ja Lee et al., 2009). Sumoylation of transcription factors often results in the repression of gene expression, thus a global increase in sumoylation in response to stress could be a mechanism of shutting down gene expression (Lee et al., 2007; Girdwood et al., 2004). This finding may be extrapolated to my results suggesting that an increase in the amount of sumoylated proteins in C2C12 cells expressing mutant lamin A/C may be an effect of damage to the myoblasts caused by a fragile nucleus or a defective nuclear lamina. Logically, the pool of non-conjugated sumo should be diminished as a result of an increased steady-state of sumoylation yet this was not the case for the p.R386K (EDMD) lamin A/C mutant. Together with the increase in both non-conjugated sumo1 and total sumoylation, this suggests that there could possibly be an overly active function of sumo1 to cause repression of gene transcription. It would be informative to examine this

phenomenon through expression microarrays which could also reveal whether the repression is pathway-specific.

4.6 Sumo1 localization altered in skeletal muscle and myoblasts of the LMNA$^{H222P/H222P}$ laminopathy mouse model

In vitro, in primary myoblasts from LMNA$^{H222P/H222P}$ mice expressing endogenous sumo1, I observed an alteration of sumo1 localization into nuclear aggregates and to the NE. In myoblasts expressing transfected sumo1, the aggregation phenotype was exacerbated however the NE localization was not observed. This has revealed possible implications for the other mutations investigated in that overexpression of sumo1 may override its localization to the NE. Still, these observations recapitulated the results from exogenous p.H222P lamin A/C and sumo1 expression in C2C12 cells. I also observed an increase in the level of transfected non-conjugated sumo1. *In vivo*, I observed that sumo1 was mislocalized and concentrated at the nuclear envelope in approximately 25% of myocytes in LMNA$^{H222P/H222P}$ skeletal muscle tissue yet there was no detectable difference in the formation of nuclear sumo1 aggregates between wild-type and mutant myocytes. As previously reported, lamin A/C localization was normal in the LMNA$^{H222P/H222P}$ mice although the primary myoblasts showed somewhat convoluted nuclear membranes and small localization discontinuities.

4.7 Mutant lamin A/C may be detrimental to nuclear pores and nuclear bodies

Interestingly, certain sumoylation-desumoylation enzymes localize to the nuclear pore complexes (NPCs) (Palancade and Doye, 2008) and the proper assembly and positioning of NPCs is dependent on lamin A/C (Furukawa, 2009). In fact, ubc9, which is critical for conjugation of sumo1 to targets, is found both in the nucleus and at NPCs (Palancade and Doye,

2008) and moreover, we have observed that ubc9 co-localizes with both wild-type and mutant lamin A/C (Boudreau et al., in preparation). SENP1 and SENP2 are sumo-specific proteases that de-sumoylate modified proteins and are found in the nucleus and at the nucleoplasmic face of the NPCs, respectively (Hang and Dasso, 2002; Zhang et al., 2002). Also, RanBP2, a protein with sumoylation E3 ligase function localizes to the cytosolic filaments of the NPCs (Mahajan et al., 1997). Altered localization and exclusion of NPCs from nuclear blebs has been demonstrated in patient fibroblasts expressing lipodystrophy-associated mutant lamins (Vigouroux et al., 2001). Fibroblasts from $LMNA^{-/-}$ mice showed exclusion of NPCs from blebs and also some NPC clustering (Sullivan et al., 1999). NPC clustering has also been reported directly in cardiomyocyte nuclei from laminopathy DCM patients (Verga et al., 2003) and this clustering was absent from DCM patients without lamin mutations (Arbustini et al., 2002). Taken together, mutant lamins may not be supporting proper nuclear envelope architecture and could be detrimental to the assembly or function of the NPCs. As p.H222P mutant lamin A/C retains its localization to the NE and we observed sumo1 to be more concentrated there, mutant lamins may be disrupting the location or protein-protein interactions of the enzymes involved in the sumoylation cascade. Future work could investigate the localization of these proteins in the presence of mutant lamins.

Nuclear PML bodies are known to increase in size and number during cellular stress and act as storage sites for repressed transcription factors and mutant proteins (Bernardi and Pandolfi, 2007). The PML protein is sumoylated by sumo1 and also phosphorylated by ERK1/2 of the MAPK pathway. Furthermore, it was shown that ubc9 is required for the proper formation of PML bodies (Bernardi and Pandolfi, 2007). This implicates sumoylation and PML in MAPK signalling which was shown to be upregulated in p.H222P mice and thus could possibly

represent one of the links to the cellular targets which are disrupted by mutant lamin A/C (Muchir et al., 2007). Moreover, as PML bodies are one of the main sites of active sumoylation and they were shown to colocalize with protein aggregates (Bernardi and Pandolfi, 2007), it would very intriguing to determine if PML bodies are increased in size/number or co-localize with the lamin A/C and sumo1 aggregates.

4.8 Altered sumo1 in $LMNA^{H222P/H222P}$ mice may be linked to fibrosis

Although an increase of overall sumoylation in primary $LMNA^{H222P/H222P}$ mutant myoblasts expressing tagged sumo1 was not detected, I observed an increase in the level of non-conjugated transfected sumo1. Previous research in cardiac and skeletal muscles of the homozygous p.H222P mouse demonstrated an increase in the nuclear accumulation of Smad proteins, which are potent effectors of the $TGF\beta_1$ signalling cascade resulting in fibrosis and alteration of cardiac gene expression (Arimura et al., 2005; Rosenkranz, 2004). Both the TGFβ receptor type I (TβRI) which activates the Smad proteins as well as Smad4 itself are sumoylated (Lin et al., 2003; Kang et al., 2008). TβRI is sumoylated in response to TGFβ and activates the phosphorylation of Smad3, signalling translocation into the nucleus and thus amplifying the TGFβ signal by modulating gene expression (Kang et al., 2008). With regards to Smad4, there are conflicting reports as to the effect of sumoylation. Certain groups report that overexpression of sumo1 or ubc9 result in increased smad4 stability and transcriptional responses to TGFβ signalling (Lin et al., 2003; Lin et al., 2003; Ohshima and Shimotohno, 2003; Liang et al, 2004; Shimada et al., 2008). Others maintain that sumoylation of Smad4 inhibits TGFβ response while overexpressing a sumo1 protease potently increases the inhibition (Long et al., 2004). It would be intriguing to investigate whether there is a correlation between the nuclear accumulation of

Smad4 and an alteration of its sumoylation status in $LMNA^{H222P/H222P}$ mice as well as in laminopathy patients with cardiac or skeletal muscle fibrosis.

4.9 Sumoylation of one unknown substrate is altered in laminopathic myoblasts

Interestingly, one unknown sumoylated substrate protein displayed an increase in sumoylation only in homozygous p.H222P myoblasts transfected with sumo1 and not in wild-type myoblasts. This band would correspond to a small sumoylated protein with an estimated molecular weight in the range of 10-20kDa. Determining the identity of this protein would be beneficial as misregulation of sumoylation in myoblasts expressing mutated lamin A/C prior to muscle differentiation in a mouse model would give insight into early disease pathogenesis. Further research should investigate whether this protein is the Histone H4 protein, a sumoylated lamin A/C binding partner and has a molecular weight of ~11kDa. Through sumoylation, H4 recruits histone deaceytlase complexes (HDACs) or blocks acetylation at the target lysine to mediate transcriptional repression (Shiio and Eisenman, 2003; Nathan et al., 2006) and thus may be responding to stress due to a defective nuclear lamina as discussed above. Identification could be achieved through co-immunoprecipitation of wild-type and p.H222P mutant lamin A/C then probing for H4 and sumo1 or through mass spectrometry of the unknown band.

4.10 Significance of research

Overall, from the results I have observed throughout this research, I propose that the expression of myopathic disease-linked mutant lamin A/C results in an alteration of the dynamics of sumo1 *in vitro* and *in vivo*. *In vitro* I have shown aberrant localization of sumo1 into nuclear aggregates of DCM- and EDMD-associated mutant lamin A/C. There was consequently an up-regulation of the sumoylation process that I suggest to be caused by interplay between an

increased steady state level of sumoylation, deficient sumo1 deconjugation and/or deficient degradation of the sumo1 protein. In primary myoblasts I have also shown an altered localization of sumo1 into nuclear aggregates and an increase in sumoylation of an unknown protein. *In vivo* in affected laminopathic mouse muscle tissue, I found sumo1 to be more concentrated at the nuclear envelope where mutant lamin A/C and multiple sumoylation enzymes are also targeted. Sumoylation is a highly conserved, very dynamic, and tightly regulated cellular process with numerous targets in cardiac and skeletal muscle. Lamins A and C are also highly conserved with roles in many cell processes, they interact with sumoylated proteins, and their functions coincide with some sumo1-regulated processes. Thus, laminopathic lamin A/C-mediated misregulation of sumoylation could account, in part, for the tissue-specific effects observed in laminopathies especially those involving striated muscles as I have shown. Determining the identities of the precise targets involved would give great insight into tissue specificity, disease pathogenesis, and possibly uncover novel targets for molecular therapies.

References

Anckar J, Sistonen L. SUMO: getting it on. Biochem Soc Trans 2007;35:1409-1413. [PubMed: 18031233]

Arbustini E, Pilotto A, Repetto A, Grasso M, Negri A, Diegoli M, Campana C, Scelsi L, Baldini E, Gavazzi A, Tavazzi L. Autosomal Dominant Dilated Cardiomyopathy with atrioventricular block: a lamin A/C defect-related disease. J Am Coll Cardiol 2002;39:981-990. [PubMed: 11897440]

Arimura T, Helbling-Leclerc A, Massart C, Varnous S, Niel F, Lacène E, Fromes Y, Toussaint M, Mura AM, Keller DI, Amthor H, Isnard R, Malissen M, Schwartz K, Bonne G. Mouse model carrying H222P-Lmna mutation develops muscular dystrophy and dilated cardiomyopathy similar to human striated muscle laminopathies. Hum Mol Genet 2005;14:155-169. [PubMed: 15548545]

Asakura M, Kitakaze MD. Global gene expression profiling in the failing myocardium. Circ J 2009;73:1568-1576. [PubMed: 19638707]

Barton PJ, Felkin LE, Koban MU, Cullen ME, Brand NJ, Dhoot GK. The slow muscle troponin T gene is expressed in developing and diseased human heart. Mol Cell Biochem 2004;263:91-97. [PubMed: 15524170]

Bernardi R, Pandolfi PP. Structure, dynamics and functions of promyelocytic leukaemia nuclear bodies. Nat Rev Mol Cell Biol 2007;8:1006-1016. [PubMed: 17928811]

Bonne G, Di Barletta MR, Varnous S, Becane HM, Hammouda EH, Merlini L, Muntoni F, Greenberg CR, Gary F, Urtizberea JA, Duboc D, Fardeau M, Toniolo D, Schwartz K. Nat Genet 1999;21:285-288. [PubMed: 10080180]

Bonne G, Mercuri E, Muchir A, Urtizberea A, Becane HM, Recan D, Merlini L, Wehnert M, Boor R, Reuner U, Vorgerd M, Wicklein EM, Eymard B, Duboc D, Penisson-Besnier I, Cuisset JM, Ferrer X, Desguerre I, Lacombe D, Bushby K, Pollitt C, Toniolo D, Fardeau M, Schwartz K, Muntoni F. Clinical and molecular genetic spectrum of autosomal dominant Emery-Dreifuss muscular dystrophy due to mutations of the lamin A/C gene. Ann Neurol 2000;48:170-180. [PubMed: 10939567]

Bridger JM, Kill IR, O'Farrell M, Hutchison CJ. Internal lamin structures within G1 nuclei of human dermal fibroblasts. J Cell Sci 1993;104:297-306. [PubMed: 8505362]

Capanni C, Cenni V, Mattioli E, Sabatelli P, Ognibene A, Columbaro M, Parnaik VK, Wehnert V, Maraldi NM, Squarzoni S, Lattanzi G. Failure of lamin A/C to functionally assemble in R482L mutant familial partial lipodystrophy fibroblasts: altered in intermolecular interaction with emerin implications for gene transcription. Exp Cell Res 2003;291:122-134. [PubMed: 14597414]

Capanni C, Mattioli E, Columbaro M, Lucarelli E, Parnavik VK, Novelli G, Wehnert M, Cenni V, Maraldi NM, Squarzoni S, Lattanzi G. Altered pre-lamin A processing is a common mechanism leading to lipodystrophy. Hum Mol Genet 2005;14:1489-1502. [PubMed: 1584304]

Cutler DA, Sullivan T, Marcus-Samuels B, Stewart CL, Reitman ML. Characterization of adiposity and metabolism in Lmna-deficient mice. Biochem Biophys Res Commun 2002;291:522-527. [PubMed: 11855819]

Dec GW, Fuster V. Idiopathic dilated cardiomyopathy. N Engl J Med 1994;331:1564-1575. [PubMed: 7969328]

Dechat T, Pfleghaar K, Sengupta K, Shimi T, Shumaker DK, Solimando K, Goldman RD. Nuclear lamins: major factors in the structural organization and function of the nucleus and chromatin. Genes Dev 2008;22:832-853. [PubMed: 18381888]

Dechat T, Adam SA, Goldman RD. Nuclear lamins and chromatin: when structure meets function. Adv Enzyme Regul 2009;49;157-166. [PubMed 19154754]

Dellaire G, Bazett-Jones DP. PML nuclear bodies: dynamic sensors of DNA damage and cellular stress. Bioessays 2004;26:963-977. [PubMed: 15351967]

Dino Rockel T, von Mikecz A. Proteasome-dependent processing of nuclear proteins is correlated with their subnuclear localization. J Struct Biol 2002;140:189-199. [PubMed: 12490167]

Dorval V, Fraser PE. SUMO on the road to neurodegeneration. Biochim Biophys Acta 2007;1773:694-706. [PubMed: 17475350]

Dreuillet C, Tillit J, Kress M, Ernoult-Lange M. In vivo and in vitro interaction of human transcription factor MOK2 and nuclear lamin A/C. Nucleic Acids Res 2002;30:4634-4642. [PubMed: 12409453]

Dreuillet C, Harper M, Tillit J, Kress M, Ernoult-Lange M. Mislocalization of human transcription factor MOK2 in the presence of pathogenic mutations of lamin A/C. Biol Cell 2008;100:51-61. [PubMed: 17760566]

Emery AE. Emery-Dreifuss muscular dystrophy – a 40 year retrospective. Neuromuscul Disord 2000;10:228-232. [PubMed: 10838246]

Fatkin D, MacRae C, Sasaki T, Wolff MR, Porcu M, Frenneaux M, Atherton J, Vidaillet HJ Jr, Spudich S, De Girolami U, Seidman JG, Seidman C, Muntoni F, Müehle G, Johnson W, McDonough B. Missense mutations in the rod domain of the lamin A/C gene as causes of dialated cardiomyopathy and conduction-system disease. N Engl J Med 1999;341:1715-1724. [PubMed: 10580070]

Favreau C, E Dubosclard, Ostlund C, Vigoureux C, Capeau J, Wehnert W, Higuet D, Worman HJ, Courvalin JC, Buendita B. Expression of lamin A mutated in the carboxyl-terminal tail generates an aberrant nuclear phenotype similar to that observed in cells from patients with Dunnigan-type partial-lipodystrophy and Emery-Dreifuss muscular dystrophy. Exp Cell Res 2003;282:14-23. [PubMed: 12490190]

Favreau C, Higuet D, Courvalin JC, Buendia B. Expression of a mutant lamin A that causes Emery-Dreifuss muscular dystrophy inhibits in vitro differentiation of C2C12 myoblasts. Mol Cell Biol 2004;24:1481-1492. [PubMed: 14749366]

Fidzianska A, Bilinska ZT, Tesson F, Wagner T, Walski M, Grzybowski J, Ruzyllo W, Hausmanowa-Petrusewicz I. Obliteration of cardiomyocyte nuclear architecture in a patient with LMNA gene mutation. J Neurol Sci 2008;271:91-96. [PubMed: 18502446]

Flick K, Kaiser P. Proteomic revelation: SUMO changes partners when the heat is on. Sci Signal 2009;2:pe45. [PubMed: 19638612]

Frock RL, Kudlow BA, Evans AM, Jameson SA, Hauscka SD, Kennedy BK. Lamin A/C and emerin are critical for skeletal muscle satellite cell differentiation. Genes Dev 2006;20:486-500. [PubMed: 16481476]

Fu L, Gao YS, Tousson A, Shah A, Chen TL, Vertel BM, Sztul E. Nuclear aggresomes form by fusion of PML-associated aggregates. Mol Cell Biol 2005;16:4905-4917. [PubMed: 16055507]

Furukawa K, Inagaki H, Hotta Y. Identification and cloning of an mRNA coding for a germ cell-specific A-type lamin in mice. Exp Cell Res 1994;212:4266-430. [PubMed: 8187835]

Furukawa K, Ishida K, Tsunoyama TA, Toda S, Osoda S, Horigome T, Fisher PA, Sugiyama S. A-type and B-type lamins initiate layer assembly at distinct areas of the nuclear envelope in living cells. Exp Cell Res 2009;315:1181-1189. [PubMed: 19210986]

Geiss-Friedlander R, Melchior F. Concepts in sumoylation: a decade on. Nat Rev Mol Cell Biol 2007;8:947-956. [PubMed: 18000527]

Gerace L, Comeau C, Benson M. Organization and modulation of nuclear lamina structure. J Cell Sci Suppl 1984;1:137-160. [PubMed: 6597817]

Gerdes AM, Capasso JM. Structural remodeling and mechanical dysfunction of cardiac myocytes in heart failure. J Mol Cell Cardiol 1995;27:849-856. [PubMed: 7602601]

Girdwood DW, Tatham MH, Hay RT. SUMO and transcriptional regulation. Semin Cell Dev Biol 2004;15:201-210. [PubMed: 15209380]

Gluzman Y. SV40-transformed simian cells support the replication of early SV40 mutants. Cell 1981;23:175-182. [PubMed: 6260373]

Goldberg M, Harel A, Brandeis M, Rechsteiner T, Richmond TJ, Weiss AM, Gruenbaum Y. The tail domain of lamin Dm0 binds histones H2A and H2B 1999;96:2852-2857. [PubMed: 10077600]

Goldberg MW, Fiserova J, Huttenlauch I, Stick R. A new model for nuclear lamina organization. Biochem Soc Trans 2008;36:1339-1343. [PubMed: 19021552]

Gonzalez-Suarez I, Redwood AB, Perkins SM, Vermolen B, Lichtensztejin D, Grotsky DA, Morgado-Palacin L, Gapud EJ, Sleckman BP, Sullivan T, Sage J, Stewart CL, Mai S, Gonzalo S. Novel roles for A-type lamns in telomere biology and the DNA damage response pathway. EMBO J 2009;28:2414-2427. [PubMed: 19629036]

Gupta P, Bilinska ZT, Sylvius N, Boudreau E, Veinot JP, Labib S, Bolongo PM, Hamza A, Jackson T, Ploski R, Walski M, Grzybowski J, Walczak E, Grzegorz R, Fidzianska A, Tesson F. Genetic and ultrastructural studies in dilated cardiomyopathy patients: a large deletion in the lamin A/C gene is associated with cardiomyocyte nuclear envelope disruption. Basic Res Cardiol 2010;105:365-377. [PubMed: 20127487]

Haas M, Jost E. Functional analysis of phosphorylation sites in human lamin A controlling lamin disassembly, nuclear transport, and assembly. Eur J Cell Biol 1993;62:237-247. [PubMed: 7925482]

Hammer E, Heilbronn R, Weger S. The E3 ligase Topors induces the accumulation of polysumoylated forms of DNA topisomerase I in vitro and in vivo. FEBS Lett 2007;581:5418-5424. [PubMed: 17976381]

Hang J, Dasso M. Association of the human SUMO-1 protease SENP2 with the nuclear pore. J Biol Chem 2002;277:19961-19966. [PubMed: 11896061]

Heald R, McKeon F. Mutations of phosphorylation sites in lamin A that prevent nuclear lamina disassembly in mitosis. Cell 1990;61:579-589. [PubMed: 2344612]

Heun P. SUMOrganization of the nucleus. Curr Opin Cell Biol 2007;19:350-355. [PubMed: 17467254]

Holt I, Ostlund C, Stewart CL, Man N, Worman HJ, Morris GE. Effect of pathogenic mis-sense mutations in lamin A on its interaction with emerin in vivo. J Cell Sci 2003;116:3027-3025. [PubMed: 12783988]

Holtz D, Tanaka RA, Hartwig J, McKeon F. The CaaX motif of lamin A functions in conjunction with the nuclear localization signal to target assembly to the nuclear envelope. Cell 1989;59:969-977. [PubMed: 2557160]

Hozak P, Sasseville MJ, Raymond Y, Cook PR. Lamin proteins form an internal nucleoskeleton as well as a peripheral lamina in human cells. J Cell Sci 1995;106:635-644. [PubMed: 7769007]

Hubner S, Eam JE, Hubner A, Jans DA. Laminopathy-inducing lamin A mutants can induce redistribution of lamin binding proteins into nuclear aggregates. Exp Cell Res 2006;312:171-183. [PubMed: 16289535]

Hutchison CJ. Lamins: building blocks or regulators of gene expression? Nat Rev Mol Cell Biol 2002;3:848-858. [PubMed: 12415302]

Hwang JJ, Allen PD, Tseng GC, Lam CW, Fananapazir L, Dzau VJ, Liew CC. Microarray gene expression profiles in dilated and hypertrophic cardiomyopathic end-stage heart failure. Physiol Genomics 2002;10:31-44. [PubMed: 12118103]

Ivorra C, Kubicek M, Gonzalez JM, Sanz-Gonzalez SM, Alvarez-Barrientos A, O'Connor JE, Burke B, Andres V. A mechanism of AP-1 suppression through interaction of c-Fos with lamin A/C. Genes Dev 2006;20:307-20. [PubMed: 16452503]

Ja Lee Y, Castri P, Bembry J, Maric D, Auh S, Hallenbeck JM. SUMOylation participates in induction of ischemic tolerance. J Neurochem 2009;109:257-267. [PubMed: 19200349]

Johnson ES. Protein modification by SUMO. Annu Rev Biochem 2004;73:355-382. [PubMed: 15189146]

Joseph J, Tan SH, Karpova TS, McNally JG, Dasso M. SUMO-1 targets RanGAP1 to kinetochores and mitotic spindles. J Cell Biol 2002;156:595-602. [PubMed: 11854305]

Kang JS, Saunier EF, Akhurst RJ, Derynck R. The type I TGF-beta receptor is covalently modified and regulated by sumoylation. Nat Cell Biol 2008;10:654-664. [PubMed: 18469808]

Karkkainen S, Peuhkurinen K. Genetics of dilated cardiomyopathy. Ann Med 2007;39:91-107. [PubMed: 17453673]

Kimes BW, Brandt BL. Properties of a clonal muscle cell line from rat heart. Exp Cell Res 1976;98:367-381. [PubMed: 943302]

Kirsh O, Seeler JS, Pichler A, Gast A, Muller S, Miska E, Mathieu M, Harel-Bellan A, Kouzarides T, Melchior F, Dejean A. The SUMO E3 ligase RanBP2 promotes modification of the HDAC4 deacetylase. EMBO J 2002;21:2682-2691. [PubMed: 12032081]

Kislinger T, Gramolini AO, Pan Y, Rahman K, MacLennan DH, Emili A. Proteome dynamics during C2C12 myoblast differentiation. Mol Cell Proteomics 2005;4:887-901. [PubMed: 15824125]

Kuehn MR. Mouse Ubc9 knock-out: many path(way)s to ruin. Dev Cell 2005;9:727-728. [PubMed: 16326385]

Kumar PP, Bischof O, Purbey PK, Notani D, Urlaub H, Dejean A, Galande S. Functional interaction between PML and SATB1 regulates chromatin-loop architecture and transcription of the MHC class I locus. Nat Cell Biol 2007;9:45-56. [PubMed: 17173041]

Kuwahara K, Saito Y, Takano M, Arai Y, Yasuno S, Nakagawa Y, Takahashi N, Adachi Y, Takemura G, Horie M, Miyamoto Y, Morisaki T, Kuratomi S, Noma A, Fujiwara H,

Yoshimasa Y, Kinoshita H, Kawakami R, Kishimoto I, Nakanishi M, Usami S, Saito Y, Harada M, Nakao K. NSRF regulates the fetal cardiac gene program and maintains normal cardiac structure and function. EMBO J 2003;22:6310-6321. [PubMed: 14633990]

Lammerding J, Schulze PC, Takahashi T, Kozlov S, Sullivan T, Kamm RD, Stewart CL, Lee RT. Lamin A/C deficiency causes defective nuclear mechanics and mechanotransduction. J Clin Invest 2004;113:370-378. [PubMed: 14755334]

Lammerding J, Fong LG, Ji JY, Reue K, Stewart CL, Young SG, Lee RT. Lamins A and C but not lamin B1 regulate nuclear mechanics. J Biol Chem 2006;281:25768-25780. [PubMed: 16825190]

Lee YJ, Miyake S, Wakita H, McMullen DC, Azuma Y, Auh S, Hallenbeck JM. Protein SUMOylation is massively increased in hibernation torpor and is critical for the cytoprotection provided by ischemic preconditioning and hypothermia in SHSY5Y cells. J Cereb Blood Flow Metab 2007;27:950-962. [PubMed: 16955077]

Lee DC, Welton KL, Smith ED, Kennedy BK. A-type lamins act as transcriptional repressors when targeted to promoters. Exp Cell Res 2009;315:996-1007. [PubMed: 19272320]

Liang M, Melchior F, Feng XH, Lin X. Regulation of Smad4 sumoylation and transforming growth factor-beta signalling by protein inhibitor of activated STAT1. J Biol Chem 2004;279:22857-22865. [PubMed: 15028714]

Lin X, Liang M, Liang YY, Brunicardi FC, Feng XH. SUMO-1/Ubc9 promotes nuclear accumulation and metabolic stability of tumour suppressor Smad4. J Biol Chem 2003;278:31043-31048. [PubMed: 12813045]

Lin X, Liang M, Liang YY, Brunicardi FC, Melchior F, Feng XH. Activation of transforming growth factor-beta signalling by SUMO-1 modification of tumor suppressor Smad4/DPC4. J Biol Chem 2003;278:18714-18719. [PubMed: 12621041]

Liu B, Wang, J, Chan KM, Tija WM, Deng W, Guan X, Huang JD, Li KM, Chau PY, Chen DJ, Pei D, Pendas AM, Cadinanos J, Lopez-Otin C, Tse HF, Hutchison C, Chen J, Cheah KS, Tryggvason K, Zhou Z. Genomic instability in laminopathy-based premature aging. Nat Med 2005;11:780-785. [PubMed: 15980864]

Lloyd DJ, Trembath RC, Shackleton S. A novel interaction between lamin A and SREBP1: implications for partial lipodystrophy and other laminopathies. Hum Mol Genet 2002;11:769-777. [PubMed: 11929849]

Long J, Wang, He D, Liu F. Repression of Smad4 transcriptional activity by SUMO modification. Biochem J 2004;379:23-29. [PubMed: 14750902]

Machiels BM, Zorenc AH, Endert JM, Kuijpers HJ, van Eys GJ, Ramaekers FC, Broers JL. An alternative splicing product of the lamin A/C gene lacks exon 10. J Biol Chem 1996;271:9249-9253. [PubMed: 8621584]

Mahajan R, Delphin C, Guan T, Gerace L, Melchior F. A small ubiquitin-related polypeptide involved in targeting RanGAP1 to nuclear pore complex protein RanBP2. Cell 1997;88:97-107. [PubMed: 9019411]

Makhnevych T, Sydorskyy Y, Xin X, Srikumar T, Vizeacoumar FJ, Jeram SM, Li Z, Bahr S, Andrews BJ, Boone C, Raught B. Global map of SUMO function revealed by protein-protein interaction and genetic networks. Mol Cell 2009;33:124-135. [PubMed: 19150434]

Malhotra R, Mason PK. Lamin A/C deficiency as a cause of familial dilated cardiomyopathy. Curr Opin Cardiol 2009;24:203-208. [PubMed: 19384091]

Manju K, Muralikrishna B, Parnaik VK. Expression of disease-causing lamin A mutants impairs the formation of DNA repair foci. J Cell Sci 2006;119:2704-2714. [PubMed: 16772334]

Markiewicz E, Dechat T, Foisner R, Quinlan RA, Hutchison CJ. Lamin A/C binding protein LAP2alpha is required for nuclear anchorage of retinoblastoma protein. Mol Biol Cell 2002;13:4401-4413. [PubMed: 12475961]

Marmiroli S, Bertacchini J, Beretti F, Cenni V, Guida M, De Pol A, Maraldi NM, Lattanzi G. A-type lamins and signalling: the PI 3-kinase/Akt pathway moves forward. J Cell Physiol 2009:220:553-561. [PubMed: 1947937]

Martelli AM, Bortul R, Tabellini G, Faenza I, Cappellini A, Bareggi R, Manzoli L, Cocco L. Molecular characterization of protein kinase C-alpha binding to lamin A. J Cell Biochem 2002;86:320-330. [PubMed: 12112001]

Mestroni L, Rocco C, Gregori D, Singara G, Di Lenarda A, Miocic S, Vatta M, Pinamonti B, Muntoni F, Carforio AL, McKenna WJ, Falaschi A, GiaccaM, Camerini F. Familial dilated cardiomyopathy: evidence for genetic and phenotypic heterogeneity. Heart Muscle Disease Study Group. J Am Coll Cardiol 1999;34:181-190. [PubMed: 10400009]

Mittlebronn M, Sullivan T, Stewart CL, Bornemann A. Myonuclear degeneration in LMNA null mice. Brain Pathol 2008;18:338-343. [PubMed: 18371185]

Miyazono K, Kamiya Y, Miyazawa K. SUMO amplifies TGF-beta signalling. Nat Cell Biol 2008;10:635-637. [PubMed: 18521068]

Moir RD, Spann TP, Herrmann H, Goldman RD. Disruption of nuclear lamin organization blocks the elongation phase of DNA replication. J Cell Biol 2000;149:1179-1192. [PubMed: 10851016]

Molkentin JD, Kalvakolanu DV, Markham BE. Transcription factor GATA-4 regulates cardiac muscle-specific expression of the alpha-myosin heavy-chain gene. Mol Cell Biol 1994;14:4947-4957. [PubMed: 8007990]

Mounkes LC, Kozlov S, Hernandez L, Sullivan T, Stewart CL. A progeroid syndrome in mice is caused by defects in A-type lamins. Nature 2003;423:298-301. [PubMed: 12748643]

Mounkes LC, Kozlov SV, Rottman JN, Stewart CL. Expression of an LMNA-N195K variant of A-type lamins results in cardiac conduction defects and death in mice. Hum Mol Genet 2005;14:2167-2180. [PubMed: 15972724]

Muchir A, Medioni J, Laluc M, Massaart C, Arimura T, van der Kooi AJ, Desguerre I, Mayer M, Ferrer X, Briault S, Hirano M, Worman HJ, Mallet A, Wehnert M, Schwartz K, Bonne G. Nuclear envelope alterations in fibroblasts from patients with muscular dystrophy, cardiomyopathy, and partial lipodystrophy carrying lamin A/C gene mutations. Muscle Nerve 2004;30:444-450. [PubMed: 15372542]

Muchir A, Pavlidis P, Decostre V, Herron AJ, Arimura T, Bonne G, Worman HJ. Activation of MAPK pathways links LMNA mutations to cardiomyopathy in Emery-Dreifuss muscular dystrophy. J Clin Invest 2007;117:1282-1293. [PubMed: 17446932]

Muchir A, Shan J, Bonne G, Lehnart SE, Worman HJ. Inhibition of extracellular signal-regulated kinase signaling to prevent cardiomyopathy caused by mutation in the gene encoding A-type lamins. Hum Mol Genet 2009;18:241-247. [PubMed18927124]

Mukhopadhyay D, Dasso M. Modification in reverse: the SUMO proteases. Trends Biochem Sci 2007;32:286-295. [PubMed: 17499995]

Muralikrishna B, Dhawan J, Rangaraj N, Parnaik VK. Distinct changes in intranuclear lamin A/C organization during myoblast differentiation. J Cell Sci 2001;114:4001-4011. [PubMed: 11739632]

Nacerddine K, Lehembre F, Bhaumik M, Artus J, Cohen-Tannoudji M, Babinet C, Pandolfi PP, Dejean A. The SUMO pathway is essential for nuclear integrity and chromosome segregation in mice. Dev Cell 2005;9:769-779. [PubMed: 1632639]

Nathan D, Ingvarsdottir K, Sterner DE, Bylebyl GR, Dokmanovic M, Dorsey JA, Whelan KA, Krsmanovic M, Lane WS, Meluh PB, Johnson ES, Berger SL. Histone sumoylation is a negative regulator in Saccharomyces cerevisiae and shows dynamic interplay with positive-acting histone modifications. Genes Dev 2006;20:966-976. [PubMed: 16598039]

Nigg EA. Assembly-disassembly of the nuclear lamina. Curr Opin Cell Biol 1992;4:105-109. [PubMed: 1421170]

Ohshima T, Shimotohno K. Transforming growth factor-beta-mediated signaling via the p38 MAP kinase pathway activates Smad-dependent transcription through SUMO-1 modification of Smad4. J Biol Chem 2003;278:50833-50842. [PubMed: 14514699]

Oka T, Maillet M, Watt AJ, Schwartz RJ, Aronow BJ, Duncan SA, Molkentin JD. Cardiac-specific depletion of Gata4 reveals its requirement for hypertrophy, compensation, and myocyte viability. Circ Res 2006;98:837-845. [PubMed 16514068]

Oka T, Xu J, Molkentin JD. Re-employment of developmental transcription factors in adult heart disease. Semin Cell Dev Biol 2007;18:117-131. [PubMed: 17161634]

Padmakumar VC, Libotte T, Lu W, Zaim H, Abraham S, Noegel AA, Gotzmann J, Foisner R, Karakesisoglou I. The inner membrane protein Sun1 mediates the anchorage of Nesprin-2 to the nuclear envelope. J Cell Sci 2005;118:3419-3430. [PubMed: 16079285]

Palancade B, Doye V. Sumoylating and desumoylating enzymes at nuclear pores: underpinning their unexpected duties? Trends Cell Biol 2008;18:174-183. [PubMed: 18313922]

Parnaik VK. Role of nuclear lamins in nuclear organization, cellular signalling, and inherited diseases. Int Rev Cell Mol Biol 2008;266:157-206. [PubMed: 18544494]

Pekovic V, Harborth J, Broers JL, Ramaekers FC, van Engelen B, Lammens M, von Zglinicki T, Foisner R, Hutchison C, Markiewicz E. Nucleoplasmic LAP2alpha-lamin A

complexes are required to maintain a proliferative state in human fibroblasts. J Cell Biol 2007;176:163-172. [PubMed: 17227891]

Perrot A, Hussein S, Ruppert V, Schmidt HH, Wehnert MS, Duong NT, Posch MG, Panek A, Dietz R, Kindermann I, Böhm M, Michalewska-Wludarczyk A, Richter A, Maisch B, Pankuweit S, Ozcelik C. Identification of mutational hot spots in LMNA encoding lamin A/C in patients with familial dilated cardiomyopathy. Basic Res Cardiol 2009;104:90-99. [PubMed: 18795223]

Pichler A. Analysis of sumoylation. Methods Mol Biol 2008;446:131-138. [PubMed: 18373254]

Prokocimer M, Davidovich M, Nissim-Rafini m, Wiesel-Motiuk N, Bar D, Barkan R, Meshorer E, Gruenbaum Y. Nuclear lamins: key regulators of nuclear structure and activities. J Cell Mol Med 2009 epub ahead of print. [PubMed: 19210577]

Raharjo WH, Enarson P, Sullivan T, Stewart CL, Burke B. Nuclear envelope defects associated with LMNA mutations cause dilated cardiomyopathy and Emery-Dreifuss muscular dystrophy. J Cell Sci 2001;114:4447-4457. [PubMed: 11792810]

Richardson P, McKenna W, Bristow M, Maisch B, Mautner C, O'Connell J, Olsen E, Thiene G, Goodwin J, Gyarfas I, Martin I, Nordet P. Report of the 1995 World Health Oganization/International Society and Federation of Cardiology Task Force on the Definition and Classification of cardiomyopathies. Circulation 1996;93:841-842. [PubMed: 8598070]

Riquelme C, Barthel KK, Qin XF, Liu X. Ubc9 expression is essential for myotube formation in C2C12 cells. Exp Cell Res 2006;312:2132-2141. [PubMed: 16631162]

Rosenblatt JD, Lunt AI, Parry DJ, Partridge TA. Culturing satellite cells from living single muscle fibre explants. In Vitro Cell Dev Biol Anim 1995;31:773-779. [PubMed: 8564066]

Rosenkranz S. TGF-beta1 and angiotensin networking in cardiac remodelling. 2004;63:423-432. [PubMed: 15276467]

Sacher M, Pfander B, Jentsch S. Identification of SUMO-protein conjugates. Methods Enzymol 2005;399:392-404. [PubMed 16338371]

Saitoh H, Hinchey J. Functional heterogeneity of small ubiquitin-related protein modifiers SUMO-1 versus SUMO-2/3. J Biol Chem 2000;275:6252-6258. [PubMed: 10692421]

Saitoh N, Uchimura Y, Tachibana T, Sugahara S, Saitoh H, Nakao M. In situ SUMOylation analysis reveals a modulatory role of RanBP2 in the nuclear rim and PML bodies. Exp Cell Res 2006;312:1418-1430. [PubMed: 16688858]

Saitoh N, Uchimura Y, Tachibana T, Sugahara S, Saitoh H, Nakao M. In situ SUMOylation analysis reveals a modulatory role of RanBP2 in the nuclear rim and PML bodies. Exp Cell Res 2006;312:1418-1430. [PubMed: 16688858]

Salomoni P, Pandolfi PP. The role of PML in tumor suppression. Cell 2002;108:165-170. [PubMed: 11832207]

Shiio Y, Eisenman RN. Histone sumoylation is associated with transcriptional repression. Proc Natl Acad Sci USA 2003;100:13225-13230. [PubMed: 14578449]

Shimada K, Suzuki N, Ono Y, Tanaka K, Maeno M, Ito K. Ubc9 promotes the stability of Smad4 and the nuclear accumulation of Smad1 in osteoblast-like Saos-2 cells. Bone 2008;42:886-893.

Spann TP, Goldman AE, Wang C, Huang S, Goldman RD. Alteration of nuclear lamin organization inhibits RNA polymerase II-dependent transcription. J Cell Biol 2002;156:603-608. [PubMed: 11854306]

Stewart CL, Kozlov S, Fong LG, Young SG. Mouse models of laminopathies. Exp Cell Res 2007;313:2144-2156. [PubMed: 17493612]

Stierle V, Couprie J, Ostlund C, Krimm I, Zinn-Justin S, Hossenlopp P, Worman HJ, Courvalin JC, Duband-Goulet I. The carboxy-terminal region common to lamins A and C contains a DNA binding domain. Biochemistry 2003;42:4819-4828. [PubMed: 12718522]

Strelkov SV, Herrmann H, Aebi U. Molecular architecture of intermediate filaments. Bioessays 2003;25:243-251. [PubMed: 12596228]

Strelkov SV, Schumacher J, Burkhard P, Aebi U, Herrmann H. Crystal structure of the human lamin A coil 2B dimer: implications for the head-to-tail association of nuclear lamins. J Mol Biol 2004;343:1067-1080. [PubMed: 15476822]

Sullivan T, Escalante-Alcalde D, Bhatt H, Anver M, Bhat N, Nagashima K, Stewart CL, Burke B. Loss of A-type lamin expression compromises nuclear envelope integrity leading to muscular dystrophy. J Cell Biol 1999;147:913-920. [PubMed: 10579712]

Sun Y, Durrin LK, Krontiris TG. Specific interaction of PML bodies with the TP53 locus in Jurkat interphase nuclei. Genomics 2003;82:250-252. [PubMed: 12837275]

Sylvius N, Bilinska ZT, Veinot JP, Fidzianska A, Bolongo PM, Poon S, McKeown P, Davies RA, Chan KL, Tang AS, Dyack S, Grzybowski J, Ruzyllo W, McBride H, Tesson F. In vivo and in vitro examination of the functional significances of novel lamin gene mutations in heart failure patients. J Med Genet 2005;42:639-647. [PubMed: 16061563]

Sylvius N, Tesson F. Lamin A/C and cardiac diseases. Curr Opin Cardiol 2006;21:159-165. [PubMed: 16601451]

Sylvius N, Hathaway A, Boudreau E, Gupta P, Labib S, Bolongo PM, Rippstein P, McBride H, Bilinska ZT, Tesson F. Specific contribution of lamin A and lamin C in the development of laminopathies. Exp Cell Res 2008;314:2362-2375. [PubMed: 185383321]

Taniura H, Glass, C, Gerace L. A chromatin binding site in the tail domain of nuclear lamins that interacts with core histones. J Cell Biol 1995;131:33-44. [PubMed: 7559784]

Taylor MR, Fain PR, Sinagra G Robinson ML, Robertson AD, Carniel E, Di Lenarda A, Bohlmeyer TJ, Ferguson DA, Brodsky GL, Boucek MM, Lascor J, Moss AC, Li WL, Stetler GL, Muntoni F, Bristow MR, Mestroni L. Natural history of dilated cardiomyopathy due to lamin A/C gene mutations. J Am Coll Cardiol 2003;41:771-780. [PubMed: 12628721]

Tomczak KK, Marinescu VD, Ramoni MF, Sanoudou D, Montanaro F, Han M, Kunkel LM, Kohane IS, Beggs AH. Expression profiling and identification of novel genes involved in myogenic differentiation. FASEB J 2004;18:403-405. [PubMed: 14688207]

van Berlo JH, Voncken JW, Kubben N, Broers JL, Duisters R, van Leeuwen RE, Crijns HJ, Ramaekers FC, Hutchison CJ, Pinto YM. A-type lamins are essential for TGF-beta1 induced PP2A to dephosphorylate transcription factors. Hum Mol Genet 2005;14:2839-2849. [PubMed: 16115815]

van Engelen BG, Muchir A, Hutchison CJ, van der Kooi AJ, Bonne G, Lammens M. The lethal phenotype of a homozygous mutation in the lamin A/C gene. Neurology 2005;64:374-376. [PubMed: 15668447]

Varela I, Cadinanos J, Pendas AM, Gutierrez-Fernandez A, Folgueras AR, Sanchez LM, Zhou Z, Rodriguez FJ, Stewart CL, Vega JA, Tryggvason K, Freije JM, Lopez-Otin C. Accelerated ageing in mice deficient in Zmpste24 protease is linked to p53 signalling activation. Nature 2005;437:564-568. [PubMed: 16079796]

Verga L, Concardi M, Pilotto A, Bellini O, Pasotti M, Repetto A, Tavazzi L, Arbustini E. Loss of lamin A/C expression revealed by immune-electron microscopy in dilated cardiomyopathy with atrioventricular block caused by LMNA gene defects. Virchows Arch 2003;443:664-671. [PubMed 12898247]

Verstraeten VL, Broers JL, Ramaekers FC, van Steensel MA. The nuclear envelope, a key structure in cellular integrity and gene expression. Curr Med Chem 2007;14:1231-1248. [PubMed: 17504143]

Vertegaal AC, Andersen JS, Ogg SC, Hay RT, Mann M, Lamond Al. Distinct and overlapping sets of SUMO-1 and SUMO-2 target protein sets revealed by quantitative proteomics. Mol Cell Proteomics 2006;5:2298-2310. [PubMed: 17000644]

Vertegaal AC. Small ubiquitin-like modifiers in chains. Biochem Soc Trans 2007;35:1422-1423. [PubMed: 18031236]

Vigouroux C, Auclair M, Dubosclard E, Pouchelet M, Capeau J, Courvalin JC, Buendia B. Nuclear envelope disorganization in fibroblasts from lipodystrophic patients with heterozygous R482Q/W mutations in the lamin A/C gene. J Cell Sci 2001;114:4459-4468. [PubMed: 11792811]

Vytopil pil M, Benedetti S, Ricci E, Galluzzi G, Dello Russo A, Merlini L, Boriani G, Gallina M, Morandi L, Politano L, Moggio M, Chiveri L, Hausmanova-Petrusewicz I, Ricotti R, Vohanka S, Toman J, Toniolo D. Mutational analysis of the lamin A/C gene (LMNA) among patients with different cardiomuscular phenotypes. J Med Genet 2003;40:e132. [PubMed: 14684700]

Wang J, Feng XH, Schartz RJ. SUMO-1 modification activated GATA4-dependent cardiogenic activity. J Biol Chem 2004;279:49091-49098. [PubMed 15337742]

Wang J, Shiels C, Sasieni P, Wu PJ, Islam SA, Freemont PS, Sheer D. Promyelocytic leukemia nuclear bodies associate with transcriptionally active genomic regions. J Cell Biol 2004;164:515-526. [PubMed: 14970191]

Wang Y, Herron AJ, Worman HJ. Pathology and nuclear abnormalities in hearts of transgenic mice expressing M371K lamin A encoded by an LMNA mutation causing Emery-Dreifuss muscular dystrophy. Hum Mol Genet 2006;15:2479-2489. [PubMed: 16825283]

Wang J, Li A, Wang Z, Feng X, Olson EN, Schwartz RJ. Myocardin sumoylation transactivates cardiogenic genes in pluripotent 10T1/2 fibroblasts. Mol Cell Biol 2007;27:622-632. [PubMed: 17101795]

Wang J. SUMO conjugation and cardiovascular development. Front Biosci 2009;14:1219-1229. [PubMed: 19273126]

Ward GE, Kirschner MW. Identification of cell cycle-regulated phosphorylation sites on nuclear lamin C. Cell 1990;61:561-577. [PubMed: 2188730]

Wei W, Yang P, Pang J, Zhang S, Wang Y, Wang MH, Dong Z, She JX, Wang CY. A stress-dependent SUMO4 sumoylation of its substrate proteins. Biochem Biophys Res Commun 2008;375:454-459. [PubMed: 18708028]

Wessely R, Seidl S, Schomig A. Cardiac involvement in Emery-Dreifuss muscular dystrophy 2005;67:220-223. [PubMed: 15691357]

Yaffe D, Saxel O. Serial passaging and differentiation of myogenic cells isolated from dystrophic mouse muscle. Nature 1977;270:725-727. [PubMed: 563524]

Yang M, Hsu CT, Ting CY, Liu LF, Hwang J. Assembly of a polymeric chain of SUMO1 on human topoisomerase I in vitro. J Biol Chem 2006;28:8264-8274. [PubMed: 16428803]

Yang W, Paschen W. Gene expression and cell growth are modified by silencing SUMO2 and SUMO3 expression. Biochem Biophys Res Commun 2009;382:215-218. [PubMed: 19275883]

Yasugi T and Howley PM. Identification of the structural and functional human homolog of the yeast ubiquitin conjugating enzyme UBC9. Nucleic Acids Res 1996;24:2005-2010. [PubMed: 8668529]

Zhang X, Azhar G, Chai J, Sheridan P, Nagano K, Brown T, Yang J, Khrapko K, Borras AM, Lawitts J, Misra RP, Wei JY. Cardiomyopathy in transgenic mice with cardiac-specific overexpression of serum response factor. Am J Physiol Heart Circ Physiol 2001;280:H1782-1792. [PubMed: 11247792]

Zhang H, Saitoh H, Matunis MJ. Enzymes of the SUMO modification pathway localize to filaments of the nuclear pore complex. Mol Cell Biol 2002;22:6498-6508. [PubMed: 12192048]

Zhang YQ, Sarge KD. Sumoylation regulates lamin A function and is lost in lamin A mutants associated with familial cardiomyopathies. J Cell Biol 2008;182:35-39. [PubMed: 18606848]

Zhao X, Sternsdorf T, Bolger TA, Evans RM, Yao TP. Regulation of Mef2 by histone deacetylase 4- and SIRT1 deacetylase-mediated lysine modifications. Mol Cell Biol 2005;25:8456-8464. [PubMed: 16166628]

Zhong N, Radu G, Ju W, Brown WT. Novel progerin-interactive partner proteins hnRNP E1, EGF, Mel 18, and UBC9 interact with lamin A/C. Biochem Biophys Res Commun 2005;338:855-861. [PubMed: 16248985]

Appendix I

Basic Res Cardiol (2010) 105:365–377
DOI 10.1007/s00395-010-0085-4

ORIGINAL CONTRIBUTION

Genetic and ultrastructural studies in dilated cardiomyopathy patients: a large deletion in the lamin A/C gene is associated with cardiomyocyte nuclear envelope disruption

Pallavi Gupta · Zofia T. Bilinska · Nicolas Sylvius · Emilie Boudreau · John P. Veinot · Sarah Labib · Pierrette M. Bolongo · Akil Hamza · Tracy Jackson · Rafal Ploski · Michal Walski · Jacek Grzybowski · Ewa Walczak · Grzegorz Religa · Anna Fidzianska · Frédérique Tesson

Received: 26 October 2009 / Revised: 12 January 2010 / Accepted: 13 January 2010 / Published online: 3 February 2010

Abstract Major nuclear envelope abnormalities, such as disruption and/or presence of intranuclear organelles, have rarely been described in cardiomyocytes from dilated cardiomyopathy (DCM) patients. In this study, we screened a series of 25 unrelated DCM patient samples for (a) cardiomyocyte nuclear abnormalities and (b) mutations in *LMNA* and *TMPO* as they are two DCM-causing genes that encode proteins involved in maintaining nuclear envelope architecture. Among the 25 heart samples investigated, we identified major cardiomyocyte nuclear abnormalities in 8 patients. Direct sequencing allowed the detection of three heterozygous *LMNA* mutations (p.D192G, p.Q353K and p.R541S) in three patients. By multiplex ligation-dependant probe amplification (MLPA)/quantitative real-time PCR, we found a heterozygous deletion encompassing exons 3–12 of the *LMNA* gene in one patient. Immunostaining demonstrated that this deletion led to a decrease in lamin A/C expression in cardiomyocytes from this patient. This *LMNA* deletion as well as the p.D192G mutation was found in patients displaying major cardiomyocyte nuclear envelope abnormalities, while the p.Q353K and p.R541S mutations were found in patients without specific nuclear envelope abnormalities. None of the DCM patients included in the study carried a mutation in the *TMPO* gene. Taken together, we found no evidence of a genotype–phenotype relationship between the onset and the severity of DCM, the presence of nuclear abnormalities and the presence or absence of *LMNA* mutations. We demonstrated

P. Gupta · N. Sylvius · E. Boudreau · S. Labib · P. M. Bolongo · A. Hamza · T. Jackson · F. Tesson (✉)
Faculty of Health Sciences, University of Ottawa, 451 Smyth, Ottawa, ON K1H 8M5, Canada
e-mail: ftesson@uottawa.ca

Z. T. Bilinska · J. Grzybowski
1st Department of Coronary Artery Disease, Institute of Cardiology, Alpejska 42, 04-6 28 Warsaw, Poland

Present Address:
N. Sylvius
Department of Biochemistry, University of Leicester, Leicester LE1 9HN, UK

J. P. Veinot
Department of Pathology and Laboratory Medicine, University of Ottawa, Anatomical Pathology, Ottawa Hospital, Ottawa, ON K1Y 4E9, Canada

R. Ploski
Department of Medical Genetics, Warsaw Medical University, Pawinskiego Street 3c, 02-106 Warsaw, Poland

M. Walski
Department of Cell Ultrastructure, M Mossakowski Medical Research Centre, Polish Academy of Science, Pawinskiego Street 5, 02-106 Warsaw, Poland

E. Walczak
Department of Pathology, Institute of Rheumatology, Spartanska 1, 02-637 Warsaw, Poland

G. Religa
2nd Department of Cardiac Surgery, Institute of Cardiology, Alpejska 42, 04-628 Warsaw, Poland

A. Fidzianska
Neuromuscular Unit, Medical Research Center, Polish Academy of Science, ul.Pawińskiego 5, 02-097 Warsaw, Poland

that a large deletion in *LMNA* associated with reduced levels of the protein in the nuclear envelope suggesting a haploinsufficiency mechanism can lead to cardiomyocyte nuclear envelope disruption and thus underlie the pathogenesis of DCM.

Keywords Lamin A/C · Thymopoietin · Mutation · Dilated cardiomyopathy · Cardiomyocyte · Nucleus ultrastructure

Introduction

Dilated cardiomyopathy (DCM) is characterized by dilatation of cardiac chambers and impaired contraction. Severity of symptoms and age of onset are highly variable. To date, mutations in 28 genes have been associated with autosomal dominant DCM [3, 9–11, 18, 19, MIM#115200]. *LMNA*, which encodes lamin A/C, is one of the most commonly implicated genes in DCM. Mutations in *LMNA* are associated with a high risk of dysrhythmia, sudden death and heart failure [4, 35]. Furthermore, symptomatic DCM patients carrying *LMNA* mutations display a worse prognosis than DCM patients carrying a mutation in another DCM-associated gene [2, 17, 19, 26, 44, 46, 48].

The A-type lamins A and C, alternatively spliced products from *LMNA*, are type V intermediate filament proteins expressed in terminally differentiated somatic cells. They are components of a thin filamentous meshwork—the nuclear lamina—underlying the nucleoplasmic side of the inner nuclear membrane, and are also present in the nucleoplasm [8, 20, 28, 30]. Lamins have traditionally been considered key components in providing structural support to the nucleus and anchoring chromatin and nuclear pore complexes to the nuclear envelope [24, 40, 52]. Intranuclear lamins have proposed functions in DNA replication [20, 25, 28, 29], transcription [41] and chromatin organization [38, 50]. In order to carry out their functions, lamins interact with a number of nuclear envelope proteins, chromatin and transcription factors. Among the genes encoding the lamin A/C interacting proteins, *TMPO*, the gene encoding nucleoplasmic thymopoietin alpha [also called lamina-associated polypeptide 2 (LAP2) alpha] has been shown to harbour a mutation in DCM patients [47]. The identified mutation occurred in the C-terminal domain of thymopoietin alpha, a region known to interact with lamin A/C (residues 319–566) [9]. Three thymopoietin isoforms, alpha, beta and gamma are encoded by *TMPO* [6]. The three isoforms share an identical amino terminal sequence but have divergent carboxy terminal sequences [9]. Thymopoietin is thought to play an important role in maintaining nuclear architecture through its binding with lamins and other proteins.

Cardiomyocytes from DCM patients with *LMNA* mutations exhibit the following characteristics: (a) reduced lamin A/C expression in myocyte nuclei on immunofluorescence/immunohistochemistry studies and (b) two types of ultrastructural changes, minor nuclear envelope damage, such as focal disruptions, blebs and nuclear pore clustering, and major morphologic alterations, including a complete loss of the nuclear envelope and accumulation of mitochondria, glycogen and/or lipofuscin in the nucleoplasm [2, 7, 13, 44, 51]. To date, these major nuclear envelope defects were only found in a DCM patient carrying the p.D192G *LMNA* mutation [7, 13, 44]. However, in non-genotyped DCM patients as well as in heart failure patients, minor nuclear defects such as irregular nuclear envelope, enlarged and bizarre shaped nuclei, indentations, giant and multiple nucleoli and irregularly distributed chromatin are commonly found [1, 4, 34, 37]. There is considerable heterogeneity in the abnormalities observed from one cardiac sample to the next as well as within one particular sample [1, 37].

The aim of the present study was to ascertain whether: (1) major nuclear envelope abnormalities are a common feature in patients with DCM and (2) *LMNA* and/or *TMPO* mutations are associated with nuclear envelope defects in cardiomyocytes from a series of 25 unrelated DCM patients.

Materials and methods

Patient recruitment

Written informed consent was obtained from all patients in accordance with study protocols approved by the hospital ethics committees. Diagnosis of DCM was established based on WHO/ISFC criteria modified by Mestroni and colleagues [27] that included severe LV systolic dysfunction (LV dilatation exceeding 117% of normal value corrected for age and body surface area) and LV ejection fraction (LVEF) $\leq$ 45% measured in angiography, without significant coronary artery disease (>50% lumen diameter reduction of one of the main coronary arteries). Exclusion criteria included hypertension, or acquired or congenital heart disease. All patients underwent clinical examination, evaluation of functional status according to NYHA classification, ECG study, two-dimensional echocardiography with Doppler and/or coronary angiography to exclude coronary artery disease. Left ventricular enlargement was calculated according to the method of Henry. A total of 25 index cases recruited in Canada and Poland were enrolled in the study.

Cardiac tissue collection, electron microscopy and immunostaining

Cardiac tissue samples were collected from endomyocardial biopsies performed on clinical indication or from explanted heart tissue. Samples were immediately processed in 1.6–3% gluteraldehyde. Fixed heart tissues were processed into thick and thin sections according to the standard methods. Tissue sections were examined with a Hitachi 7100 or JEM 1200EX electron microscope.

For indirect immunofluorescence examinations, 8 μm cryostat sections were stained with two monoclonal antisera against lamin A/C (NCL-LAM-A/C) (Novocastra Laboratories, Newcastle, UK) and A4, kindly provided by Dr. Hutchison (Department of Biological Science, University of Dundee, UK). A4 antibody detects only lamin A as its recognition site lies after amino acid 572. NCL-LAM-A/C recognizes both lamin A and lamin C. In brief, antibodies diluted 1:10 were applied to tissue sections for 60 min. Sections were rinsed with PBS and incubated for another 60 min with the appropriate Rodamine Red X conjugated goat anti-rabbit IgG secondary antibody diluted 1:30 with PBS. After being washed with PBS, the sections were mounted in gelmount and viewed with an Opton Zeiss standard LAB16 microscope with epifluorescence optics.

Screening of *LMNA* and *TMPO* coding sequences

Genomic DNA was isolated from white blood cells (Qiagen Flexigene kit). To screen for somatic mutations, DNA was extracted from cardiac tissues using a Qiamp Mini DNA extraction kit (Qiagen).

Intronic oligonucleotide primers flanking each of the exons were designed based on published sequences (Genbank accession number: L123399, L12400 and L12401 for *LMNA* and UCSC genome bioinformatics database for *TMPO*). All DNA samples were subjected to PCR and direct sequencing (ABI Prism Big Dye, ABI PRISM 3100 genetic analyzer). If there was any suspicion of genomic variation in a given patient, another sample of DNA collected independently was systematically double-strand sequenced (Table 1). Sequences were compared to two control samples from individuals without known cardiovascular disease. Each sample's electropherogram was analyzed by two independent investigators.

Multiplex-ligation dependant probe amplification (MLPA) analysis was performed to screen for deletions and duplications in the *LMNA* gene coding sequence according to the manufacturer's instructions (SALSA MLPA KIT P048 LMNA, MRC Holland). The probe mix contained probes for 10 of the 12 coding exons of *LMNA*, but not

Table 1 Primer pairs and annealing temperatures used to amplify *LMNA* and *TMPO* coding regions

		Primer sequences (5′ to 3′)		PCR annealing temperature (°C)
LMNA	Exon	Forward	Reverse	
	1A	TCTGTCCTTCGACCCGAG	GTAGACCGCCAAGCGATC	51
	2A	GGAGGACCTGCAGGAGCT	GCCCTCTCACTCCCTTCC	50
	3	CCTTCAAGTTCTTGTGTTCTGTGAC	CCTAGCCCAGCCCAAGTCTGTC	58
	4	GGCCTCCCAGGAACTAATTCTG	CTCCCTGCCACCATCTGC	63
	5	GCTGTAGCAGTGATGCCCAAC	CCAAAGCCCTGAGAAGTGAAG	62
	6	ATCCTGGAGAGAGTAGCCAG	TCTAGTCAAGGCCAGTTGCC	60
	7	CCCCACTTGGTCTCCCTCTCC	CCCTGATGCAGCTGTATCCCC	60
	8	GAGGCCTCAATTGCAGGCAGGC	GAAAAGGACACTTACCCCAGC	62
	9	GGAGCGCTGGGGTAAGTGTC	CTCGTCCAGCAAGCAGCCAG	60
	10	GTAAGCAGCAGGCCGGACAAAG	GATGCCATGGAATATTCCTGTG	58
	11A	GGTCAGTCCCAGACTCGC	ACCAGATTGTCCCCGAAG	55
	11B	GTCACTCGCAGCTACCGC	CCACCTCGTCCTACCCCT	52
	12	CTTGTCTGAGCCCCAGACTGGAG	AGGGAAAAGGAAGGGAGGAGAAAT	65
TMPO	1	GTCTAAGGGGAAGGGTGGAG	CAGACCCACACGTCAAAGAAC	60
	2	CCAATTTGGTAGTGAGTTTGCA	TAATTTGGGGTCCTGCTTCA	60
	3	TGAGCTGCATCCTAAATGAAAC	TGAGCTGCATCCTAAATGAAAC	57
	4	GCTTTGTCTACCAGGGCAAATC	GGCAGCCATCTTCACTCATC	60
	5	AAACCAGGGTTCCCGATTA	TGGATTAGTGTTGTCAGGAGGTT	60
	6	CCAGTATGGCCGTTATTAAAGTA	CTCCCTCCCACTCCAAAAA	60
	7	AAGAGAGCCTTGGAAGCATGTG	ACCATTGTACCTGGCTCCAAA	60
	8	TCAGGGAATGTGCTTGGAAT	GCAGTTTTTATTCAGCAGAGAA	60

for exons 5 and 9 because of the close proximity of exons 4 and 5, and exons 8 and 9. The probe mix also contained 13 probes for other human genes. Two of these probes recognize genes localized on chromosome 1. One of these probes was located 94 kb upstream of *LMNA* exon 1 and another 100 kb downstream of *LMNA* exon 12. MLPA amplification products were analyzed on an ABI model 3130XL Genetic Analyzer (Applied Biosystems) with the GeneMapper software V.3.7, using Genescan 500LIZ internal size standard (Applied Biosystems). Each patient's electropherogram was compared to three controls. We used the Coffalyzer MLPA DAT (MRC-Holland) software to analyze MLPA data. Resulting normalized ratios were ~1.0 for every wild-type peak, 0.5 for heterozygous deletions and 1.5 for heterozygous duplications.

Quantitative real-time PCR was used to confirm the deletion found in *LMNA* (Roche LightCycler 2.0) [36]. Primers were designed for *LMNA* exon 9 (forward: 5′-ggagcgctggggtaagtgtc-3′; reverse: 5′-ctcgtccagcaagcagcccag-3′). PCR was set up in capillaries in a total volume of 20 µl; each PCR mixture contained 2.5 mM $MgCl_2$ (2.5 mM), 2 µl of sybr green mix, 0.6 µM of mixture of forward and reverse primers and 20 ng of DNA. Standard curves for both the housekeeping gene (β2-microglobulin) and target gene were generated. Two different types of sample DNA (i.e., one sample from the DCM patient carrying the deletion and one sample from a DCM patient without the deletion) were utilized to ensure that the gene dosage ratio of the target to the housekeeping gene was disrupted only when a deletion was present. Using the slope and y-intercept of the standard curve, the LightCycler system calculated the concentrations (M) of sample and control DNA for both the reference gene (β2 microglobulin) and the target gene (Lamin A/C). These concentrations were then used to calculate the gene dosage ratio using the following equation:

$$R = \frac{M_{\text{target}}(\text{patient})/M_{\text{reference}}(\text{patient})}{M_{\text{target}}(\text{control})/M_{\text{reference}}(\text{control})}$$

where $R = 0.5$ (0.4–0.7) indicates deletion, $R = 1$ (0.8–1.2) indicates normal copy number and $R = 1.5$ (1.3–1.7) indicates duplication

Statistical analysis

LVEF and LVEDD in percentage values were compared between patients with major cardiomyocyte nuclear abnormality and patients with non-specific cardiomyocyte nuclear abnormality using a two-tailed Student's t test (level of significance 5%).

Results

Ultrastructural characteristics of endomyocardial samples

Ultrastructural analysis of endomyocardial samples enabled us to distinguish two groups of DCM patients. One group consisted of eight individuals exhibiting major nuclear envelope abnormalities on electron micrographs (Fig. 1) and the second consisted of 17 patients with minor and non-DCM specific abnormalities.

Among the patients with nuclear envelope defects, the proportion of defective cells ranged from a small percentage to as much as 30% (patients 2 and 6). The most obvious abnormality, occurring in four of eight patients, was intrusion and accumulation of mitochondria and other cytoplasmic organelles into the nuclear matrix (patients 1, 2, 5 and 7) (Fig. 1a, d). The membranes of these organelles appeared discontinuous from the nuclear envelope (Fig. 1a, d). The nuclear envelope was usually irregular (Fig. 1a–c) and partially disrupted or totally missing in six of eight patients (patients 1, 2, 4, 5, 6 and 7) (Fig. 1a, c, d). Chromatin disorganization was also observed (patients 2 and 6). In contrast, samples from the 17 patients in the second group displayed modest and non-specific nuclear membrane alterations, such as nuclear irregularity, that are commonly found in DCM patients regardless of the presence of *LMNA* mutations (Fig. 1e, f).

Clinical characteristics of the patient cohort

Clinical characteristics of the 25 DCM patients (19 males and 6 females) included in our study are shown in Table 2. There was considerable heterogeneity in terms of the clinical characteristics and severity of DCM across the cohort of 25 patients.

In the group of eight patients who exhibited nuclear envelope abnormalities, age at disease onset ranged from 14 to 63 years, four patients had a family history of DCM (Table 2, Fig. 2, [44]), while none had a suspicion of muscular dystrophy. Disease severity ranged from mild DCM to progressive heart failure and LVEF values ranged from <10 to 50%. Various arrhythmias were present in all eight patients; two patients required ICD (patients 1 and 7) and one required pacemaker (patient 5). Three patients had received a heart transplant (patients 4, 5 and 6) and two patients had died of heart failure (patients 2 and 3). In addition, patient 5 presented with hypothyroidism and patient 7 with mild mental retardation. No other phenotypic abnormality was identified within this population.

A similar degree of heterogeneity was also observed among the 17 patients with no major nuclear envelope

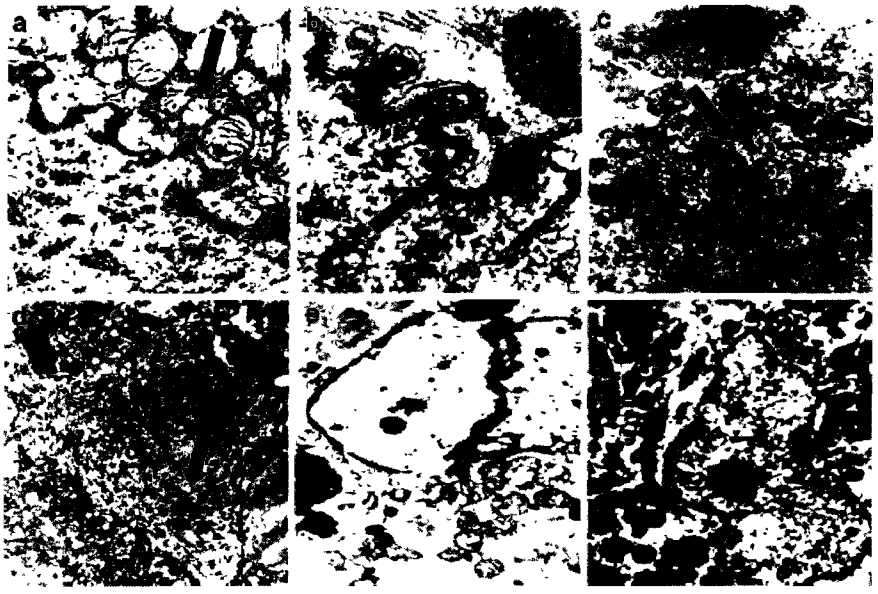

Fig. 1 Electron micrographs of cardiomyocytes from dilated cardiomyopathy patients with or without *LMNA* mutation. a, b, c and d Major nuclear abnormalities in, respectively, patient 1, 3, 4 and 5 (Table 2). Patient 1 carried the *LMNA* deletion exons 3–12, while patients 3, 4 and 5 had no *LMNA* nor *TMPO* mutation; a accumulation of mitochondria around the nuclear envelope; b blebbing of the nuclear envelope and separation of the inner and the outer nuclear membrane; c extrusion of nucleoplasm from the cardiomyocyte nucleus into the cytoplasm; d accumulation of cytoplasmic organelles in the nucleoplasm; e non specific nuclear alteration in patient 10 (Table 2) carrying the p.Q353K *LMNA* mutation; f non specific alterations in dilated cardiomyopathy patient 14 (Table 2) with wild type *LMNA* and *TMPO* (original magnifications: a. 20,000×; b. 18,000×; c. 12,000×; d. 10,000×; e. 4,000×; and f. 4,000×)

abnormalities: age at disease onset ranged from 12 to 61 years, 10 patients had a family history of DCM (Table 2, Fig. 2, [44]), 1 patient had documented skeletal myopathy (patient 10) and 1 had elevated CPK values [up to 600 U/l (patient 18)]. LVEF values ranged from 10 to 38%; conduction defects were present in all but two patients (data were not available for four patients), four patients required ICD and two had pacemakers. Twelve patients had received heart transplants and two patients had died of heart failure (patients 13 and 21).

We compared mean LVEF and LVEDD in percentage values between patients exhibiting major nuclear envelope abnormalities and patients with minor and non-DCM-specific abnormalities. No significant correlation between the severity of the phenotype and the presence of nuclear envelope defect was detected ($p > 0.05$).

Screening of *LMNA* and *TMPO* coding sequences

We screened the complete coding sequence as well as the intron–exon boundaries of *LMNA* (12 exons) and *TMPO* (8 exons) for mutations using direct sequencing of DNA extracted from white blood cells of all 25 patients. We identified three patients with *LMNA* mutations, one in the group with major nuclear envelope defects (patient 2, p.D192G) and two in the group with non-specific nuclear envelope abnormalities (patient 9, p.R541S and patient 10, p.Q353K). Patient 2 and 9 and their *LMNA* mutations have been described previously [7, 44]. All these variations were absent in DNA from more than 100 controls. No mutation was found in *TMPO*. Previously reported polymorphisms in both *LMNA* (synonymous polymorphisms rs538089, rs505058, rs4641) and *TMPO* (non-synonymous polymorphism rs17459334) were detected. We also found a c.C1341A synonymous polymorphism in *LMNA* exon 6, which has not been previously reported, in two control individuals. Mutations in the corresponding codon have been previously reported in patients with limb-girdle muscular dystrophy 1B (p.R377H, [31]; p.R377L, [21]).

Sequencing analysis cannot detect large heterozygous deletions or duplications. In an attempt to ascertain whether the defects resulted from deletions or duplications in *LMNA*, we performed multiplex ligation-dependant probe amplification (MLPA) on the *LMNA* coding sequence in all 25 DCM patients. One DCM patient (Table 2, patient 1) with major nuclear abnormality displayed a MLPA normalized ratio peak area of ~0.5 for exons 3–12 (Fig. 3). This indicated the presence of a heterozygous deletion encompassing exons 3 to 12 (>4,704 bp). The remaining probes, including those for exons 1 and 2, displayed a normalized ratio of ~1.0 indicating normal copy number (Fig. 3). We confirmed the presence of the deletion using

Table 2 Patients' clinical characteristics at the time of the heart sampling, *LMNA* mutation status and nuclear envelope defect status

Patient	*LMNA* mutation	Family history	Nuclear envelope defect	Sex/age at onset (years)	NYHA class	Echocardiography	Weight (kg)/height (cm)/LVEDD (%)	Dysrhythmias	Clinical status
Major nuclear envelope defects and *LMNA* mutation									
1	Deletion exons 3–12	Yes	Irregular and broken nuclear envelope; accumulation of mitochondria within and around the nuclei	F/39	II	LVEDD 54 mm, LVEF 50%	57/164/120.0	nsVT, couplets, frequent VE, ICD	Mild progressive HF No MD
2*	p.D192G (c.575A > G)	Yes	Complete loss of nuclear envelope, accumulation of mitochondria, glycogen and/or lipofuscin in the nucleoplasm, chromatin disorganization	M/26	IV	LVEDD 60 mm, LVEF 20%	67/175/127.2	1 AVB, LAFB	Died at 27 while awaiting for a heart transplant No MD
Major nuclear envelope defects and no *LMNA* mutation									
3	No	Yes	Blebbing of nuclear envelope, separation of inner and outer nuclear membrane	M/63	III	LVEDD 64 mm, LVEF 26%	71/180/136.5	SVT, VT	Died of progressive HF, 4 years after diagnosis No MD
4	No	Yes	Extrusion of nucleoplasm from the cardiomyocyte nucleus into the cytoplasm	M/21	III	LVEDD 75 mm, LVEF 25%	80/176/153.7	nsVT	HTx at 24 No MD
5	No	No	Irregular nucleus border; lack of nuclear membrane, presence of mitochondria within nuclear matrix	M/29	III	LVEDD 59 mm, LVEF 30%	84/176/120.5	RBBB, LPFB, nsVT. Pacemaker at 32	Progressive HF, HTx at 40 No MD
6	No	No	Local disruption of nuclear envelope, chromatin disorganization	F/14	IV	LVEDD 64 mm, LVEF < 10%	55/152/144.7	Recurrent VT/VF	HTx at 14 No MD
7	No	No	Misshapen nuclei, local disruption of nuclear envelope, penetration of mitochondria into nucleus	M/14	III	LVEDD 71 mm, LVEF 20%	57/168/155.6	nsVT, couplets, frequent VE, ICD at 20	Progressive HF No MD
8	No	No	Irregular shape of nuclei	M/18	III	LVEDD 68 mm, LVEF 20%	47/160/156.0	LBBB, nsVT	Progressive HF No MD
Non-specific nuclear envelope defects and *LMNA* mutation									
9*	p.R541S (c. 1621C > A)	Yes	No	M/12	IV	LVEDD 64 mm, LVEF 25%	49/152/147.3	NA	HTx at 13 No MD
10	p.Q353K (c.1057C > A)	Yes	No	M/38	IV	LVEDD 62 mm, LVEF 22%.	59/163/138.1	ICD	HTx at 38 Skeletal myopathy

Table 2 continued

Patient	*LMNA* mutation	Family history	Nuclear envelope defect	Sex/age at onset (years)	NYHA class	Echocardiography	Weight (kg)/height (cm)/LVEDD (%)	Dysrhythmias	Clinical status
Non-specific nuclear envelope defects and no *LMNA* mutation									
11	No	Yes	No	M/27	II	LVEDD 60 mm, LVEF 38%	100/186/117.2	Permanent AF, single VE	Improved after AF ablation, LVEF 45%
									No MD
12	No	Yes	No	M/26	III	LVEDD 75 mm, LVEF 20%	73/183/154.8	Single VE	Stable HF
									No MD
13	No	Yes	No	M/40	NA	LVEDD 77 mm, LVEF 19%	73/168/164.3	ICD, pacemaker	Died at 59, poor candidate denied for HTx
									No MD
14	No	Yes	No	F/14	IV	LVEDD 58 mm, LVEF 14%	37/155/139.4	No	HTx at 14
									No MD
15	No	Yes	No	M/36	II	LVEDD 78 mm, LVEF 25%	94/185/154.9	Single Vex	Stable HF
									No MD
16	No	Yes	No	M/27	III	LVEDD 78 mm, LVEF 10%	72/186/160.7	Sinus tachycardia	HTx within several months
									No MD
17	No	Yes	No	M/34	IV	LVEDD 78 mm, LVEF 20%	73/178/163.1	1-degree AVB	Fulminant HF leading to HTx within several months
									No MD
18	No	Yes	No	M/35	III	LVEDD 58 mm, LVEF 15%	80/170/121.1	Frequent sVT	Atrial septal aneurysm; HTx at 39
									No MD
									CPK value up to 600 U/l
19	No	No	No	F/13	NA	LVEDD 69 mm, LVEF 10%	41/164/160.3	NA	HTx at 13
									No MD
20	No	No	No	F/61	NA	LVEDD 69 mm, LVEF 12%	88/165/145.3	ICD	Pericarditis, HTx at 62
									No MD
21	No	No	No	M/54	III	LVEDD 88 mm, LVEF 20%	109/175/175.1	Pacemaker	Died at 60, waiting for HTx
									No MD

Table 2 continued

Patient	*LMNA* mutation	Family history	Nuclear envelope defect	Sex/age at onset (years)	NYHA class	Echocardiography	Weight (kg)/height (cm)/LVEDD (%)	Dysrhythmias	Clinical status
22	No	No	No	M/40	III-IV	LVEDD 68 mm, LVEF 27%	71/160/147.8	No	HTx at 62 No MD
23	No	No	No	M/27	NA	LVEDD 96 mm, LVEF 13%	70/170/203.8	ICD	HTx at 57 No MD
24	No	No	No	F/12	NA	LVEF 13%	42/153/NA	NA	HTx at 12 No MD
25	No	No	No	M/20	NA	LVEF 13%	86.5/197/NA	NA	HTx at 22 No MD

Clinical characteristics and mutation where previously described for patients 2 and 9 [7, 40]

AF atrial fibrillation, *AVB* atrioventricular block, *HF* heart failure, *HTx* heart transplantation, *ICD* implantable cardioverter defibrillator, *LAFB* left anterior fascicular block, *LPFB* left posterior fascicular block, *LVEDD* left ventricle end diastolic diameter, *LVEF* left ventricle ejection fraction, *MD* muscular disease, *NA* not available, *RBBB* right bundle branch block, *VEX* ventricular extrasystole, *VE* ventricular ectopy, *VT* ventricular tachycardia, *nsVT* nonsustained ventricular tachycardia, *SVT* supraventricular tachycardia, *VT/VF* ventricular tachycardia/ventricular fibrillation

qPCR (*R* value of 0.5 for the patient with the deletion and 1 for the patient without the deletion) (Fig. 4).

Lastly, to assess whether the nuclear envelope defects in the remaining patients could result from somatic mutations, we screened for *LMNA* and *TMPO* mutations in the heart from sporadic cases with nuclear envelope defect for which cardiac tissue was available (patients 5, 6) as well as in heart from patients without defective nuclear envelope (patients 19, 20, 21, 22, 23, 24 and 25). This analysis did not reveal any somatic mutations.

In summary, a large degree of clinical heterogeneity was evident in the cohort of DCM patients studied regardless of the presence of nuclear envelope abnormalities, *LMNA* mutation or family history of DCM.

Immunostaining results

To gain further insight into the functional significance of the heterozygous deletion of exons 3–12 of *LMNA* observed in patient 1, we performed indirect immunofluorescence analysis of endomyocardial samples from this patient as well as a control patient without *LMNA* mutation, using antibodies directed against both lamin A and C. All cardiomyocyte nuclei were immunostained with antibodies directed against lamin A and C epitopes (Fig. 5). The immunostaining was reduced in patient 1 as compared to the control patient indicating significant attenuation of lamin expression (Fig. 5).

Discussion

Among heart samples from 25 unrelated DCM patients, we identified major cardiomyocyte nuclear abnormalities in 8 individuals and non-specific nuclear abnormalities in the remaining patients. The presence of nuclear abnormalities, along with the fact that all patients presented with dysrhythmias and/or severe heart failure leading to cardiac transplantation, prompted us to analyze the sequence of *LMNA* and *TMPO*, two DCM-causing genes involved in maintaining nuclear envelope architecture.

Direct sequencing allowed the identification of three heterozygous *LMNA* genomic variations (p.D192G, p.R541S and p.Q353K) in three patients. Since sequencing analysis cannot detect large heterozygous deletions or duplications, we performed multiplex ligation-dependant probe amplification (MLPA) on the *LMNA* coding sequence in all 25 DCM patients. We found a heterozygous deletion encompassing exons 3–12 of the *LMNA* gene. This deletion was confirmed using quantitative real-time PCR. All variations were absent in DNA from more than 100 controls. The occurrence of *LMNA* mutation in our population is high probably due to fact that the studied

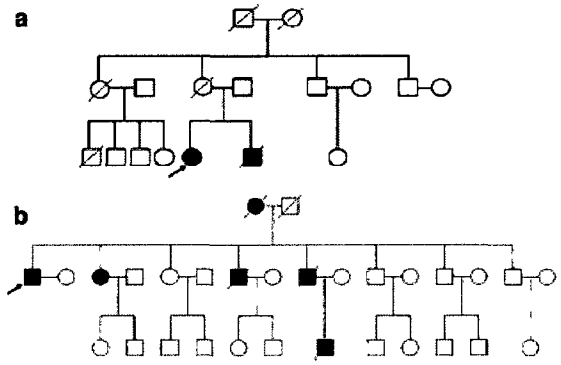

Fig. 2 Pedigree of the families with *LMNA* mutations. *Arrow* indicates proband; *black filled symbol* dilated cardiomyopathy patient, *open symbol* asymptomatic individual. a Deletion of exons 3–12; b p.Q353K

population presented with cardiac condition requiring undergoing endomyocardial biopsies or cardiac transplantation. Moreover, various arrhythmias were present in all but two patients. Since mutations in *LMNA* are usually associated with a worse prognosis than any other DCM-associated gene mutation [2, 17, 18, 26, 44, 46, 48] as well as with dysrhythmia [4, 35], our population was probably biased toward *LMNA* mutations carriers. None of the patients carried a mutation in the *TMPO* gene.

While rare findings of small deletions in the lamin A/C gene in patients with laminopathies have been reported previously, to our knowledge, this study is the first to document a large deletion encompassing most exons of the lamin A/C gene in a DCM patient. Walter et al. [53] found a 15 amino acid deletion (−3 to 12 nucleotides) in the 5′ end of the *LMNA* gene in a patient with Emery–Dreifuss muscular dystrophy (EDMD) that resulted in loss of the

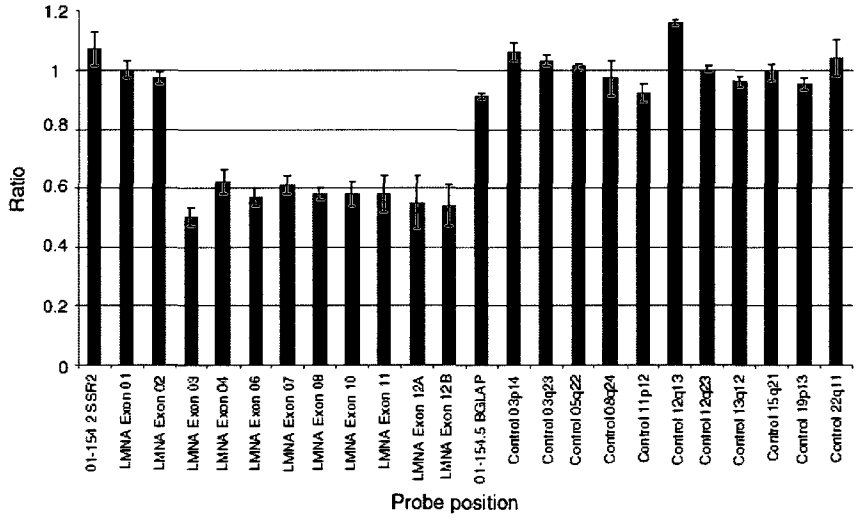

Fig. 3 MLPA analysis graph showing the heterozygous *LMNA* deletion of exons 3–12 in patient 1. Exons 3–12 display a normalized ratio of ~0.5; indicating a loss of genetic material. Exons 1, 2 and the remaining control probes display a normalized ration of ~1.0; indicating normal copy number. The control probes are targeted within the same chromosome and to different chromosomes as indicated by their locus

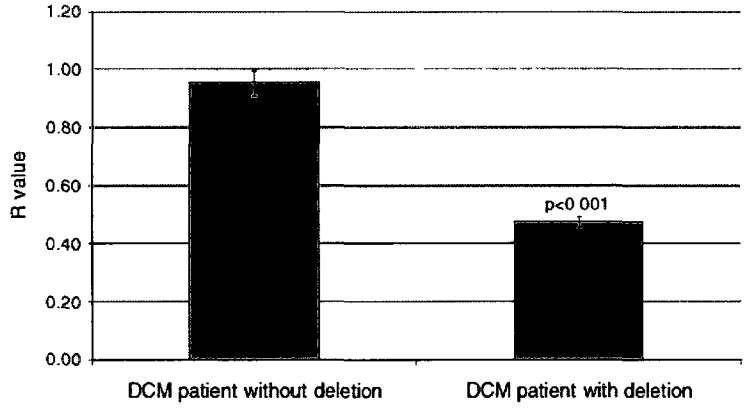

Fig. 4 Confirmation of the deletion of exons 3–12 in *LMNA* in patient 1 using qPCR. *R* values were calculated as described in the "Materials and methods". Patient 14 without the deletion had a *R* value of 0.955, which indicates a normal copy number of the exon. The *R* value for patient 1 is 0.476, which indicates the presence of only one copy of the exon ($n = 3$)

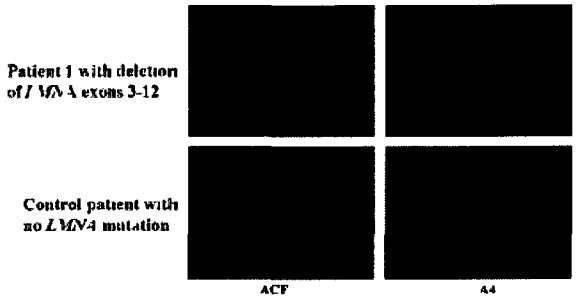

Fig. 5 Indirect immunofluorescence analysis of endomyocardial biopsy from patient 1 carrying the *LMNA* heterozygous exon 3–12 deletion and from a control patient with no *LMNA* mutation. Endomyocardial biopsy was taken from the right ventricle. Immunostaining was performed using anti-lamin A–C monoclonal antibodies ACF and antibody A4 which detects lamin A only (see Materials and methods) and the goat anti-rabbit IgG secondary antibody (original magnification 1,050×)

translation initiator codon. van Tintelen et al. [49] reported a 674-bp deletion encompassing exon 1 and the adjacent non-coding exon in a patient with myocardial fibrosis. The presence of the exon 1 p.Q6Stop *LMNA* mutation resulting in reduced levels of lamin A/C proteins has also been reported in a family with EDMD [5].

Most *LMNA* mutations that cause DCM are heterozygous point mutations, only some of which have been associated with cardiomyocyte nuclear envelope defects [2, 7, 13, 44, 51]. It has been suggested that mutations causing such abnormalities have a dominant-negative effect on the functions of normal lamin protein. Impaired lamin integration into the nuclear lamina due to the dominant-negative effects of a mutation may cause disruption of the lamina and ultimately compromise nuclear envelope integrity. Our results suggest that apart from the dominant-negative effects of mutant lamin A/C protein, lamin haploinsufficiency can also cause nuclear envelope defects and underlie the pathogenesis of DCM. Since the deletion encompasses *LMNA* exon 3 to 12, it is likely that the observed nuclear abnormalities are not due to the expression of a putative truncated protein composed of exons 1–2 only. It was shown that the potential truncated protein resulting from the Y259X nonsense mutation (exon 4) was not detectable in patient fibroblasts [33]. Similarly, in the mouse model with the *LMNA* exon 8–11 deletion, the 54-kDa truncated protein resulting from this deletion was not detected [43]. Furthermore, immunostaining revealed reduced lamin A/C in the patient's cardiomyocyte nuclei. That lamin haploinsufficiency can cause such defects is further corroborated by the fact that a heterozygous $LMNA^{+/-}$ mouse model in which cardiac lamin A/C levels were diminished by 50% compared to wild-type, demonstrated early-onset conduction system disease and late-onset DCM [54]. Furthermore, misshapen cardiomyocyte nuclei and heterochromatin clumping were also observed [54].

The *LMNA* deletion of exons 3–12 was observed in a patient presenting with major nuclear envelope abnormalities—notably broken nuclear envelope and accumulation of mitochondria within and around the nuclei. This suggests that haplo-insufficiency is the mechanism underlying the observed nuclear abnormalities. Among their many functions, lamins play an integral role in maintaining the mechanical stability of the nucleus; hence we can speculate that the nuclear envelope defects observed in the patient carrying this *LMNA* deletion results from the reduced levels of lamin A/C protein.

Apart from the observed deletion, one of our patients with nuclear envelope defects carried a p.D192G point mutation in the *LMNA* gene. When expressed in COS-7 cells, this mutation resulted in a discontinuous nuclear lamina due to the formation of multiple lamin aggregates [14, 15]. These results therefore corroborated the pathological findings from the patient with the mutation.

In our study, not all *LMNA* mutations were found to cause nuclear envelope abnormalities in patients' cardiomyocytes. Indeed, two patients with *LMNA* point mutations demonstrated no specific nuclear envelope abnormalities in the samples taken from explanted heart tissue: one patient carried a p.Q353K mutation, while the second carried the p.R541S mutation. It is possible that the number of abnormal nuclei was so low in these two patients that it resulted in a false-negative finding. Patient age at the time of tissue collection and the protein domain affected by the mutation were considered as possible explanations for the observed discrepancy in nuclear envelope phenotype. Age at the time of tissue collection was 38 and 12 years for the patients carrying mutations p.Q353K and p.R541S, respectively, both of which were associated with normal nuclear envelope ultrastructure. The patients with *LMNA* deletion and p.D192G mutation, both of whom demonstrated nuclear envelope abnormalities, were 39 and 26 years of age, respectively. Hence, there was no apparent relationship between age and observed nuclear envelope phenotype. It was also considered possible that the presence of nuclear envelope abnormalities may depend upon the protein domain affected by each mutation [12, 32]. The p.D192G mutation, which was associated with major nuclear envelope abnormalities, is located in the central α helical rod domain at the distal end of coil 1B. This highly conserved region of the lamin A/C protein is critical for the formation of the α helical coiled-coil dimer, the basic building block for the construction of lamin filaments. In contrast, the p.Q353K mutation in exon 6 affected a highly conserved residue localized in the central rod domain coil 2B fragment. Based on the coil 2B fragment crystal

structure, mutations in this domain are unlikely to alter the dimer structure but may interfere with essential molecular interactions occurring in later stages of filament assembly, lamina formation and/or chromatin interaction [42]. Similarly, the p.R541S mutation is located in highly conserved residues in a region of gene shared by lamin A and C isoforms within the carboxyl-terminal end. The buried side chain of R541 participates in the stabilization of the carboxy-terminal β-sandwich through hydrophobic contacts with the core of the domain [22]. Mutations in this domain could therefore destabilize the three-dimensional structure of the C-terminal domain of lamin A/C. This domain also carries sites for many lamin A/C interacting proteins. Therefore, both p.Q353K and p.R541S mutations could theoretically disrupt multiple functions of lamin A and C, including the maintenance of nuclear architecture. Unexpectedly, the ultrastructural phenotype associated with these mutations was indistinguishable from controls. Hence, our results do not support the presence of a relationship between the position of the mutation and the resulting ultrastructural phenotype.

The six patients demonstrating nuclear ultrastructural defects without *LMNA* or *TMPO* mutations showed that germ-line mutations in these genes are not a prerequisite for nuclear envelope defects. However, we could not discount the possibility that some of these individuals possessed somatic *LMNA* or *TMPO* mutations restricted to diseased cardiac tissue. The fact that only a percentage of observed cardiomyocytes from these patients displayed an abnormal nucleus lends support to this hypothesis. Indeed, somatic mutation occurring in a selective subpopulation of progenitor cell lineage is one of the molecular mechanisms leading to such tissue mosaicism. Furthermore, in other cardiovascular diseases such as idiopathic ventricular tachycardia or idiopathic atrial fibrillation, both germ-line and somatic missense mutations have been linked to the disease [14, 23]. We therefore screened for the presence of *LMNA* and *TMPO* mutations in DNA extracted from heart tissues of patients who did not have familial DCM, but were unable to identify any somatic mutations. Another possibility is that mutation in genes encoding lamin A/C-binding proteins are responsible for the major cardiomyocyte nuclear abnormalities observed in these patients [15, 16, 39, 55–57].

We showed here that there is no clear correlation between the presence or position of the *LMNA* mutation and either clinical phenotype with respect to DCM onset or severity or cardiomyocyte ultrastructural phenotype. We also found no apparent correlation between genotype and either severity of the ultrastructural aberration (i.e., the degree of nuclear envelope disruption), or the proportion of observed cells displaying abnormal nuclei. Furthermore, there was no significant correlation between the severity of the disease and the presence of ultra-structural nuclear envelope defects. Although a quantitative analysis was not possible due to the small sample size, overall, we found no evidence of a relationship between the onset and the severity of DCM, the presence of nuclear abnormalities and the presence or absence of *LMNA* mutations.

Taken together, our results suggest that lamin A/C haplo-insufficiency, documented by reduced protein level in the patient's cardiomyocyte nuclear envelope caused by a large deletion in the *LMNA* gene, can lead to nuclear envelope disruption and underlie the pathogenesis of DCM. However, the finding that two patients without cardiomyocyte nuclear abnormalities had *LMNA* mutations indicates that *LMNA* mutations may not necessarily lead to major cardiomyocyte nuclear envelope defects. Furthermore, patients with major nuclear envelope abnormalities may not have *LMNA* or *TMPO* mutation. This demonstrates that patients with a clinical suspicion of laminopathy and marked abnormality of cardiomyocyte nuclei can be free of both *LMNA* and *TMPO* mutations and may carry a mutation in another gene encoding a protein involved in the maintenance of the nuclear architecture.

Acknowledgments The work was supported by Canadian Institutes for Health Research operating grants 38054, 65152 and 77685, and by Heart and Stroke Foundation Grants NA 5101 and 6628 awarded to F. Tesson and by an internal grant from the Institute of Cardiology (Warsaw, Poland) no:2.57/VII/03. At the time the study was conducted, N. Sylvius was the recipient of the fellowships awarded by the Heart and Stroke Foundation of Ontario Program Grant 5275 and Astra Zeneca/Canadian Society of Hypertension/CIHR, and Pallavi Gupta was the recipient of Ontario Graduate Scholarship in Science and Technology (OGSST). We acknowledge the important contribution of the Canadian Cardiovascular Genetics Centre (Ottawa, Canada).

Conflict of interest statement The authors declare that they have no conflict of interest.

References

1. Arbustini E, Gavazzi A, Pozzi R, Grasso M, Pucci A, Campana C, Graziano G, Martinetti M, Cuccia M, Salvaneschi L, Martinelli L, Montemartini C, Vigano M (1989) The morphologic spectrum of dilated cardiomyopathy and its relation to immune-response genes. Am J Cardiol 64:991–995
2. Arbustini E, Pilotto A, Repetto A, Grasso M, Negri A, Diegoli M, Campana C, Scelsi L, Baldini E, Gavazzi A, Tavazzi L (2002) Autosomal dominant dilated cardiomyopathy with atrioventricular block: a lamin A/C defect-related disease. J Am Coll Cardiol 39:981–990
3. Arimura T, Hayashi T, Matsumoto Y, Shibata H, Hiroi S, Nakamura T, Inagaki N, Hinohara K, Takahashi M, Manatsu S, Sasaoka T, Izumi T, Bonne G, Schwartz K, Kimura A (2007) Structural analysis of four and half LIM protein-2 in dilated cardiomyopathy. Biochem Biophys Res Commun 357:162–167
4. Baandrup U, Florio RA, Roters F, Olsen EG (1981) Electron microscopic investigation of endomyocardial biopsy samples in

hypertrophy and cardiomyopathy. A semiquantitative study in 48 patients. Circulation 63:1289–1298
5. Bécane HM, Bonne G, Varnous S, Muchir A, Ortega V, Hammouda EH, Urtizberea JA, Lavergne T, Fardeau M, Eymard B, Weber S, Schwartz K, Duboc D (2000) High incidence of sudden death with conduction system and myocardial disease due to lamins A and C gene mutation. J Pac Clin Electrophysiol 23:1661–1666
6. Berger R, Theodor L, Shoham J, Gokkel E, Brok-Simoni F, Avraham KB, Copeland NG, Jenkins NA, Rechavi G, Simon AJ (1996) The characterization and localization of the mouse thymopoietin/lamina-associated polypeptide 2 gene and its alternatively spliced products. Genome Res 6:361–370
7. Bilinska ZT, Sylvius N, Grzybowski J, Fidzianska A, Michalak E, Walczak E, Walski M, Bieganowska K, Szymaniak E, Kusmierczyk-Droszcz B, Lubiszewska B, Wagner T, Tesson F, Ruzyłło W (2006) Dilated cardiomyopathy caused by *LMNA* mutations. Clinical and morphological studies. Polish Heart J 64:812–818
8. Bridger JM, Kill IR, O'Farrell M, Hutchison CJ (1993) Internal lamin structures within G1 nuclei of human dermal fibroblasts. J Cell Sci 104:297–306
9. Daehmlow S, Erdmann J, Knueppel T, Gille C, Froemmel C, Hummel M, Hetzer R, Regitz-Zagrosek V (2002) Novel mutations in sarcomeric protein genes in dilated cardiomyopathy. Biochem Biophys Res Commun 298:116–120
10. Dechat T, Korbei B, Vaughan OA, Vlcek S, Hutchison CJ, Foisner R (2000) Lamina-associated polypeptide 2 (alpha) binds intranuclear A-type lamins. J Cell Sci 113:3473–3484
11. Dubosc-Bidot L, Xu P, Charron P, Neyroud N, Dilanian G, Millaire A, Bors V, Komajda M, Villard E (2008) Mutations in the z-band protein myopalladin gene and idiopathic dilated cardiomyopathy Cardiovasc Res 77:118–125
12. Favreau C, Dubosclard E, Ostlund C, Vigouroux C, Capeau J, Wehnert M, Higuet D, Worman HJ, Courvalin JC, Buendia B (2003) Expression of lamin A mutated in the carboxyl-terminal tail generates an aberrant nuclear phenotype similar to that observed in cells from patients with Dunnigan-type partial lipodystrophy and Emery–Dreifuss muscular dystrophy. Exp Cell Res 282:14–23
13. Fidziańska A, Bilińska ZT, Tesson F, Wagner T, Walski M, Grzybowski J, Ruzyłło W, Hausmanowa-Petrusewicz I (2008) Obliteration of cardiomyocyte nuclear architecture in a patient with *LMNA* gene mutation. J Neurol Sci 271:91–96
14. Gollob MH, Jones DL, Krahn AD, Danis L, Gong XQ, Shao Q, Liu X, Veinot JP, Tang AS, Stewart AF, Tesson F, Klein GJ, Yee R, Skanes AC, Guiraudon GM, Ebihara L, Bai D (2006) Somatic mutations in the connexin 40 gene (GJA5) in atrial fibrillation. N Engl J Med 354:2677–2688
15. Gruenbaum Y, Margalit A, Goldman RD, Shumaker DK, Wilson KL (2005) The nuclear lamina comes of age. Nature Rev Mol Cell Biol 6:21–31
16. Haque F, Lloyd DJ, Smallwood DT, Dent CL, Shanahan CM, Fry AM, Trembath RC, Shackleton S (2006) SUN1 interacts with nuclear lamin A and cytoplasmic nesprins to provide a physical connection between the nuclear lamina and the cytoskeleton. Mol Cell Biol 26:3738–3751
17. Hermida-Prieto M, Monserrat L, Castro-Beiras A, Laredo R, Soler R, Peteiro J, Rodriguez E, Bouzas B, Alvarez N, Muniz J, Crespo-Leiro M (2004) Familial dilated cardiomyopathy and isolated left ventricular noncompaction associated with lamin A/C gene mutations. Am J Cardiol 94:50–54
18. Inagaki N, Hayashi T, Arimura T, Koga Y, Takahashi M, Shibata H, Teraoka K, Chikamori T, Yamashina A, Kimura A (2006) α-B crystallin mutation in dilated cardiomyopathy. Biochem Biophys Res Commun 342:379–386
19. Karkkainen S, Peuhkurinen K (2007) Genetics of dilated cardiomyopathy. Ann Med 39:91–107
20. Kennedy BK, Barbie DA, Classon M, Dyson N, Harlow E (2000) Nuclear organization of DNA replication in primary mammalian cells. Genes Dev 14:2855–2868
21. Ki CS, Hong JS, Jeong GY, Ahn KJ, Choi KM, Kim DK, Kim JW (2002) Identification of lamin A/C (*LMNA*) gene mutations in Korean patients with autosomal dominant Emery–Dreifuss muscular dystrophy and limb-girdle muscular dystrophy 1B. J Hum Genet 47:225–228
22. Krimm I, Östlund C, Gilquin B, Couprie J, Hossenlopp P, Mornon JP, Bonne G, Courvalin J-C, Worman HJ, Zinn-Justin S (2002) The Ig-like structure of the C-terminal domain of lamin A/C, mutated in muscular dystrophies, cardiomyopathy and partial lypodystrophy. Structure 10:811–823
23. Lerman BB, Dong B, Stein KM, Markowitz SM, Linden J, Catanzaro DF (1998) Right ventricular outflow tract tachycardia due to a somatic cell mutation in G protein subunit alpha i2. J Clin Inves 101:2862–2868
24. Liu J, Ben-Shahar TR, Riemer D, Treinin M, Spann P, Weber K, Fire A, Gruenbaum Y (2000) Essential roles for Caenorhabditis elegans lamin gene in nuclear organization, cell cycle progression, and spatial organization of nuclear pore complexes. Mol Biol Cell 11:3937–3947
25. Meier J, Campbell KH, Ford CC, Stick R, Hutchison CJ (1991) The role of lamin LIII in nuclear assembly and DNA replication, in cell-free extracts of *Xenopus* eggs. J Cell Sci 98:271–279
26. Mercuri E, Brown SC, Nihoyannopoulos P, Poulton J, Kinali M, Richard P, Piercy RJ, Messina S, Sewry C, Burke MM, McKenna W, Bonne G, Muntoni F (2005) Extreme variability of skeletal and cardiac muscle involvement in patients with mutations in exon 11 of the lamin A/C gene. Muscle Nerve 31:602–609
27. Mestroni L, Maisch B, McKenna WJ, Schwartz K, Charron P, Rocco C, Tesson F, Richter A, Wilke A, Komajda M (1999) Guidelines for the study of familial dilated cardiomyopathies. Collaborative research group of the European Human and Capital Mobility Project on familial dilated cardiomyopathy. Eur Heart J 20:93–102
28. Moir RD, Montag-Lowy M, Goldman RD (1994) Dynamic properties of nuclear lamins: lamin B is associated with sites of DNA replication. J Cell Biol 125:1201–1212
29. Moir RD, Spann TP, Herrmann H, Goldman RD (2000) Disruption of nuclear lamin organization blocks the elongation phase of DNA replication. J Cell Biol 149:1179–1792
30. Moir RD, Yoon M, Khuon S, Goldman RD (2000) Nuclear lamins A and B1: different pathways of assembly during nuclear envelope formation in living cells. J Cell Biol 151:1155–1168
31. Muchir A, Bonne G, van der Kooi AJ, van Meegen M, Baas F, Bolhuis PA, de Visser M, Schwartz K (2000) Identification of mutations in the gene encoding lamins A/C in autosomal dominant limb girdle muscular dystrophy with atrioventricular conduction disturbances (LGMD1B). Hum Mol Genet 9:1453–1459
32. Muchir A, Medioni J, Laluc M, Massart C, Arimura T, van der Kooi AJ, Desguerre I, Mayer M, Ferrer X, Briault S, Hirano M, Worman HJ, Mallet A, Wehnert M, Schwartz K, Bonne G (2004) Nuclear envelope alterations in fibroblasts from patients with muscular dystrophy, cardiomyopathy, and partial lipodystrophy carrying lamin A/C gene mutations. Muscle Nerve 30:444–450
33. Muchir A, van Engelen BG, Lammens M, Mislow JM, McNally E, Schwartz K, Bonne G (2003) Nuclear envelope alterations in fibroblasts from LGMD1B patients carrying nonsense Y259X heterozygous or homozygous mutation in lamin A/C gene. Exp Cell Res 291:352–362
34. Rowan RA, Masek MA, Billingham ME (1998) Ultrastructural morphometric analysis of endomyocardial biopsies. Idiopathic dilated cardiomyopathy, anthracycline cardiotoxicity, and normal myocardium. Am J Cardiovasc Pathol 2:137–144

35. Perrot A, Hussein S, Ruppert V, Schmidt HH, Wehnert MS, Duong NT, Posch MG, Panek A, Dietz R, Kindermann I, Böhm M, Michalewska-Wludarczyk A, Richter A, Maisch B, Pankuweit S, Ozcelik C (2009) Identification of mutational hot spots in LMNA encoding lamin A/C in patients with familial dilated cardiomyopathy. Basic Res Cardiol 104:90–99
36. Schiender M, Franziska J, Sanz J, Kanel TV, Gallati S (2006) Detection of exon deletions (CFTR) by relative quantification on the lightcycler. Clin Chem 52:2005–2012
37. Scholz D, Diener W, Schaper J (1994) Altered nucleus/cytoplasm relationship and degenerative structural changes in human dilated cardiomyopathy. Cardioscience 5:127–138
38. Shimi T, Pfleghaar K, Kojima S, Pack CG, Solovei I, Goldman AE, Adam SA, Shumaker DK, Kinjo M, Cremer T, Goldman RD (2008) The A- and B-type nuclear lamin networks: microdomains involved in chromatin organization and transcription. Genes Dev 22:3409–3421
39. Shumaker DK, Kuczmarski ER, Goldman RD (2003) The nucleoskeleton: lamins and actin are major players in essential nuclear functions. Curr Opin Cell Biol 15:358–366
40. Smythe C, Jenkins HE, Hutchison CJ (2000) Incorporation of the nuclear pore basket protein nup153 into nuclear pore structures is dependent upon lamina assembly: evidence from cell-free extracts of *Xenopus* eggs. EMBO J 19:3918–3931
41. Spann TP, Goldman AE, Wang C, Huang S, Goldman RD (2002). Alteration of nuclear lamin organization inhibits RNA polymerase II-dependent transcription. J Cell Biol 156:603–308
42. Strelkov SV, Schumacher J, Burkhard P, Aebi U, Herrmann H (2004) Crystal structure of the human lamin A coil 2B dimer: implications for the head-to-tail association of nuclear lamins. J Mol Biol 343:1067–1080
43. Sullivan T, Escalante-Alcalde D, Bhatt H, Anver M, Bhat N, Nagashima K, Stewart CL, Burke B (1999) Loss of A-type lamin expression compromises nuclear envelope integrity leading to muscular dystrophy. J Cell Biol 147:913–920
44. Sylvius N, Bilinska ZT, Veinot JP, Fidzianska A, Bolongo PM, Poon S, McKeown P, Davies RA, Chan KL, Tang AS, Dyack S, Grzybowski J, Ruzyllo W, McBride H, Tesson F (2005) In vivo and in vitro examination of the functional significances of novel lamin gene mutations in heart failure patients. J Med Genet 42:639–647
45. Sylvius N, Hathaway A, Boudreau E, Gupta P, Labib S, Bolongo P, Rippstein P, Mcbride H, Bilinska ZT, Tesson F (2008) Specific contributions of lamin A and lamin C in the development of laminopathies. Exp Cell Res 314:2362–2375
46. Taylor MR, Fain PR, Sinagra G, Robinson ML, Robertson AD, Carniel E, Di Lenarda A, Bohlmeyer TJ, Ferguson DA, Brodsky GL, Boucek MM, Lascor J, Moss AC, Li WL, Stetler GL, Muntoni F, Bristow MR, Mestroni L (2003) Natural history of dilated cardiomyopathy due to lamin A/C gene mutations. J Am Coll Cardiol 41:771–780
47. Taylor MR, Slavov D, Gajewski A, Vlcek S, Ku L, Fain PR, Carniel E, Di Lenarda A, Sinagra G, Boucek MM, Cavanaugh J, Graw SL, Ruegg P, Feiger J, Zhu X, Ferguson DA, Bristow MR, Gotzmann J, Foisner R, Mestroni L (2005) Thymopoietin (lamina-associated polypeptide2) gene mutation associated with dilated cardiomyopathy. Hum Mutat 26:566–574
48. van Berlo JH, de Voogt WG, van der Kooi AJ, van Tintelen JP, Bonne G, Yaou RB, Duboc D, Rossenbacker T, Heidbuchel H, de Visser M, Crijns HJ, Pinto YM (2005) Meta-analysis of clinical characteristics of 299 carriers of *LMNA* gene mutations: do lamin A/C mutations portend a high risk of sudden death? J Mol Med 83:79–83
49. van Tintelen JP, Tio RA, Kerstjens-Frederikse WS, van Berlo JH, Boven LG, Suurmeijer AJH, White SJ, den Dunnen JTD, te Meerman GJ, Vos YJ, van der Hout AH, Osinga J, van den Berg MP, van Veldhuisen DJ, Buys CHC, Hofstra RMW, Pinto YM (2007) Severe myocardial fibrosis caused by a deletion of the 5′ end of the lamin A/C gene. J Am Coll Cardiol 49:2430–2439
50. Vaughan OA, Whitefield WGF, Hutchinson CJ (2000) Functions of nuclear lamins. Protoplasma 211:1–7
51. Verga L, Concardi M, Pilotto A, Bellini O, Pasotti M, Repetto A, Tavazzi L, Arbustini E (2003) Loss of lamin A/C expression revealed by immuno-electron microscopy in dilated cardiomyopathy with atrioventricular block caused by *LMNA* gene defects. Virchows Arch 443:664–671
52. Vlcek S, Dechat T, Foisner R (2001) Nuclear envelope and nuclear matrix: Interactions and dynamics. Cell Mol Life Sci 58:1758–1765
53. Walter MC, Witt TN, Weigel BS, Reilicha P, Richard P, Pongratza D, Bonne G, Wehnert MS, Lochmuller H (2005) Deletion of the *LMNA* initiator codon leading to a neurogenic variant of autosomal dominant Emery–Dreifuss muscular dystrophy. Neuromuscular Disord 15:40–44
54. Wolf CM, Wang L, Alcalai R (2008) Lamin A/C haploinsufficiency causes dilated cardiomyopathy and apoptosis-triggered cardiac conduction system disease. J Mol Cell Cardiol 44: 293–303
55. Zastrow MS, Flaherty DB, Benian GM, Wilson KL (2006) Nuclear titin interacts with A- and B-type lamins in vitro and in vivo. J Cell Sci 119:239–249
56. Zastrow MS, Vlcek S, Wilson KL (2004) Proteins that bind A-type lamins: Integrating isolated clues. J Cell Sci 117:979–987
57. Zhong N, Radu G, Ju W, Brown WT (2005) Novel progerin-interactive partner proteins hnRNP E1, EGF, Mel 18, and UBC9 interact with lamin A/C. Biochem Biophys Res Commun 338:855–861

Appendix II

EXPERIMENTAL CELL RESEARCH 314 (2008) 2362–2375

available at www.sciencedirect.com

ScienceDirect

www.elsevier.com/locate/yexcr

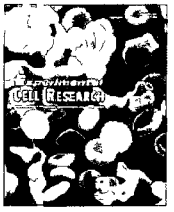

Research Article

Specific contribution of lamin A and lamin C in the development of laminopathies

Nicolas Sylvius[a,*,1], *Andrea Hathaway*[a], *Emilie Boudreau*[a], *Pallavi Gupta*[a], *Sarah Labib*[a], *Pierrette M. Bolongo*[a], *Peter Rippstein*[b], *Heidi McBride*[b], *Zofia T. Bilinska*[c], *Frédérique Tesson*[a]

[a]*Laboratory of Genetics of Cardiac Diseases, University of Ottawa Heart Institute, 40 Ruskin Street, Ottawa, Canada K1Y 4W7*
[b]*University of Ottawa Heart Institute, 40 Ruskin Street, Ottawa, Canada K1Y 4W7*
[c]*First Department of Cardiac Disease, Institute of Cardiology, Alpejska 42, 04-628 Warsaw, Poland*

ARTICLE INFORMATION

Article Chronology
Received 4 January 2008
Revised version received
28 April 2008
Accepted 28 April 2008
Available online 10 May 2008

Keywords:
Lamin A/C gene
Laminopathy
Nuclear envelope
FRAP
Electron microscopy

ABSTRACT

Mutations in the lamin A/C gene are involved in multiple human disorders for which the pathophysiological mechanisms are partially understood. Conflicting results prevail regarding the organization of lamin A and C mutants within the nuclear envelope (NE) and on the interactions of each lamin to its counterpart. We over-expressed various lamin A and C mutants both independently and together in COS7 cells. When expressed alone, lamin A with cardiac/muscular disorder mutations forms abnormal aggregates inside the NE and not inside the nucleoplasm. Conversely, the equivalent lamin C organizes as intranucleoplasmic aggregates that never connect to the NE as opposed to wild type lamin C. Interestingly, the lamin C molecules present within these aggregates exhibit an abnormal increased mobility. When co-expressed, the complex formed by lamin A/C aggregates in the NE. Lamin A and C mutants for lipodystrophy behave similarly to the wild type. These findings reveal that lamins A and C may be differentially affected depending on the mutation. This results in multiple possible physiological consequences which likely contribute in the phenotypic variability of laminopathies. The inability of lamin C mutants to join the nuclear rim in the absence of lamin A is a potential pathophysiological mechanism for laminopathies.

Introduction

The lamin A/C gene (*LMNA*) has been implicated in numerous diseases referred to as "laminopathies" that affect the heart, skeletal muscle, adipose tissue, bones, peripheral nerves, skin, or cause premature aging [1].

Lamins A and C are type V intermediate filament proteins expressed in terminally differentiated somatic cells, and synthesized by alternative splicing of *LMNA*. Both proteins share the same first 566 amino acids but differ in their carboxyl terminus. Lamins A and C have 646 and 572 amino acids respectively and are known for their structural role in supporting the nuclear architecture and anchoring chromatin and the nuclear pore complexes to the nuclear membrane. Indeed, along with B-type lamins, they are the main components of the lamina, a filamentous meshwork underlying the inner nuclear

* *Corresponding author* CEA/Institut de Génomique, Centre National de Génotypage, 2 rue Gaston Crémieux, Bâtiment G2, CP 5721, 91057 Evry Cedex, France.
E-mail address: sylvius@cng.fr (N. Sylvius).
[1] Current address. Centre National de Génotypage, 2 rue Gaston Crémieux, CP 5721, 91 057 Evry Cedex, France.

0014-4827/$ – see front matter
doi:10.1016/j.yexcr.2008.04.017

membrane. However, they are also present within the nucleus [2]. In addition to participating in nuclear architecture, there is a growing body of evidence showing that lamin A/C plays a key role in gene transcription regulation, DNA repair and replication [1,3], and cell differentiation regulation [1,4,5]. The list of lamins A and C partners is regularly growing [2,6–9], which confirms that these proteins are involved in multiple functions, some of which are still being unravelled. For instance, it has recently been shown that lamins A and C are tightly connected to the cytoskeleton, thus revealing a nuclear–cytoskeletal continuity [10]. Also, some LMNA mutations have been reported to affect the posttranslational machinery of the cell. It has been shown that the nuclear localization of SUMO1 (ubiquitin-related modifier1) is totally disrupted in the presence of the DCM-associated D192G lamin C mutant [11].

Whether or not lamin A is required for lamin C to be localized into the nuclear envelope remains debated. The early death of lmna knockout mice ($lmna^{-/-}$) [12] or the dramatic lamina defects observed when silencing lamin A/C in human endometrial stromal cells [13], clearly demonstrates that at least one of the two proteins is required for survival. However, a recent study in fibroblasts from mice expressing only lamin C have shown that lamin C is normally targeted to the nuclear envelope [14]. As well, nuclei shape from these fibroblasts is only mildly altered and the mice do not exhibit any symptoms of muscle diseases. Furthermore, lamin C has also been shown to be sufficient for proper localization of both emerin [14] and nesprin-2 [15] at the nuclear envelope. These studies therefore suggest that lamin C can substitute for lamin A on its own and provide functional support to the nuclear envelope. However, these results strikingly contradict several other studies which showed that lamin A targets both lamin C and emerin to the nuclear envelope [16–19].

Furthermore, nuclear envelope alterations associated with LMNA mutations have long been reported [11,20–23]. Mice expressing M371K lamin A exhibit cardiomyocytes with convoluted nuclear envelopes, intranuclear inclusions and chromatin clumps in nuclei [24]. Several LMNA mutations are known to result in the aggregation of lamin A *in vitro* [18,25–27]. In a previous report, we found DCM-causing LMNA mutations leading to the aggregation of nuclear lamin C as well [11]. However, the physiological consequences of these aggregates as well as the impact of these mutations on lamin C specifically or on the complex lamin A/lamin C have only been partially investigated. It is unclear whether or not these lamin A and lamin C aggregates retain the capability to incorporate themselves into the nuclear envelope either in combination or independently.

In humans, most reported LMNA mutations are found in Emery–Dreifuss muscular dystrophy and dilated cardiomyopathy (DCM) but the spectrum of phenotypes is constantly extending [28]. Nuclear fragility and/or abnormalities in the tissue/cell-specific gene expression are the main two hypotheses proposed to explain how mutations in this gene cause such a large spectrum of diseases [1]. However, the exact pathophysiological mechanisms remain puzzling. In this study, we propose to further examine wild type and mutated lamin A and C behaviour separately and then in combination. In an attempt to better clarify the lamin A and lamin C respective functions and shed light on the properties of lamin A/C affected in laminopathies, we compared various LMNA mutations previously reported in DCM (L85R, D192G, N195K) [29], autosomal dominant Emery–Dreifuss muscular dystrophy (R386K) [30] or lipodystrophy (R482W) [31].

Methods

Expression plasmid and mutagenesis

Our cloning procedures of wild type and mutated full-length human lamins A and C as C-terminal fusions to either the enhanced cyan, yellow or red fluorescent protein sequence of, respectively pECFP-C1, pEYFP-C1, and pDsRed2-C1 fluorescent expression vectors, have previously been described [11]. L85R, D192G, N195K, R386K and R482W point mutations were introduced in the lamin A and lamin C cDNAs by site directed mutagenesis using primers previously published [11,18,27]. All clones were systematically sequenced.

Fluorescent microscopy

Images were captured on an Olympus 1×70 inverted microscope and processed using TILLvisION software (version 4.0), or an Olympus Fluoview FV1000 confocal microscope with a 100× 1.4 NA oil immersion objective (UplanSApo) and using the Olympus FV-10 acquisition software, version 5.0, to acquire images.

Fluorescence recovery after photobleaching experiments (FRAP)

FRAP experiments were performed on living transfected COS7 cells at 37 °C. Only the transfected cells displaying a phenotype characteristic of the mutation investigated were considered for FRAP experiments. To minimize cell physiology disturbance, we chose to photobleach selected areas for 10 iterations at 16% power of the argon laser. After photobleaching, 42 images were captured every 5 s for 210 s at 1.5% power of the argon laser. FRAP was performed during such a short period of time to limit bias due to nuclear rotation and cell movement. Average fluorescence intensity in each region of interest was normalized to total cellular fluorescence loss during bleach and imaging phase as $I_{rel}=T_0 I_t/T_t I_0$ as described by Phair et al. [32] (T_0, total cellular intensity during prebleach; T_t, total cellular intensity at time t; I_0, average intensity in the region of interest during prebleach, I_t, average intensity in the region of interest at time t). Fluorescence of surrounding cells was taken into account in cases of cells exhibiting a single speckle (mutation D192G and R386K). A non linear regression was used to create a best fit curve. Difference in the $t_{1/2}$ between L85R, D192G, R386K and wild type lamin C aggregates was assessed by a *T*-test.

Immunocytochemistry

Transfected cells were fixed on coverslips with 4% paraformaldehyde in phosphate buffered saline (PBS) and permeabilized with 10% Triton-100 for 5 min. Cells were incubated with the primary antibody (RanGap1 (N-19) polyclonal antibody (Santa Cruz)) in 10% fetal bovine serum (1:50) and with Alexa Fluor 594-labeled Rabbit Anti-Goat antibody (Molecular Probes) for 30 min. The coverslips were mounted on a glass slide with mowiol.

Immunoblotting

Western blot analyses were performed as previously described by Sylvius et al. [11]. The primary antibody used was goat anti-lamin A/C (N-18) polyclonal antibody and mouse anti beta actin (C4) monoclonal antibody (Santa Cruz) and the secondary antibodies were peroxidase-linked anti-goat and anti-rabbit antibodies (Santa Cruz).

Cell preparation for EM

Cells were fixed in 1.6% glutaraldehyde in 0.1 M sodium cacodylate buffer pH 7.2. They were then resuspended in 15% bovine serum albumin infiltrated for 30 min and pelleted by centrifugation. The supernatant was removed and the cell pellets were coagulated with 1.6% glutaraldehyde in 0.1 M sodium cacodylate buffer pH 7.2. The resulting firm pellets were cut into 1 mm pieces post-fixed in 1% osmium tetroxide dehydrated in ascending alcohols and embedded in Spurr epoxy resin. Thin sections were stained with uranyl acetate and lead citrate and examined with a Jeol 1230 TEM equipped with AMT software.

Results

We transiently expressed the full-length human wild type and the various mutant lamins A and C cDNAs fused to the C-terminus of variants of the *Aequorea victoria* green fluorescent protein (GFP) (lamin-FP) in fibroblast COS7 and rat cardiomyoblast H9C2 cells. To assess the consequences of mutations on

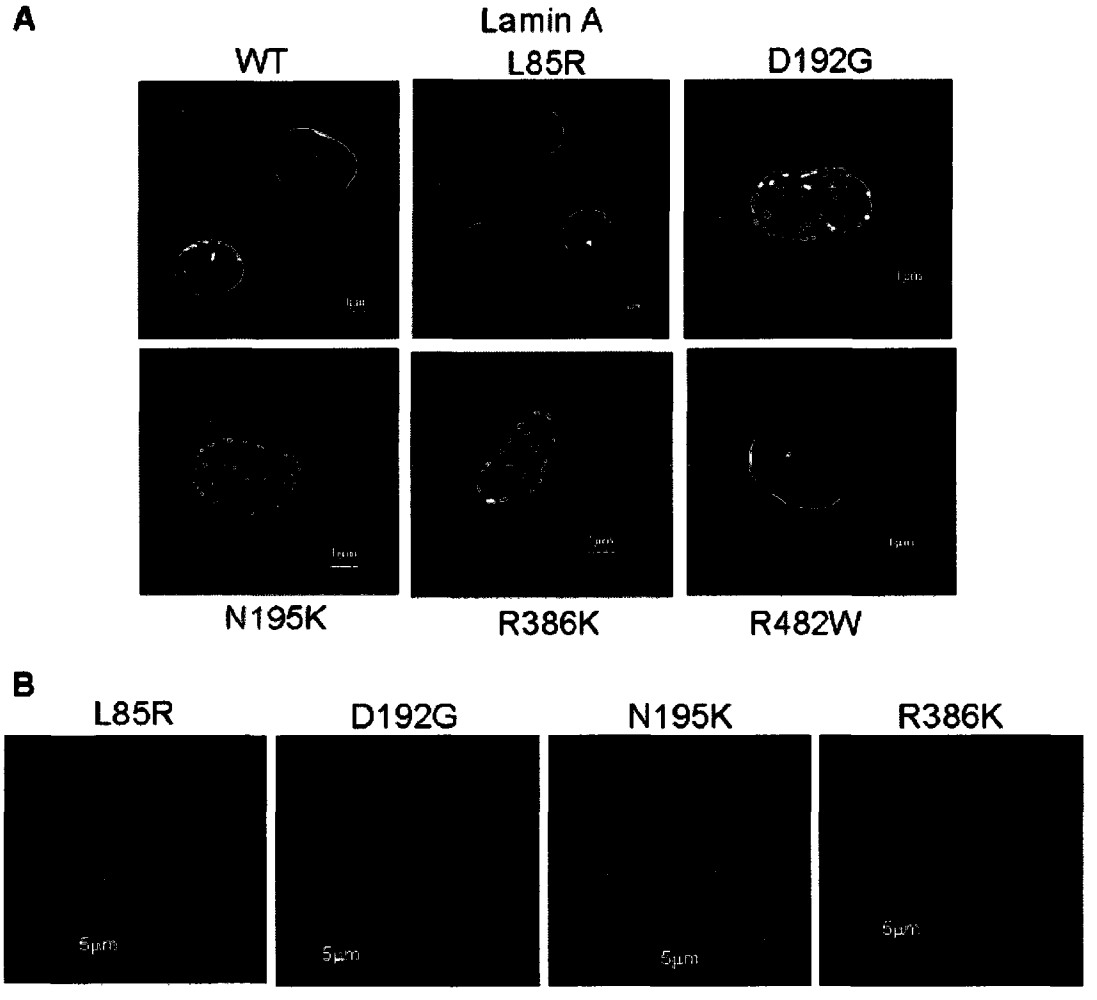

Fig. 1 – A. Nuclei expressing wild type or the various lamin A mutant constructs transiently expressed as ECFP fusion protein in COS7 cells. Cells were visualized by wide-field fluorescence microscopy with an excitation wavelength of 433 nm. Wild type lamin A, as well as L85R and R482W lamin A mutants homogeneously organize throughout the nucleus. In contrast, D192G, N195K and R386K lamin A mutants accumulate in abnormal aggregates. The nuclear membrane appears granular and discontinued. B. The abnormal lamin A aggregation previously found in COS7 cells expressing D192G, N195K and R386K lamin A, was confirmed in nuclei of rat cardiomyoblast H9C2 cells as opposed to cells expressing wild type or L85R lamin A (not shown).

Fig. 2 – Confocal microscopy picture of H9C2 cell nuclei transiently expressing D192G lamin A as ECFP fusion protein. Mutated lamin A organizes as aberrant aggregates. However, the spherical organization of these aggregates reveal that they are likely embedded in the nuclear envelope.

lamin A and C properties specifically, we used confocal immunofluorescence microscopy to examine the cells expressing lamins A-FP and C-FP separately and then together.

Lamin A mutants aggregate

The wild type phenotype was characterized by a homogeneous distribution of the protein throughout the nucleus (Fig. 1A). L85R and R482W lamin A-FP did not exhibit any aberrant phenotype compared to the wild type (Figs. 1A and B). It is noted that the images of cells expressing L85R lamin A were carefully analyzed since this mutant was previously reported as slightly different from the wild type [18]. In contrast, D192G, N195K and R386K lamin A-FP accumulated in abnormal, giant aggregates (Figs. 1A and B), which is consistent with results already described in C2C12 or COS7 cells [11,26,27]. Several immunofluorescence microscopy studies performed on cells lines transfected with lamin A/C have reported the aggregation of lamin A as intranuclear foci or nuclear aggregates inside the nucleoplasm [18,25–27]. To confirm this statement in our analyses, we used confocal immunofluorescence microscopy and 3D reconstruction of the cell (Fig. 2). Although we could not exclude the presence of nucleoplasmic aggregates, it was obvious that the aggregates were massively present at the periphery of the nucleus and led to a punctate aspect of the nucleus, as shown on Fig. 2. This punctate aspect suggests that lamin A-FP mutants retain the ability to locate at the nuclear envelope, albeit not properly.

Abnormal lamin C aggregation is a common feature of several LMNA mutations

We then examined the effect of these mutations on lamin C only. As previously described, wild type lamin C-FP gave rise to multiple small intranuclear aggregates, known as speckles.

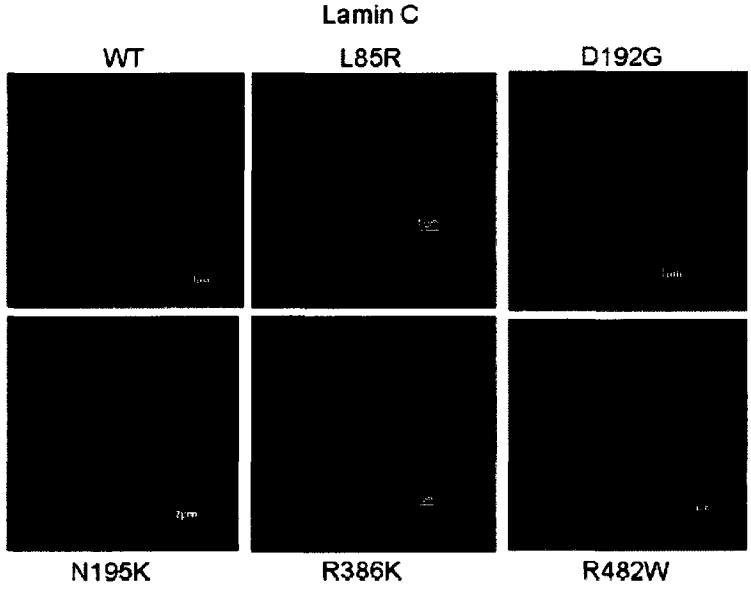

Fig. 3 – Nuclei expressing wild type or the various mutated lamin C constructs transiently expressed as ECFP fusion protein in COS7 cells. Prior to visualization by wide-field fluorescence microscopy, Hoechst 33258 dye was used to locate the nuclei (in blue). Excitation wavelengths were 433 nm for lamin C-ECFP and 365 nm for Hoechst 33258. Note that the aberrant aggregation of the lamin C (in red) within the nucleus visualized by Hoechst 33258 dye is common to several *LMNA* mutations. Only R482W lamin C mutants responsible for lipodystrophy gave rise to a phenotype similar to the wild type.

that are evenly distributed throughout the nucleus [11]. R482W lamin C-FP showed a phenotype similar to the wild type whereas D192G lamin C-FP accumulated in one or two intranuclear giant speckles (Fig. 3), which agrees with previously published studies performed on COS7 or HeLa cells [11,18]. Interestingly, L85R, D192G, N195K, and R386K lamin C-FP mutants also showed a dramatic aggregation in the vast majority of transfected cells (Fig. 3). In COS7 cells, the respective mean speckle diameters were 4.7+/ 2 μm (n=9) for L85R lamin C-FP, 5.2+/- 1 μm (n=11) for D192G lamin C-FP, 5.3+/- 2.5 μm (n=3) for N195K lamin C-FP, 7.1+/- 4 μm (n=10) for R386K lamin C-FP, and 2.9+/- 1.5 μm (n=11) for wild type lamin C-FP. The mean nuclear diameter was 15 μm (+/- 1.5 μm) for all transfected COS7 cells. Intriguingly, L85R lamin C-FP exhibited an aberrant phenotype compared to wild type lamin C-FP, as opposed to its counterpart lamin A-FP which behaved similarly

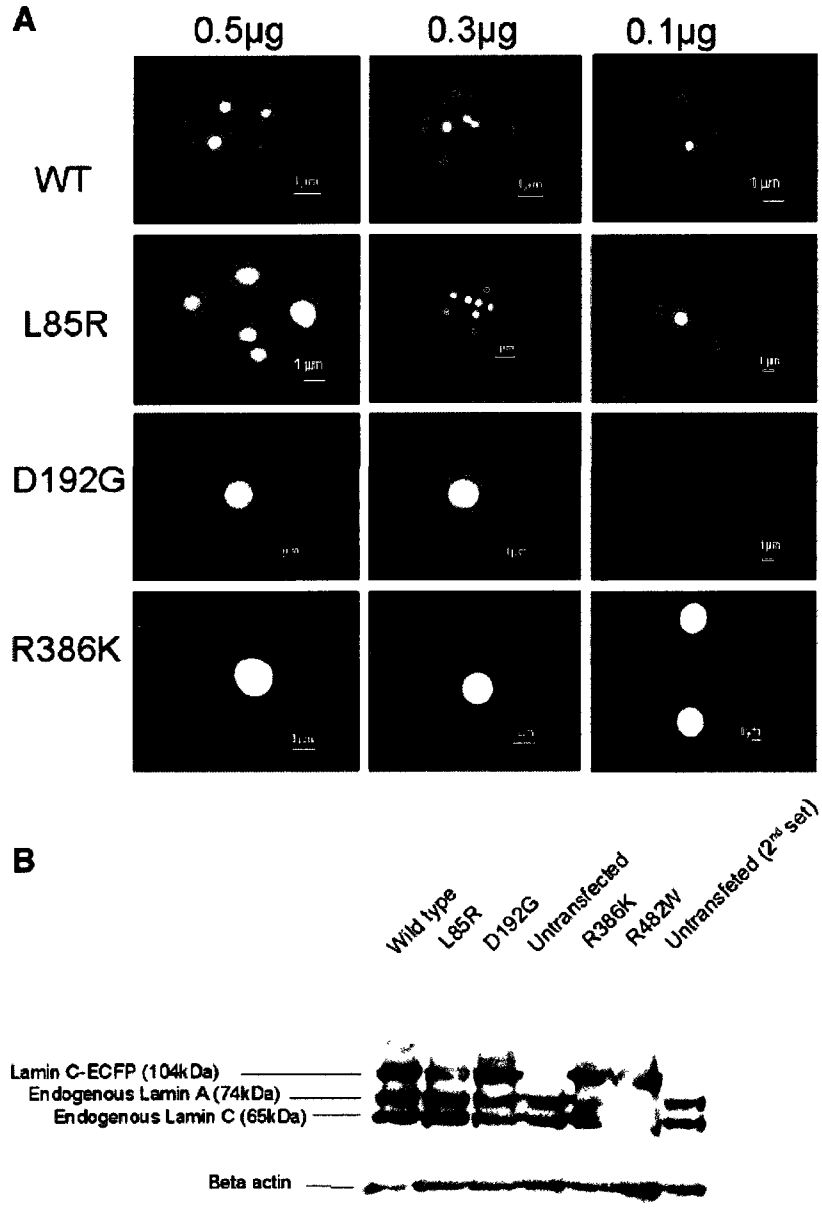

Fig. 4 – A. Transient transfections of COS7 cells with varying quantity of either wild type or mutated lamin C-FP constructs. Cells were visualized by wide-field fluorescence microscopy with an excitation wavelength of 433 nm. The phenotype observed with mutated lamin C-FP is not due to a too elevated quantity of vectors used to transfect the cells. B. Representative Western blot analysis of COS7 cells transfected with the different lamin C-FP variants and using anti lamin A/C antibody. Results show equal over-expression for all construct.

to the wild type lamin A-FP. This suggests that both proteins were differentially affected by the mutation. Aberrant aggregation of nuclear lamin C-FP was observed in less than 20% of COS7 cells expressing wild type lamin C-FP. This proportion was similar to that we previously reported [11].

To ensure that this abnormal lamin C aggregation was not an artifact due to the over-expression of the protein we transfected COS7 cells using lower concentrations of constructs (0.3 μg and 0.1 μg). Lamin C-FP mutants formed giant aggregates at each tested concentration indicating that the formation of large

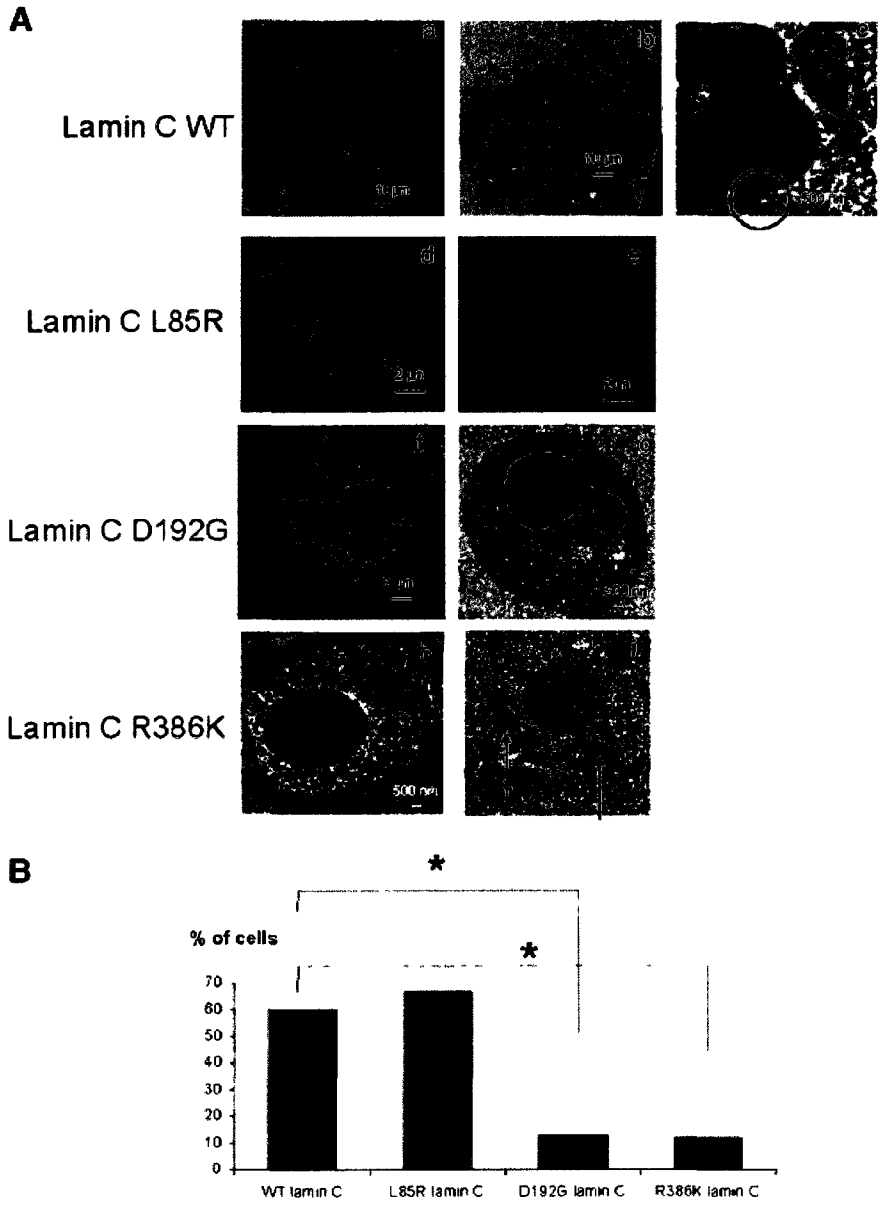

Fig. 5 – A. Electron micrographs of COS7 cells transiently transfected with lamin C-FP constructs. In 60% of cells, wild type lamin C nuclear aggregates were localized in close contact with the nuclear envelope (a–c). Notably, wild type aggregates were able to establish close contact with the nuclear envelope (circle) (c). Similarly, L85R lamin C aggregates organized in contact with the nuclear envelope (d–e). Conversely, in 88% and 87.5% of cells respectively, D192G and R386K lamin C aggregates were found within the nucleoplasm without any contact with the nuclear envelope (f–i). In 30% of cells expressing R386K lamin C, nuclei presented with lamin C aggregates localized outside the nuclear envelope (j–k). B. Percentage of transfected cells displaying lamin C nuclear aggregates in direct contact with the nuclear envelope. χ^2 test showed that the number of cells displaying lamin C aggregates in close contact with the nuclear envelope is significantly different in transfected cells expressing D192G or R386K lamin C mutants compared to the wild type ($p<0.01$).

aggregates was not an artifact due to an exaggerated dose of DNA (Fig. 4A). Furthermore, Western blotting quantification of lamin mutants did not reveal any difference in the transfection efficiency compared to the wild type, confirming that these giant aggregates did not result from transfection artifact (Fig. 4B).

Mutated lamin C loses its ability to incorporate into the nuclear envelope

We further assessed whether lamin C aggregates retain their ability to join the nuclear envelope. As a means to better see envelope shape and potential misshapen nuclei, we chose to

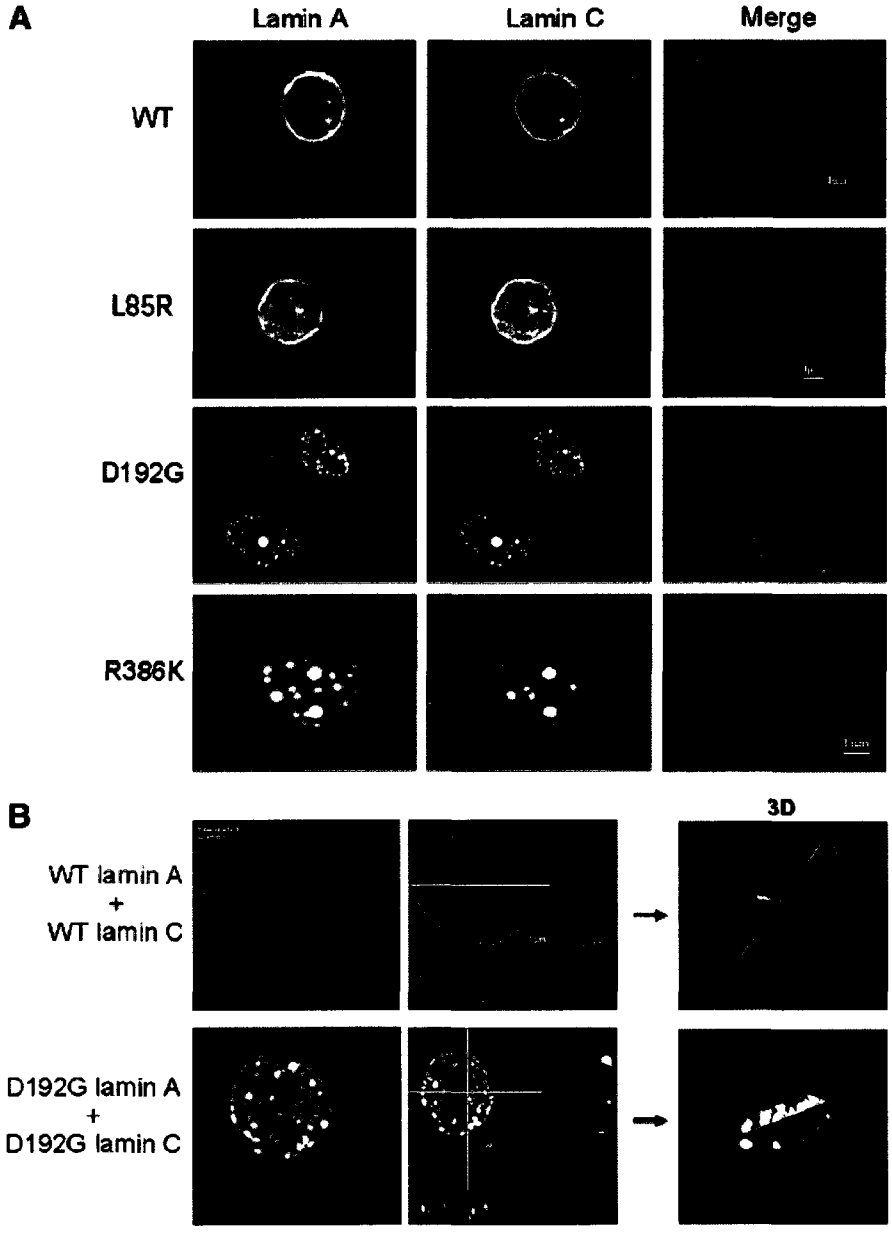

Fig. 6 – A. COS7 cell nuclei transiently co-expressing wild type or mutated lamin A and lamin C constructs. Lamins A and C were inserted into pECFP-C1 and pDsRed2-C1 fluorescent expression vectors respectively. Cells were visualized by wide-field fluorescence microscopy with excitation wavelengths of 433 nm for lamin A-FP and 558 nm for DsRed2-lamin C. Compared to the wild type, the complex lamin A/C forms aggregates and the membrane appears granular and discontinued.
B. Laser-scanning confocal microscopy of COS7 cells nuclei transiently co-transfected with either wild type or mutated lamin A and lamin C. Lamin A (in red) and lamin C (in green) were inserted into pECFP-C1 and pEYFP-C1 fluorescent expression vectors; respectively. Excitation wavelengths were 433 nm for lamin A-FP and 558 nm for DsRed2-lamin C.

perform electron microscopy on COS7 cells expressing the wild type or the various lamin C-FP mutants. We restricted the analysis to wild type lamin C and L85R, D192G and R386K lamin C mutants since each of these mutants are representative of a single phenotype. No nuclear deformation was observed in any of the transfected cells. However, in most cells expressing wild type lamin C-FP (60%), lamin C aggregates were in close contact with the nuclear envelope (Fig. 5Aa–b). Clearly, close connections between wild type lamin C aggregates and the nuclear envelope are possible (Fig. 5Ac). Conversely, the number of cells exhibiting such a proximity between aggregates and the nuclear envelope was dramatically reduced in the case of D192G and R386K lamin C-FP (12% and 12.5% respectively; wild type: $n=47$; D192G: $n=38$, $p<0.01$; R386K: $n=17$, $p<0.01$) (Figs. 5Af–i and B). In most of these cells, speckles were found within the nucleoplasma and did not exhibit any close connection with the nuclear envelope as opposed to cells expressing wild type lamin C-FP. In the case of L85R lamin C-FP, the percentage of cells exhibiting lamin C aggregates in contact with the nuclear envelope was similar to the wild type (L85R, $n=24$, $p<0.1$) (Fig. 5B). This finding implies that wild type lamin C is able to establish connections with the nuclear envelope in the absence of lamin A. This also implies that mutations D192G and R386K caused the inhibition of the lamin C/nuclear envelope connection. The L85R mutation had no effect on this contact. Again, this supports the hypothesis that each LMNA mutation has specific consequences in regards to lamin A/C properties. It is noteworthy to mention that a significant proportion of cells (30%, $n=17$, $p<0.05$) expressing R386K lamin C exhibited aggregates abnormally localized outside the nuclear membrane (Arrows in Fig. 5Ai). This is rarely observed in nuclei of cell expressing wild type (<8%, $n=47$), or the other lamin C mutants (<18% for D192G, $n=38$, $p>0.05$; <12% for L85R, $n=24$, $p>0.05$). However, electron microscopy analysis of the nuclear envelope of cells expressing R386K lamin C did not reveal any obvious abnormality.

Nuclear localization of lamin A/C mutant complexes in COS7 cells

To find out whether lamin A/C complexes localized in the nuclear envelope, we then co-expressed the wild type and each mutated lamin A-FP with its corresponding lamin C, except for N195K and R482W lamin A/C since these mutants are similar to D192G and wild type respectively. To circumvent bleedthrough issues due to confluent spectral profiles exhibited by C-FP and YFP fluorophores, the wild type and the various lamin A-FP mutants were expressed concomitantly with their counterpart lamin C cloned in pDsRed2-C1 expression vectors. When co-expressed, wild type lamin A-FP and wild type DsRed2-lamin C were homogeneously distributed throughout the nuclear envelope, conferring the nucleus with a veil-like appearance (Fig. 6A). In contrast, D192G and R386K mutants resulted in abnormal aggregations of the complex lamin A/C, which is

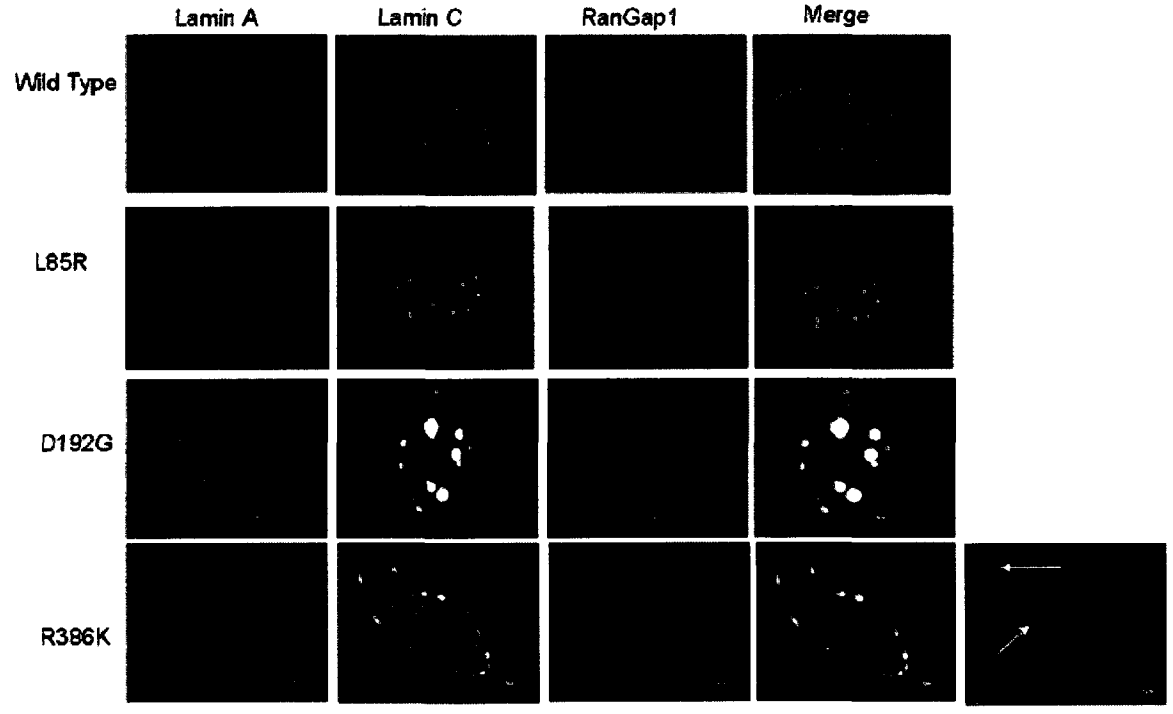

Fig. 7 – Confocal immunofluorescence microscopy pictures of COS7 cells nuclei transiently co-expressing wild type or mutated lamin A-FP and lamin C-FP and immunostained with the anti RanGaP1 polyclonal antibody (N-19). RanGap appears normally distributed in the nuclear envelope. Arrows indicate nuclei with R386K lamin C aggregates localized outside the nuclear envelope.

consistent with previous results [11,18]. Cells expressing L85R lamin A-FP and L85R DsRed2-lamin C exhibited a phenotype similar to the wild type, which suggests that co-expression of both lamins rescues the wild type phenotype. Although L85R DsRed2-lamin C formed speckles within the nucleus (Figs. 3 and 4), we showed that these speckles retained the capacity to make contact with the nuclear envelope (Fig. 5A). Most importantly, even when mutated, lamins A and lamin C always co-localized and were situated in close contact with the nuclear envelope as made evident by confocal microcopy (Fig. 6B). However, in some cells expressing R386K lamins A and C, we observed aberrant localizations of lamin A/C aggregates outside of the nuclear envelope visualized by anti RanGap1 (Arrows in Fig. 7), similarly to cells expressing R386K lamin C-FP only (Fig. 5Ai). Furthermore, the expression of lamin A mutants did not disturb the distribution of endogenous RanGap1 as revealed by immunostaining with an anti RanGap1 (N-19) polyclonal antibody (Fig. 7). Notably, Rangap1 was not enriched in lamin A/C aggregates (Fig. 7). Since RanGAP1 is a Ran GTPase-activating protein present on the cytoplasmic side of nuclear pore complex during interphase, this result suggests that the nuclear pore complexes were correctly localized in the nuclear rim of transfected cells.

Mutated lamin C molecules present in giant aggregates exhibit increased mobility

It has been shown that some *LMNA* mutations are associated with an increased mobility of lamin A within the nuclear envelope [33] which indicates that some *LMNA* mutations affect the mobility of lamin A/C molecules. We hypothesized that the inability of lamin C mutants to properly incorporate into the nuclear envelope would reflect a different rigidity of the molecular structure of lamin C aggregates compared to the wild type. This would lead to defective connection with the nuclear envelope. To assess the mobility of the lamin C molecules inside the aggregates, we performed Fluorescence Recovery After Photobleaching (FRAP) on living COS7 cells expressing L85R, D192G, R386K or wild type lamin C-FP. A defined area of selected aggregates was bleached by a series of high-powered spot laser pulses (Fig. 8A). The recovery of fluorescence in this area was then monitored as a mean to assess the mobility of lamin C

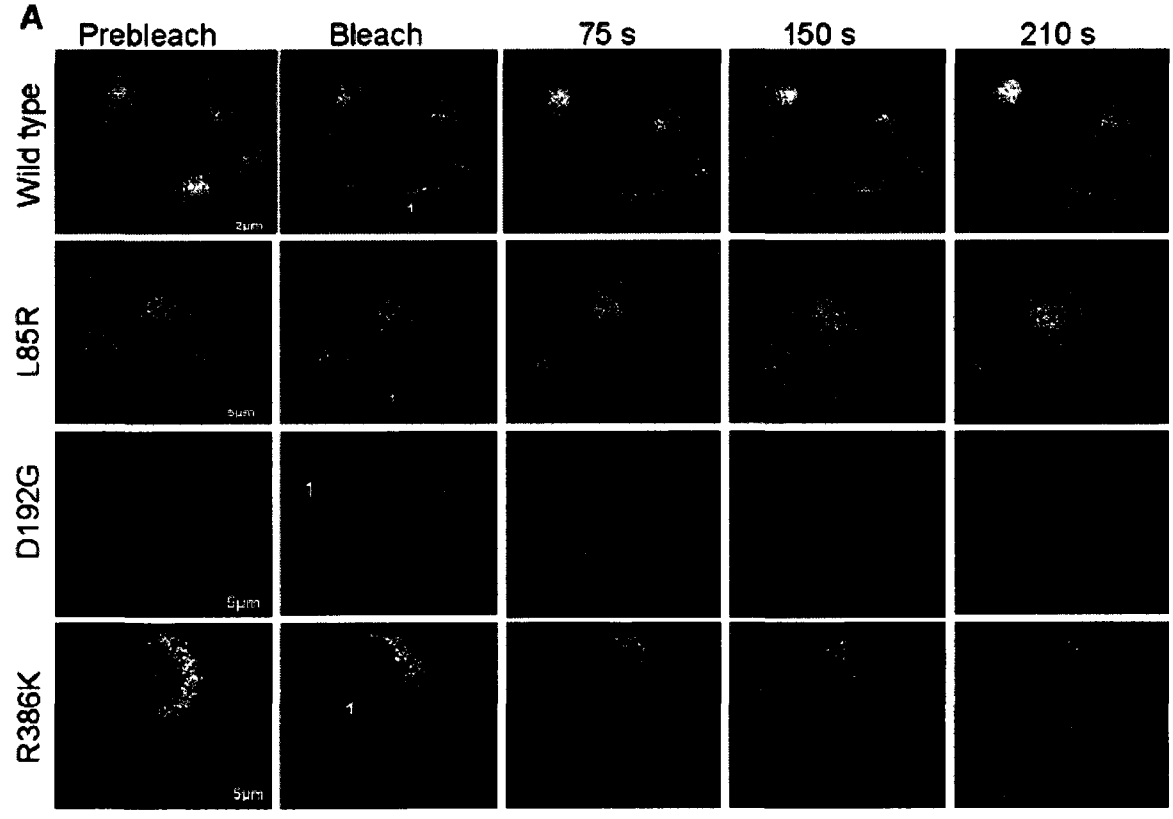

Fig. 8 – A. FRAP experiments on wild type and L85R, D192G and/or R386K lamin C nuclear aggregates of COS7 cells. The boxed regions were bleached and the fluorescence recovery was monitored over a 210 s period. B. Quantitative experiments showing normalized fluorescence recovery after photobleaching of a targeted region of the lamin C nuclear aggregates in COS7 cells. (a) The fluorescence intensity in the bleached area is expressed as a relative recovery. Error bars indicates SEM, $n=7$. 1 is the level of fluorescence before bleaching. (b) We assessed the time after photobleaching required for fluorescence to recover the median value between the prebleach and just after the bleach ($t_{1/2}$) as a mean to reflect the dynamics of molecule.

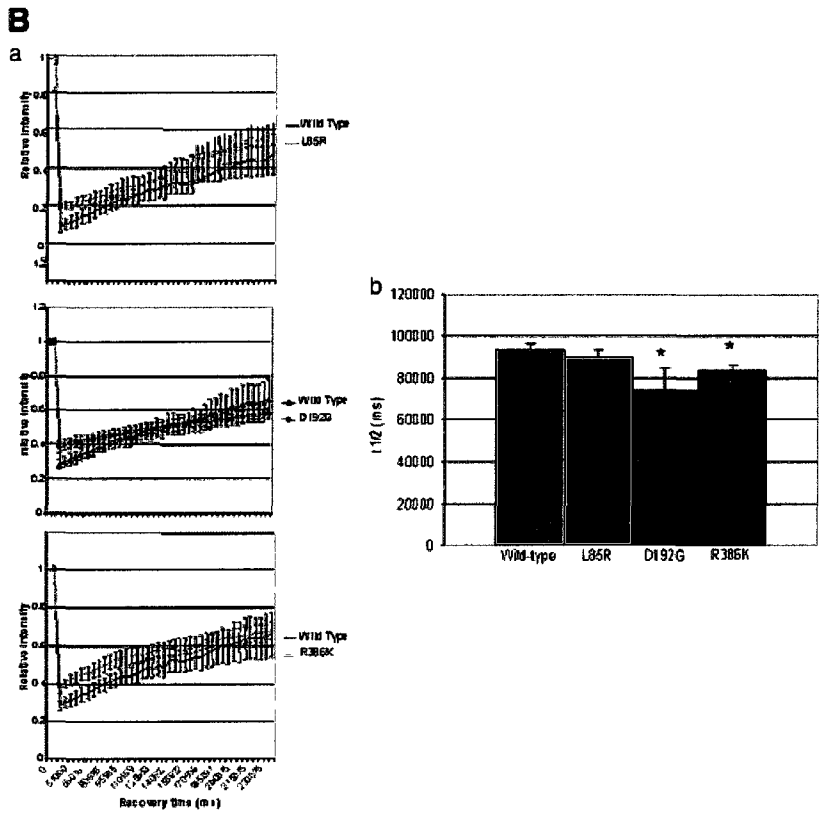

Fig. 8 (continued).

molecules within each aggregate. T-test confirmed that the time after bleaching required to recover 50% of the plateau ($t_{1/2}$, half time recovery) was significantly decreased in D192G ($p=0.02$) or R386K ($p=0.03$) lamin C-FP aberrant speckles compared to wild type lamin C-FP speckles (Fig. 8B), thus revealing that the dynamics of mutated lamin C molecules is significantly higher within D192G and R386K lamin C aggregates than within wild type aggregates. In contrast, in L85R lamin C aggregates, the difference is not significant. Therefore, in comparison to the wild type, the D192G and R386K lamin C intra-aggregates molecules appeared to be more mobile which is indicative of a less stable structure of the mutants. This finding was corroborated by three-minute films showing that R386K lamin C-FP speckles were more prone to move and fuse to each other (data not shown). No difference was observed with L85R (Figs. 8A and B) and R482W (data not shown) aggregates compared to the wild type.

Discussion

In order to better differentiate and define lamin A and lamin C functions, we used a cell model to express the lamins individually and then together. In view of the conflicting results in previous studies regarding the effect of *LMNA* mutations, we duplicated some of the experiments in COS7 cells and H9C2 rat cardiomyoblasts. Results are summarized in Table 1.

Mutated lamins A organize as nuclear envelope aggregates

Our results showed that some mutated lamin A (D192G, N195K, R386K) form abnormal aggregates when expressed alone, which is consistent with previous studies [11,26,27]. However, in contrast to previous studies reporting lamin aggregates described as intranuclear [18,25–27], we found that lamin A aggregates mainly localized at the nuclear periphery of the nucleus, suggesting that although unable to properly organize in the nuclear rim and form the lamina, lamin A mutants keep the capability of associating with the nuclear envelope. Alternatively, other mutants (L85R, R482W) behaved in a way that was indistinguishable from the wild type.

Lamin C mutants form aberrant intranucleoplasmic aggregates and lose their ability to join the nuclear envelope

We also expressed lamin C alone and showed that aberrant lamin C aggregation within the nucleoplasm is a defect common to several *LMNA* mutations (L85R, D192G, N195K, R386K). Interestingly, only the mutations responsible for skeletal and cardiac diseases were found to result in this atypical aggregation whereas mutation R482W involved in human lipodystrophy, did not result in noticeable abnormalities in the location or distribution of either lamin A or lamin C. This finding suggests that the pathophysiological mechanism of laminopathies with

Table 1 – Summary of the phenotypes observed for the LMNA mutations selected in the study

Variants	Diseases	Phenotypes		
		Lamin A alone	Lamin C alone	Lamin A+C
Wild type		Homogenous distribution throughout the nuclear envelope	Numerous small intranuclear aggregates mainly in close contact with the nuclear envelope	Homogenous distribution throughout the nuclear envelope
L85R	DCM	Homogenous distribution throughout the nuclear envelope similarly to the wild type	Rare intranuclear giant aggregates which may make contact with the nuclear envelope	Homogenous distribution similarly to the wild type
D192G	DCM	Aggregates located at the periphery of the nucleus	Rare intranuclear giant aggregation without contact with the nuclear envelope. Lamin C molecules display increased mobility.	Aberrant aggregation of lamin A/C complexes connected to the nuclear envelope
N195K	DCM	Aggregates located at the periphery of the nucleus	Rare intranuclear giant aggregates	
R386K	EDMD	Aggregates located at the periphery of the nucleus.	Rare intranuclear giant aggregates without contact with the nuclear envelope. Significant proportion of these aggregates localize outside the nuclear membrane. Lamin C molecules display increased mobility.	Aberrant aggregation of lamin A/C complexes connected to the nuclear envelope
R482W	FPLD	Homogenous distribution throughout the nucleus similarly to the wild type	Phenotype indistinguishable from the wild type	

AD-EDMD: Autosomal dominant muscular dystrophy, DCM: Dilated cardiomyopathy, and FPLD: Dunningan-type familial partial lipodystrophy.

cardiac involvement is distinct from lipodystrophy and engages lamin C but not lamin A as made evident by the absence of abnormal phenotype in cells expressing lamin A with the dilated cardiomyopathy mutation L85R. Other mutations responsible for cardiomyopathy or muscular dystrophy have also been reported to result in aberrant lamin A or C aggregation such as mutations E358K, M358K [27], or R453W [25]. However, all mutations should be tested to corroborate this conclusion and determine if this lamin C aggregation inside the nucleoplasm could be regarded as a potential hallmark of laminopathies with cardiac or muscular involvement. So far, more than two hundred mutations have been reported of which most are listed in the database http://www.dmd.nl/nmdb/index.php?select db=LMNA.

Compared to some previous reports [16–19], we sometimes obtained divergent phenotypes of cells expressing the lamin mutants. For example, Raharjo et al. showed that L85R lamin A exhibits a punctate distribution across the nuclear surface slightly different from the wild type, which opposes our results and other studies [27]. Also, N195K and R386K lamin A mutants have been shown to re-localize to the nucleoplasm [18,27,34]. These discrepancies may be explained by protocol differences such as i) the antibody used which can be directed against lamin A, lamin C, or both lamins; ii) the expression vectors used for the transfection which requires either direct or indirect immunofluorescence analysis; iii) the cell lines used (C2C12, HeLa, COS7, SW13, H9C2) since each cell type expresses different levels of endogenous A-type lamin and differently handles the expression of exogenous lamin A/C.

It is interesting to note that aberrant lamin C aggregation may also be present in a small proportion of nuclei expressing wild type lamin C. This suggests that the presence of these aggregates corresponds to a transient stage of the cell cycle. We can hypothesize that cells expressing these mutants would be longer fixed in this stage. Recently, it has been shown that the mutant lamin A involved in Hutchinson–Gilford Progeria Syndrome and harboring a 50 amino acid deletion alters the cell cycle progression [35].

Furthermore, several studies have suggested that lamin A plays a key role in targeting lamin C and Emerin to the nuclear envelope [16–19]. However, recent work in embryonic fibroblasts from mice expressing lamin C only (lco) showed that lamin C and emerin are normally localized into the nuclear envelope even in the absence of lamin A [14]. Furthermore, $Lmna^{lco/lco}$ fibroblasts from these mice display nuclear envelope with only very minimal alterations. The extrapolation of these results to human is hazardous since mouse models often exhibit differences compared to human laminopathies [36,37]. For example, two mutated H222P alleles are necessary to develop muscular dystrophy in mice, whereas the patients are heterozygous [36]. Similarly, the clinical phenotype of LmnaL530P/L530P mice, harboring an Emery–Dreifuss mutation, is consistent with human progeria syndrome [38]. In this study, we used a cell model expressing lamin C only, and brought evidence that wild type lamin C has the capacity to establish close connections with the nuclear envelope on its own (Figs. 5Ac and B). This strongly suggests that lamin C can behave independently and that lamin A is not necessary for lamin C to be present in the nuclear envelope. This finding also argues in favor of a potential substitution of lamin A by lamin C in the nuclear envelope which is consistent with the study by Fong et al. However, it is important to note that our finding does not contradict the fact that lamin C is intranuclear when expressed alone and is re-incorporated into the nuclear lamina when expressed with lamin A, as previously reported [11,16–19]. This likely reflects that the presence of lamin C in the nuclear lamina requires a precise lamin C/lamin A stoichiometry to be respected. This may also explain why the incorporation of lamin C into the nuclear lamina proceeds via intranuclear foci [17].

Furthermore, our results showed that the lamin C mutants tested here were seldom part of the nuclear lamina (Fig. 5A). As a consequence, an altered ability of lamin C to establish connections with the nuclear envelope due to mutations in *LMNA* gene should also be considered to explain the major alterations of the nuclear membrane observed in cardiomyocytes from patients [11,20,22]. To further analyze the pathophysiology of laminopathies and propose a potential explanation as for why the mutant lamin C connections with the nuclear envelope is altered, we performed FRAP experiments on the nuclear aggregates formed by lamin C mutants. Our result revealed that lamin C molecules were significantly more mobile within D192G and R386K lamin C-FP intranuclear aggregates compared to the wild type, thereby indicating that these aberrant lamin C aggregates were significantly less stable. Interestingly, the increased lamin C velocity was observed only with the mutants that exhibited an altered ability to interact with nuclear envelope and that led to an abnormal aggregation in the nucleoplasm (D192G, R386K). In view of these results, we can postulate that the lamin C molecules involved in these aggregates preferably interact with each other to the detriment of the nuclear envelope. However, it would be interesting to investigate other mutants to corroborate a potential correlation between the size of intranuclear aggregates, the velocity of nuclear lamin C and its capacity to associate with the nuclear envelope. Altogether, these results provide novel insight into the pathophysiological mechanism of laminopathies.

LMNA mutations alter lamin A and C interactions with their partners but not RanGap 1 distribution

We showed that L85R lamin C aggregates exhibited neither altered stability nor altered capacity to be connected to the nuclear membrane, as opposed to D192G, N195K, and R386K mutants. These findings likely indicate that the maintenance of these properties is not correlated to the size of nuclear aggregates. However, we cannot exclude that the formation of such aberrant intranuclear accumulations did not affect other lamin A/C properties, such as the interactions with lamin A/C partners. Nuclear lamina is known to participate in the organization of nuclear pores within the nuclear membrane [39]. Since we did not find any mislocalization of RanGap1 with any of the mutants tested, we can hypothesize that the localization of nuclear pore complex within the nuclear envelope is not affected. Therefore, in our cell model, the nuclear-cytoplasm trafficking of macromolecules through the nuclear envelope is most likely unaffected by the presence of mutated lamin A/C (Fig. 7). However, further experiments have to be performed to confirm this hypothesis. Indeed, it has been shown that embryonic fibroblasts from mice lacking A-type lamin exhibited a loss of the nuclear pore protein Nup153 from one pole of the nuclei indicating exclusion of nuclear pore complex from this area [40]. Similarly, Muchir et al. found that Nup153 was absent in pole of fibroblasts from patients with type 1B limb-girdle muscular dystrophy and carrying the nonsense Y259X mutation [21]. Recently, the prelamin A Y646F mutant has been found to co-localize with nuclear pore complex in embryonic kidney (HEK-293) cells [41]. Our divergent results may be explained by the fact that the mutations we investigated are not responsible for either 1B limb-girdle muscular dystrophy or progeria and that the cell type used in our model has endogenous lamin A/C which is likely sufficient to anchor nuclear pore complexes in the nuclear envelope.

Lastly, in a previous report, we showed that lamin C nuclear aggregation results in the aberrant trapping of SUMO1, a post translational modifier of numerous proteins [11]. Among these proteins, there are several transcription factors including the cardiac specific transcription factor GATA4 [42]. Similarly, Hubner et al. demonstrated that the over-expression of lamin A mutant led to the sequestration of the lamin A/C interacting partners pRb (retinoblastoma protein) and SREBP1a (sterol responsive element binding protein 1a) into lamin A nuclear aggregates [34]. Such aberrant interactions with lamin A/C partners may also be considered as a potential pathophysiological mechanism for laminopathies.

LMNA gene mutations and the variety of human phenotypes

Defects in gene regulation and/or abnormalities in nuclear architecture causing cellular fragility are the main two hypotheses that have been proposed to explain the variability of phenotypes due to *LMNA* mutations [1]. Our previous study was in favor of nuclear fragility since we observed dramatic nuclear envelope discontinuity in cardiomyocytes from *LMNA* mutated patients [11]. Here, we better dissect the properties of each of lamins A and C specifically and show that they can be differentially affected by a given mutation. These results with others [16,18,27], clearly showed that the consequences of *LMNA* mutation on the cell physiology is different from one mutation to another. Therefore, we can conclude that i) the type of mutation and ii) its consequence on the unique properties of each lamin specifically, are two key factors that has to be considered in predicting the potential consequences on nuclear function. The combination of these two factors can result in multiple consequences on the cell physiology which likely contributes to explain the variability and complexity of phenotypes in human disease and may be regarded as an additional working hypothesis to explain how mutations in *LMNA* gene lead to so many phenotypes in humans.

Lamins A and C support conjoint and also separate functions

Lastly, we showed that connections between the nuclear envelope and some mutated lamin C-FP (D192G, R386K) are absent which is not the case with the equivalent mutated lamin A. Conversely, other mutants, such as L85R led to aberrant lamin C aggregation but did not alter lamin A organization within the nuclear envelope. The fact that a mutation has different effects on lamin A and lamin C, shows that lamins A and C have to be investigated not only together but also separately in order to better dissect their function and specific role in the occurrence of disease. Also, this likely suggests that each protein may support distinct functions. This is in agreement with a previous study showing that lamins A and C do not play the same role in the nuclear lamina assembly characteristics [16]. In particular, the emerin-lamin A and emerin-lamin C interactions appear to be functionally different and are differently affected by some Emery–Dreifuss *LMNA* mutations [16]. As a conclusion, a closer look at the functions of lamins A and C specifically may allow resolution of conflicting results and may also help define

genotype–phenotype correlation in laminopathies which has been difficult thus far.

Acknowledgments

The Laboratory of Genetics of Cardiac diseases is part of the John and Jennifer Ruddy Canadian Cardiovascular Genetics Centre. This research was supported by Canadian Institutes for Health Research operating grants 38054 and 65152, and by Heart and Stroke Foundation grant NA 5101 awarded to F Tesson. N Sylvius was the recipient of the fellowship awarded by the Heart and Stroke Foundation of Ontario Program grant 5275 and by the Astra Zeneca/Canadian Society of Hypertension/CIHR fellowship.

REFERENCES

[1] N. Sylvius, F. Tesson, Lamin A/C and cardiac diseases, Curr. Opin. Cardiol. 21 (2006) 159–165.
[2] D.K. Shumaker, E.R. Kuczmarski, R.D. Goldman, The nucleoskeleton: lamins and actin are major players in essential nuclear functions, Curr. Opin. Cell Biol. 15 (2003) 358–366
[3] C.J. Hutchison, Lamins: building blocks or regulators of gene expression? Nat. Rev., Mol. Cell Biol. 3 (2002) 848–858.
[4] R.L. Boguslavsky, C.L. Stewart, H.J. Worman, Nuclear lamin A inhibits adipocyte differentiation: implications for Dunnigan-type familial partial lipodystrophy, Hum. Mol. Genet. 15 (2006) 653–663.
[5] D. Constantinescu, H.L. Gray, P.J. Sammak, G.P. Schatten, A.B. Csoka, Lamin A/C expression is a marker of mouse and human embryonic stem cell differentiation, Stem Cells 24 (2006) 177–185
[6] Y. Gruenbaum, A. Margalit, R.D. Goldman, D.K. Shumaker, K.L. Wilson, The nuclear lamina comes of age, Nat. Rev., Mol. Cell Biol. 6 (2005) 21–31.
[7] M.S. Zastrow, D.B. Flaherty, G.M. Benian, K.L. Wilson, Nuclear titin interacts with A- and B-type lamins in vitro and in vivo, J. Cell Sci. 119 (2006) 239–249.
[8] M.S. Zastrow, S. Vlcek, K.L. Wilson, Proteins that bind A-type lamins: integrating isolated clues, J. Cell Sci. 117 (2004) 979–987.
[9] N. Zhong, G. Radu, W. Ju, W.T. Brown, Novel progerin-interactive partner proteins hnRNP E1, EGF, Mel 18, and UBC9 interact with lamin A/C, Biochem. Biophys. Res. Commun. 338 (2005) 855–861.
[10] F. Haque, D.J. Lloyd, D.T. Smallwood, C.L. Dent, C.M. Shanahan, A.M. Fry, R.C. Trembath, S. Shackleton, SUN1 interacts with nuclear lamin A and cytoplasmic nesprins to provide a physical connection between the nuclear lamina and the cytoskeleton, Mol. Cell. Biol. 26 (2006) 3738–3751.
[11] N. Sylvius, Z.T. Bilinska, J.P. Veinot, A. Fidzianska, P.M. Bolongo, S. Poon, P. McKeown, R.A. Davies, K.L. Chan, A.S. Tang, S. Dyack, J. Grzybowski, W. Ruzyllo, H. McBride, F. Tesson, *In vivo and in vitro examination of the functional* significances of novel lamin gene mutations in heart failure patients, J. Med. Genet. 42 (2005) 639–647.
[12] J. Lammerding, P.C. Schulze, T. Takahashi, S. Kozlov, T. Sullivan, R.D. Kamm, C.L. Stewart, R.T. Lee, Lamin A/C deficiency causes defective nuclear mechanics and mechanotransduction, J. Clin. Invest. 113 (2004) 370–378.
[13] S. Tulac, C. Dosiou, E. Suchanek, L.C. Giudice, Silencing lamin A/C in human endometrial stromal cells: a model to investigate endometrial gene function and regulation, Mol. Hum. Reprod. 10 (2004) 705–711.
[14] L.G. Fong, J.K. Ng, J. Lammerding, T.A. Vickers, M. Meta, N. Cote, B. Gavino, X. Qiao, S.Y. Chang, S.R. Young, S.H. Yang, C.L. Stewart, R.T. Lee, C.F. Bennett, M.O. Bergo, S.G. Young, Prelamin A and lamin A appear to be dispensable in the nuclear lamina, J. Clin. Invest. 116 (2006) 743–752.
[15] T. Libotte, H. Zaim, S. Abraham, V.C. Padmakumar, M. Schneider, W. Lu, M. Munck, C. Hutchison, M. Wehnert, B. Fahrenkrog, U. Sauder, U. Aebi, A.A. Noegel, I. Karakesisoglou, Lamin A/C-dependent localization of Nesprin-2, a giant scaffolder at the nuclear envelope, Mol. Biol. Cell 16 (2005) 3411–3424.
[16] I. Motsch, M. Kaluarachchi, L.J. Emerson, C.A. Brown, S.C. Brown, M.C. Dabauvalle, J.A. Ellis, Lamins A and C are differentially dysfunctional in autosomal dominant Emery–Dreifuss muscular dystrophy, Eur. J. Cell Biol. 84 (2005) 765–781.
[17] G.E. Pugh, P.J. Coates, E.B. Lane, Y. Raymond, R.A. Quinlan, Distinct nuclear assembly pathways for lamins A and C lead to their increase during quiescence in Swiss 3T3 cells, J. Cell Sci. 110 (Pt 19) (1997) 2483–2493.
[18] W.H. Raharjo, P. Enarson, T. Sullivan, C.L. Stewart, B. Burke, Nuclear envelope defects associated with LMNA mutations cause dilated cardiomyopathy and Emery–Dreifuss muscular dystrophy, J. Cell Sci. 114 (2001) 4447–4457.
[19] A. Vaughan, M. Alvarez-Reyes, J.M. Bridger, J.L. Broers, F.C. Ramaekers, M. Wehnert, G.E. Morris, W.G.F. Whitfield, C.J. Hutchison, Both emerin and lamin C depend on lamin A for localization at the nuclear envelope, J. Cell Sci. 114 (2001) 2577–2590.
[20] E. Arbustini, A. Pilotto, A. Repetto, M. Grasso, A. Negri, M. Diegoli, C. Campana, L. Scelsi, E. Baldini, A. Gavazzi, L. Tavazzi, Autosomal dominant dilated cardiomyopathy with atrioventricular block: a lamin A/C defect-related disease, J. Am. Coll. Cardiol. 39 (2002) 981–990.
[21] A. Muchir, B.G. van Engelen, M. Lammens, J.M. Mislow, E. McNally, K. Schwartz, G. Bonne, Nuclear envelope alterations in fibroblasts from LGMD1B patients carrying nonsense Y259X heterozygous or homozygous mutation in lamin A/C gene, Exp. Cell Res. 291 (2003) 352–362.
[22] L. Verga, M. Concardi, A. Pilotto, O. Bellini, M. Pasotti, A. Repetto, L. Tavazzi, E. Arbustini, Loss of lamin A/C expression revealed by immuno-electron microscopy in dilated cardiomyopathy with atrioventricular block caused by LMNA gene defects, Virchows Arch. 443 (2003) 664–671.
[23] C. Vigouroux, M. Auclair, E. Dubosclard, M. Pouchelet, J. Capeau, J.C. Courvalin, B. Buendia, Nuclear envelope disorganization in fibroblasts from lipodystrophic patients with heterozygous R482Q/W mutations in the lamin A/C gene, J. Cell Sci. 114 (2001) 4459–4468.
[24] Y. Wang, A.J. Herron, H.J. Worman, Pathology and nuclear abnormalities in hearts of transgenic mice expressing M371K lamin A encoded by an LMNA mutation causing Emery–Dreifuss muscular dystrophy, Hum. Mol. Genet. 15 (2006) 2479–2489.
[25] J.L. Broers, H.J. Kuijpers, C. Ostlund, H.J. Worman, J. Endert, F.C. Ramaekers, Both lamin A and lamin C mutations cause lamina instability as well as loss of internal nuclear lamin organization, Exp. Cell Res. 304 (2005) 582–592.
[26] S. Hubner, J.E. Eam, K.M. Wagstaff, D.A. Jans, Quantitative analysis of localization and nuclear aggregate formation induced by GFP-lamin A mutant proteins in living HeLa cells, J. Cell Biochem. 98 (2006) 810–826.
[27] C. Ostlund, G. Bonne, K. Schwartz, H.J. Worman, Properties of lamin A mutants found in Emery–Dreifuss muscular dystrophy, cardiomyopathy and Dunnigan-type partial lipodystrophy, J. Cell Sci. 114 (2001) 4435–4445.
[28] J. Rankin, S. Ellard, The laminopathies: a clinical review, Clin. Genet. 70 (2006) 261–274.
[29] D. Fatkin, C. MacRae, T. Sasaki, M.R. Wolff, M. Porcu, M. Frenneaux, J. Atherton, H.J. Vidaillet Jr., S. Spudich, U. De

Girolami, J.G. Seidman, C. Seidman, F. Muntoni, G. Muehle, W. Johnson, B. McDonough, Missense mutations in the rod domain of the lamin A/C gene as causes of dilated cardiomyopathy and conduction-system disease, N. Engl. J. Med. 341 (1999) 1715–1724.
[30] G. Bonne, M.R. Di Barletta, S. Varnous, H.M. Becane, E.H. Hammouda, L. Merlini, F. Muntoni, C.R. Greenberg, F. Gary, J.A. Urtizberea, D. Duboc, M. Fardeau, D. Toniolo, K. Schwartz, Mutations in the gene encoding lamin A/C cause autosomal dominant Emery–Dreifuss muscular dystrophy, Nat. Genet. 21 (1999) 285–288.
[31] H. Cao, R.A. Hegele, Nuclear lamin A/C R482Q mutation in canadian kindreds with Dunnigan-type familial partial lipodystrophy, Hum. Mol. Genet. 9 (2000) 109–112.
[32] R.D. Phair, T. Misteli, High mobility of proteins in the mammalian cell nucleus, Nature 404 (2000) 604–609.
[33] S. Gilchrist, N. Gilbert, P. Perry, C. Ostlund, H.J. Worman, W.A. Bickmore, Altered protein dynamics of disease-associated lamin A mutants, BMC Cell Biol. 5 (2004) 46.
[34] S. Hubner, J.E. Eam, A. Hubner, D.A. Jans, Laminopathy-inducing lamin A mutants can induce redistribution of lamin binding proteins into nuclear aggregates, Exp. Cell. Res. 312 (2006) 171–183.
[35] T. Dechat, T. Shimi, S.A. Adam, A.E. Rusinol, D.A. Andres, H.P. Spielmann, M.S. Sinensky, R.D. Goldman, Alterations in mitosis and cell cycle progression caused by a mutant lamin A known to accelerate human aging, Proc. Natl. Acad. Sci. U. S. A. 104 (2007) 4955–4960.
[36] T. Arimura, A. Helbling-Leclerc, C. Massart, S. Varnous, F. Niel, E. Lacene, Y. Fromes, M. Toussaint, A.M. Mura, D.I. Keller, H. Amthor, R. Isnard, M. Malissen, K. Schwartz, G. Bonne, Mouse model carrying H222P-Lmna mutation develops muscular dystrophy and dilated cardiomyopathy similar to human striated muscle laminopathies, Hum. Mol. Genet. 14 (2005) 155–169.
[37] L.C. Mounkes, S.V. Kozlov, J.N. Rottman, C.L. Stewart, Expression of an LMNA-N195K variant of A-type lamins results in cardiac conduction defects and death in mice, Hum. Mol. Genet. 14 (2005) 2167–2180.
[38] L.C. Mounkes, S. Kozlov, L. Hernandez, T. Sullivan, C.L. Stewart, A progeroid syndrome in mice is caused by defects in A-type lamins, Nature 423 (2003) 298–301.
[39] J.M. Holaska, K.L. Wilson, M. Mansharamani, The nuclear envelope, lamins and nuclear assembly, Curr. Opin. Cell Biol. 14 (2002) 357–364.
[40] T. Sullivan, D. Escalante-Alcalde, H. Bhatt, M. Anver, N. Bhat, K. Nagashima, C.L. Stewart, B. Burke, Loss of A-type lamin expression compromises nuclear envelope integrity leading to muscular dystrophy, J. Cell Biol. 147 (1999) 913–920.
[41] Y. Pan, A. Garg, A.K. Agarwal, Mislocalization of prelamin A Tyr646Phe mutant to the nuclear pore complex in human embryonic kidney 293 cells, Biochem. Biophys. Res. Commun. 355 (2007) 78–84.
[42] J. Wang, X.H. Feng, R.J. Schwartz, SUMO-1 modification activated GATA4 dependent cardiogenic gene activity, J. Biol. Chem. 279 (2004) 49091–49098.

Appendix III

Lamin A/C mutants disturb sumo1 localization and sumoylation *in vitro* and *in vivo*

Émilie Boudreau[1], Sarah Labib[1], Anne Bertrand[2,3], Valerie Décostre[2,3], Pierrette Bolongo[1], Nicolas Sylvius[1], Pallavi Gupta[1], Gisele Bonne[2,3,4], and Frédérique Tesson[1]

1 Faculty of Health Sciences, University of Ottawa, Ottawa, Canada

2 Inserm, UMRS 974, Paris, F-75013, France

3 Université Pierre et Marie Curie-Paris6, UM 76, CNRS, UMR7215, Institut de Myologie, IFR14, Paris, F-75013, France

4 AP-HP, Groupe Hospitalier Pitié-Salpêtrière, U.F. Cardiogénétique et Myogénétique, Service de Biochimie Métabolique, Paris, F-75013, France

Corresponding Author

Frédérique Tesson, PhD:

Keywords: lamin type A, laminopathy, sumoylation, sumo1 protein, dilated cardiomyopathy

Word Count: 3372

ABSTRACT

A-type lamins A and C are nuclear intermediate filament proteins in which mutations have been implicated in multiple disease phenotypes commonly known as laminopathies. In COS7 cells, we previously showed that the over-expression of a lamin C mutant associated with dilated cardiomyopathy (p.Asp192Gly) resulted in nuclear aggregation of lamin C and the sequestration of a protein modifier, sumo1, within the aggregates. Sumoylation is a post-translational protein modification that regulates a wide range of cell processes through the attachment of sumo1 to various substrates. Here we observed the mislocalization of sumo1 both *in vitro* (C2C12 cells overexpressing mutant lamins A and C) and *in vivo* (myoblasts and myopathic muscle tissue from the $Lmna^{H222P/H222P}$ mouse model). In C2C12 cells, we showed that the trapping of sumo1 in p.Asp192Gly, p.Gln353Lys, and p.Arg386Lys aggregates of lamin A/C correlated with an increased steady-state level of sumoylation. However, we could not detect the sumoylation of lamin A or C by sumo1. Our results suggest that mutant lamin A/C alters the dynamics of sumo1 and thus misregulation of sumoylation may be contributing to disease progression in laminopathies.

INTRODUCTION

Laminopathies, diseases associated with mutations in the lamin A/C gene (*LMNA*), are a collection of over ten distinct disease phenotypes including but not restricted to dilated cardiomyopathy (DCM), Emery-Dreifuss muscular dystrophy (EDMD), restrictive dermopathy, familial partial lipodystrophy (FPLD), and premature ageing (OMIM # 150330). However, there is no definitive genotype-phenotype relationship for over 340 mutations reported in this gene (for the full list of mutations, see UMD-*LMNA* database at www.umd.be/LMNA/). *LMNA* is one of the most frequently reported mutated genes in familial DCM and is associated with a worse prognosis than other forms of DCM.[1] Also, mutations in *LMNA* are often responsible for an earlier onset and more severe form of EDMD than X-linked EDMD.[2]

LMNA encodes the A-type lamin proteins, lamins A and C, which are expressed in all terminally differentiated and nucleated cells. Lamins A and C are type V intermediate filament proteins which constitute major components of the inner nuclear lamina with structural roles such as nuclear membrane strength and shape, positioning of the nuclear pore complexes, anchoring chromatin, and lamina assembly.[3-5] They also support regulatory roles as they are required for proper DNA transcription and gene expression.[6, 7]

Investigations into the molecular consequences of *LMNA* mutations have shown that point mutations can affect lamina, filament, and protein complex assembly in a mutation-dependent manner.[8-10] Expression of certain lamin A/C mutants result in intranuclear aggregations of the lamins while others do not appear to affect assembly or localization of the protein.[11, 12] Furthermore, mutations in *LMNA* can differentially affect the lamin A or C isoforms.[10] The absence of the lamin A/C protein has been shown to cause mislocalization of other nuclear proteins such as emerin.[13] Previously, we demonstrated that *in vitro* over-expression of lamin C containing the p.Asp192Gly DCM-linked mutation resulted in the mislocalization and trapping of a post-translational protein modifier known as Small Ubiquitin-related MOdifier-1 (sumo1) inside lamin C aggregates.[11] The sequestration of sumo1 was abolished by the disruption of the sumo1 di-glycine motif required for sumoylation.[11] Sumoylation, which involves the covalent but reversible attachment of the ~10 kD sumo1 protein to a lysine residue on the target protein, has been shown to regulate an assortment of cell processes that include gene expression and nucleocytoplasmic transport.[14, reviewed in 15] It

was demonstrated that the ubiquitin-conjugating enzyme E2I (Ubc9), which conjugates sumo1 to target proteins, interacts with lamin A/C.[16] Furthermore, both lamins A and C contain three proposed common sumoylation consensus sequences.[17] Taken together these findings suggest that lamin A/C may be modified by sumo1 and that mutations in *LMNA* may disturb the sumoylation process by disrupting sumo1 localization. Interestingly, it was observed in HeLa cells and mouse cardiomyocytes that lamin A/C is modified by sumo2/3 and that a DCM-associated mutation within the consensus sequence decreased the sumoylation.[18] However, it was shown that lamin A/C is sumoylated preferentially by sumo2/3 and not sumo1.[18] Sumo2 and sumo3 are nearly identical paralogs of sumo1, with approximately 50% sequence identity with sumo1 and both common and unique protein substrates.[19]

In the present study we tested the sumoylation of lamin A/C by sumo1 in the C2C12 mammalian myoblast cell model. We investigated whether the expression of DCM- and EDMD-associated mutant lamin A and C alter the localization of sumo1 and disturb the sumo1 sumoylation process in C2C12 cells. We confirmed our results using myoblasts isolated from the *Lmna*$^{H222P/H222P}$ knock-in mouse, which develops adult-onset muscle dystrophy and DCM comparable to the human phenotype.[20] We also validated sumo1 mislocalization results *in vivo* in soleus muscle tissue biopsies from the *Lmna*$^{H222P/H222P}$ mouse. Although there is still much to be elucidated, our results highlight the involvement of the sumo1 sumoylation pathway in the pathophysiology of laminopathies especially those involving striated muscles.

MATERIALS AND METHODS

Expression vector preparation

Full length lamin A, lamin C, and sumo1 cDNA was previously cloned into fluorescent expression vectors (pECFP-C1, pDsRed2-C1, and pEYFP-N1 from Clonetech laboratories) as described previously.[11] The p.Leu85Arg, p.Asp192Gly, and p.Arg386Lys point mutations were previously introduced into the lamin A and C cDNA by site-directed mutagenesis as described previously.[11] The ubc9-HA vector was a kind gift from Peter Howley as seen in Yasugi and Howley (1996).[21] The p.His222Pro point mutation was introduced into the lamin A and C cDNA by site-directed mutagenesis (Stratagene) with forward primer 5'-TCTCCACCAGTCGGGTCTCAGGACGGCGCTTGGTCTCACGC-3' and reverse primer 5'-GCGTGAGACCAAGCGCCGTCCTGAGACCCGACTGGTGGAGA-3'. The p.Gln353Lys

point mutation was introduced using the forward primer 5'-CCGAGATGCGGGCAAGGATGAAGCAGCAGCTGGACGAGTAC-3' and reverse primer 5'-GTACTCGTCCAGCTGCTGCTTCATCCTTGCCCGCATCTCGG-3' All the inserts were systematically verified by sequencing.

Cell culture and transfection

C2C12 mouse myoblasts and COS7 monkey kidney cells were cultured in Dulbecco's Modified Eagle Medium (DMEM) and transiently transfected using Metafectene Pro (Biontex). Primary mouse myoblasts were harvested from wild-type and *Lmna*$^{H222P/H222P}$ mutant mice as described previously.[22] cultured in Myo-1 medium. and transfected using electroporation (Amaxa).

Co-immunoprecipitation

Nuclear protein was incubated with M280 sheep anti-mouse magnetic beads (Dynal - Invitrogen) for 1 hour at 4^0C. Each sample was incubated with 2μg primary antibody (anti-GFP sc-9996. anti-lamin A C sc-6215. Santa Cruz) then M280 sheep anti-mouse magnetic beads. Samples were washed in TEG buffer supplemented with 50mM NaCl and 0 1% TitonX-100. Washed beads were boiled with SDS sample buffer with DTT at 95°C for 5 minutes then cooled.

Immunoblotting

Cells were harvested 24 hours post-transfection and either nuclear protein (Active Motif) or total protein was extracted. N-ethylmaleimide (NEM) was added to certain extractions to preserve sumoylation.[23] Primary antibodies used included goat anti-lamin A C. rabbit anti-SP3. mouse anti-sumo1. mouse anti-β-Actin. mouse anti-GFP (Santa Cruz Biotechnology 6215. 644. 5308. 47778. and 69779). mouse anti-GAPDH (ABM G041). mouse anti-vinculin (Sigma-Aldrich 4505). and mouse anti-emerin (Novocastra NCL-EMERIN). Secondary HRP-conjugated antibodies used included goat anti-mouse. rabbit anti-goat. or goat anti rabbit (Santa Cruz 2005. 2768. 2004) Visualization was performed using ECL detection reagent (Amersham) in the Fluorochem chemiluminescent imager (Alpha Innotech). Blots were analyzed for densitometry using the AlphaEase program. GAPDH. β-actin. or vinculin were used as protein loading controls.

Densitometry and statistical analysis

Samples were normalized to GAPDH or β-actin housekeeping protein to account for protein loading differences. As densitometry values vary greatly between blots, wild-type values were set at 100% and mutant values were compared against the wild-type as a ratio. As these calculations have not been previously shown to follow a normal distribution, a non-parametric Wilcoxon rank test was used with statistical significance set at $p<0.01$.

Immunostaining and fluorescent microscopy

C2C12 images were captured on an Olympus Fluoview FV1000 confocal microscope using the Olympus FV-10 acquisition software. Cryostat soleus muscle cross sections 6μm thick were obtained from *Lmna*$^{+/+}$ and *Lmna*$^{H222P/H222P}$ mice.[20] Prior to staining, slides were treated with 0.01M citric acid (pH 6.0) and incubated with 0.05 mg ml mouse Fab. Tissue sections and primary mouse myoblasts were incubated with 1:50 mouse anti-SUMO1 (Santa Cruz Biotechnology 6215) primary antibody overnight at 4°C and then 1:200 Alexa Fluor 568 goat anti-mouse (Invitrogen A-21124) secondary antibody for 30-60min in the dark. Images were captured on a CarlZeiss Axiophot2 or Z1 Imager fluorescent microscopes.

RESULTS

To investigate the impact of *LMNA* mutations on the sumo1 sumoylation pathway, we examined sumoylation of lamin A C and sumo1 localization in the presence of wild-type lamin A and C as well as p.Leu85Arg, p.Asp192Gly, and p.Gln353Lys lamin A and C mutants associated with DCM and p.Arg386Lys and p.His222Pro lamin A and C mutants associated with EDMD.

Lamin A and C are not sumoylated by sumo1

We previously reported the disruption of sumo1 localization in COS7 cells over-expressing p.Asp192Gly mutant lamin C and demonstrated that this mislocalization was sumoylation dependent.[11] Examination of the lamin A and C protein sequence unveiled three potential sumoylation consensus sites[17] at lysine amino acid positions 171, 201, and 270. Although not essential for sumoylation, these sites are found more frequently modified by sumo1

and consist of a four residue motif. Ψ-K-X-E/D. where Ψ is any large hydrophobic amino acid. K is the target lysine to which sumo1 is attached. X is any amino acid. and E/D is aspartic or glutamic acid. To assess whether lamin A and C were sumoylated. we over-expressed tagged lamin A and lamin C in C2C12 cells. Due to the transient nature of sumoylation and the low steady-state levels of sumoylated proteins.[23] cells were also transfected with tagged sumo1. However. no slower migrating bands corresponding to sumoylated lamin A or lamin C by either endogenous or exogenous sumo1 were observed (Figure 1A). To ensure the result was not cell-type specific. we confirmed the results using COS7 cells (data not shown). As a positive control of our protocol and of the sumoylation process in the C2C12 cell line. the blot was stripped and re-probed for the reversibly sumoylated protein. SP3. We observed bands for SP3 sumoylated by both endogenously and exogenously expressed sumo1 (Figure 1B). Given that we previously demonstrated how p.Asp192Gly mutant lamin C sequesters sumo1 inside aggregates. we investigated whether the expression of this mutant and other disease associated mutant lamin C result in its sumoylation. We transfected tagged proteins: lamin C. sumo1. and Ubc9. Ubc9, the sumoylation conjugating enzyme. was co-transfected to further promote protein sumoylation. No bands corresponding to sumoylated lamin C were observed with any of the lamin C wild-type or mutants (Figure 1C) suggesting that wild-type as well the other lamin A and C mutants are not sumoylated. To confirm this result. co-immunopreciptations were performed. In C2C12 cells transfected with tagged sumo1. immunoprecipitation of endogenous lamin A/C did not reveal lamin-sumo1-conjugates (Figure 1D). These results were confirmed in COS7 cells transfected with tagged wild-type lamin A. lamin C and with sumo1 (Figure 1E). Furthermore. over-expression of ubc9 did not produce different results (data not shown).

Mutant lamin A/C expression in C2C12 cells alters localization of sumo1 and ubc9

We next investigated the effect of disease associated *LMNA* point mutations on the localization of sumo1 and ubc9 in C2C12 cells. Wild-type lamin A. lamin C. and sumo1 show a relatively even distribution in the nucleus (Figure 2). In agreement with previously published results in other cell lines. the p.Leu85Arg mutant lamin A/C shows a comparable phenotype to the wild-type samples. and the p.Asp192Gly mutant lamin A/C results in nuclear aggregation of co-localized lamin A and C. As shown previously with only p.Asp192Gly lamin C.[11] expression of p.Asp192Gly lamin A and C aggregates disturb the localization of sumo1 by

sequestering it within the aggregates. The p.Gln353Lys substitution results in variable sizes and distributions of aggregated lamins A and C within the nucleus as well as at the nuclear periphery. This mutant also sequesters sumo1 within some of the aggregates. As previously reported, the p.Arg386Lys mutation also results in the formation of lamin A/C aggregates and we demonstrate here the trapping of the sumo1 protein. The p.His222Pro mutant lamin A/C retains the ability to localize to the nuclear lamina but also develops aggregates with partial sumo1 sequestration. To assess ubc9 localization, the cells were transiently co-transfected with ubc9-GFP, and wild-type or mutant tagged lamin A and lamin C. Ubc9 was observed to always co-localize with both wild-type and any mutant lamin A/C (Figure 3).

Mutant lamin A/C expression alters cellular sumoylation in C2C12 cells

Given that mutant lamin A/C affected sumo1 localization, we next investigated the effect of p.Leu85Arg, p.Asp192Gly, p.Arg353Lys, and p.Arg386Lys lamin A/C mutations on the steady-state level of sumoylation. Western blotting was performed on nuclear extracts from C2C12 cells transfected with tagged lamin A, lamin C and sumo1 or lamin C, ubc9 and sumo1. It was observed that cells expressing mutant lamin A/C that trapped sumo1 in aggregates also showed an increase in steady-state sumoylation levels and non-conjugated sumo1-YFP (Figure 4). Densitometry analysis was then performed on the bands corresponding to proteins conjugated to sumo1 (>85kDa) and also on the band of non-conjugated sumo1 tagged with YFP (at ~41kDa). There was a statistically significant increase in the steady-state levels of conjugated sumo1-YFP in the cells expressing p.Asp192Gly, p.Gln353Lys, and p.Arg386Lys mutant lamin A/C, however the values varied from 1.3-fold to 4-fold increases thus estimating a true mean of increased sumoylation is difficult. We attribute this to the 30-40% transfection efficiency in C2C12 cells thus allowing the non-transfected cells to dilute the effect of the mutant lamins. There was also an increase in the levels of non-conjugated sumo1-YFP in the cells expressing the p.Asp192Gly, p.Gln353Lys, and p.Arg386Lys mutant lamin A/C though the trend was less pronounced and fell slightly below statistical significance.

Sumo1 localization and sumoylation are perturbed in *Lmna*$^{H222P/H222P}$ mouse myoblasts

In order to confirm our results in a more physiologically relevant model, we cultured primary skeletal muscle myoblasts harvested from *Lmna*$^{+/-}$ and *Lmna*$^{H222P/H222P}$ mice and stained

for sumo1 (Figure 5 left panel). In *Lmna*$^{+/+}$ myoblasts, sumo1 shows homogenous nuclear and cytoplasmic distribution (Figure 5A). Approximately 75% of myoblasts of *Lmna*$^{H222P/H222P}$ mice show sumo1 localizing into nuclear foci while approximately 25% of myoblasts show a pronounced appearance at the NE without foci (Figure 5A). As reported previously in striated muscles.[20] lamin A/C is normally localized in myoblasts (data not shown). Mutated myoblasts transfected with tagged sumo1 demonstrated an exacerbation of the foci phenotype to approximately 87% (Figure 5B).

To determine if the sumoylation profile is disturbed in *Lmna*$^{H222P/H222P}$ myoblasts, we performed western blotting for sumo1 in total protein from sumo1-YFP transfected *Lmna*$^{+/+}$ and *Lmna*$^{H222P/H222P}$ primary myoblasts (Figure 5C). We did not detect a significant change in the levels of sumo1 conjugated proteins yet we observed an increase in the amount of non-conjugated sumo1-YFP. There was also an increased sumoylation of one unknown protein that migrates to approximately 60kDa which would correspond to a protein with an estimated molecular weight of 10-20kDa.

Altered localization of endogenous sumo1 in *Lmna*$^{H222P/H222P}$ mouse muscle tissue

As endogenous sumo1 was found mislocalized in myoblasts cultured from *Lmna*$^{H222P/H222P}$ mice, we wanted to determine if this occurred *in vivo* in dystrophic *Lmna*$^{H222P/H222P}$ muscle tissue.[20] Therefore we examined its localization directly by immunostaining for sumo1 in cross-sections of soleus muscle from *Lmna*$^{-/-}$ and *Lmna*$^{H222P/H222P}$ mice (Figure 6). Wild-type muscle tissue sumo1 shows consistent punctate myocyte staining and homogenous punctate nuclear localization (Figure 6 left panel) that is comparable to endogenous myoblast sumo1 staining (Figure 5A). In the p.His222Pro mutant muscles, we observed a striking nuclear envelope localization of sumo1 in approximately 25% of nuclei (Figure 6 right panel). The cytoplasmic localization appears conserved in this tissue. A small proportion of nuclei (~6%) showed an intranuclear aggregation of sumo1.

DISCUSSION

In this study, we showed that the expression of mutant lamin A/C results in the mislocalization and misregulation of sumoylation and/or sumo1 turnover. The lamin A/C protein

sequence contains three sumoylation consensus sequences as well as interacts with the conjugating enzyme. ubc9.[16] yet we could not detect its sumoylation by sumo1. This is in agreement with the study that found lamin A/C to be preferentially modified by sumo2/3.[18] The mutations included in this study were located in the α-helical coiled coil rod domains of lamin A/C that are essential for both filament assembly and protein-protein interactions.[24] As we previously demonstrated the aggregation of lamin C and the sequestration of sumo1.[11] we investigated whether mutations in lamin C would produce a misfolding of the protein that might reveal an otherwise masked sumoylation site. However. we did not observe any sumoylation of mutant lamin C indicating that lamin A/C is not sumoylated by sumo1.

Over-expression of sumo1 with wild-type mutant lamin A and C showed normal localization of lamin A/C with no trapping of sumo1. as did expression of the p.Leu85Arg mutant. We observed that p.Asp192Gly and p.Arg386Lys mutant lamin A/C formed intranuclear aggregates of lamin A/C as expected[10] however we further demonstrated sequestration of sumo1 within the aggregates. We report here for the first time. the *in vitro* over-expression of p.Gln353Lys (DCM) and p.His222Pro (EDMD) mutant lamin A/C. The p.Gln353Lys mutant lamin A/C shows intranuclear aggregations that sequester sumo1. We observed that p.His222Pro mutant lamin A/C localizes to the nuclear envelope yet forms intranuclear aggregates that partially sequester sumo1. This is in contrast to the reported normal localization in both cardiac and skeletal muscle from the $Lmna^{H222P/H222P}$ mouse.[20] This discrepancy may be due to the over-expression of mutant lamins and the exaggeration of normally undetectable changes in lamin filament formation. In myoblasts solely expressing p.His222Pro mutated lamin A/C. we observed an abnormal nuclear rim and/or intranuclear aggregation of both endogenous and exogenously expressed sumo1 as was seen in C2C12 cells. In skeletal muscle cross-sections. we observed a prominent staining of sumo1 at the nuclear envelope in a subset of myocyte nuclei. Certain sumoylation-desumoylation enzymes localize to the nuclear pore complexes (NPCs)[36] and the proper assembly and positioning of NPCs is dependent on lamin A/C.[37] In fact. ubc9. which is critical for conjugation of sumo1 to targets. is found both in the nucleus and at NPCs.[36] Furthermore. we have shown in C2C12 cells that ubc9 co-localizes with wild-type and mutant lamin A/C. SENP1 and SENP2 are sumo-specific proteases that de-sumoylate modified proteins and are found in the nucleus and at the nucleoplasmic face of the NPCs.

respectively.[38. 39] Also. RanBP2. a protein with sumoylation E3 ligase function also localizes to the cytosolic filaments of the NPCs.[40] Therefore. mutant lamin A C may be altering the assembly or function of the lamina. ubc9. and NPCs and thus disrupting the location or protein-protein interactions of the enzymes involved in the sumoylation cascade.

In the C2C12 cell model. the sequestration of sumo1 within mutant lamin aggregates paralleled with an increase in the steady-state levels of sumoylated proteins in nuclear extracts. There was also a modest increase in the amount of non-conjugated sumo1. Our results suggest that the trapping of sumo1 in the lamin A C aggregates may conceal sumoylated proteins from normal regulation of de-conjugation and or sumo1 degradation. Furthermore. although not sequestered within the aggregates. we found ubc9 to co-localize with both wild-type and mutant lamin A/C regardless of aggregation phenotype. This co-localization of ubc9 at lamin aggregates may be maintaining or promoting the higher levels of sumoylation. As there are hundreds of proteins known to undergo sumoylation. the consequences of sumo1 mislocalization could have disastrous consequences on the regulation of many cell processes. Previous research in cardiac and skeletal muscles of the *Lmna*$^{H222P/H222P}$ mouse demonstrated an increase in the nuclear accumulation of Smad proteins. which are potent effectors of the TGFβ$_1$ signalling cascade correlating with increased fibrosis in the mice.[20. 28] Both the TGFβ receptor type I (TβRI) which activates the Smad proteins as well as Smad4 are sumoylated.[29. 30] TβRI is sumoylated in response to TGFβ and amplifies the signal by modulating gene expression.[30] However. there are conflicting reports whether sumoylation stimulates or represses Smad4.[29. 31-35] The nuclear accumulation of Smad proteins might result from the alteration of sumoylation of Smad4 and or TβRI in the presence of lamin A C mutants. Interestingly. we also observed an increase in the sumoylation of one unknown substrate protein only in homozygous p.His222Pro myoblasts transfected with sumo1 and not in wild-type nor heterozygous myoblasts. This band would correspond to a small (10-20kDa) sumoylated protein which we are currently investigating. Determining a protein whose sumoylation is misregulated prior to muscle differentiation could give insight into early disease pathogenesis.

Overall. our results suggest that disease-associated mutations in the *LMNA* gene that result in the expression of mutated lamin A/C mediate a mislocalization of sumo1. ubc9. and

likely sumoylated proteins in a mutation-dependent manner. There is consequently deficient deconjugation and/or degradation of sumo1 indicating a misregulation of the sumoylation process. In affected mouse tissue, sumo1 is found concentrated at the nuclear envelope where mutant lamin A/C and many of the sumoylation enzymes are targeted. As sumoylation is a highly conserved and tightly regulated cellular process with numerous targets, we propose that altered sumo1 dynamics may play a role in the pathophysiology of laminopathies.

ACKNOWLEDGEMENTS

The authors would like to thank Dr. Peter Howley (Harvard Medical School) for the kind gifts of the ubc9 vector as well as Dr. Heidi McBride (University of Ottawa Heart Institute) for her assistance with the Olympus Confocal microscope.

COMPETING INTERESTS

None

FUNDING

This research was supported by an operating grant from the Heart and Stroke Foundation (NA 6628) awarded to F. Tesson, an operating grant from the Canadian Institutes of Health Research (77685) awarded to F. Tesson, a Government of France scholarship awarded to E. Boudreau, and INSERM (Institut national de la santé et de la recherche médicale) and Université Pierre et Marie Curie - Paris 6.

REFERENCES

1 Sylvius N. Tesson F. Lamin A/C and cardiac diseases. Curr Opin Cardiol 2006:21:159-165.

2 Brown SC. Piercy RJ. Muntoni F. et al. Investigating the pathology of Emery-Dreifuss muscular dystrophy. Biochem Soc Trans 2008:36:1335-1338.

3 Glass CA. Glass JR. Taniura H. et al. The alpha-helical rod domain of human lamins A and C contains a chromatin binding site. EMBO J 1993;12:4413-4424.

4 Sullivan T. Escalante-Alcalde D. Bhatt H. et al. Loss of A-type lamin expression compromises nuclear envelope integrity leading to muscular dystrophy. J Cell Biol 1999:147:913-920.

5 Liu J. Rolef Ben-Shahar T. Riemer D. et al. Essential roles for Ceanorhabditis elegans lamin gene in nuclear organization. cell cycle progression. and spatial organization of nuclear pore complexes. Mol Biol Cell 2000:11:3089-3099.

6 Kumaran RI. Muralikrishna B. Parnavik VK. Lamin A/C speckles mediate spatial organization of splicing factor compartments and RNA polymerase II transcription. J Cell Biol 2002:159:783-793.

7 Verstraeten VL. Broers JL. Ramaekers FC, et al. The nuclear envelope. a key structure in cellular integrity and gene expression. Curr Med Chem 2007;14:1231-1248.

8 Muchir A. Medioni J. Laluc M. et al. Nuclear envelope alterations in fibroblasts from patients with muscular dystrophy. cardiomyopathy. and partial lipodystrophy carrying lamin A/C gene mutations. Muscle Nerve 2004:30:444-450.

9 Weisel N. Mattout A. Melamed-Book N. et al. Laminopathic mutations interfere with the assembly. localization. and dynamics of nuclear lamins. Proc Natl Acad Sci USA 2008:105:180-185.

10 Sylvius N. Hathaway A. Boudreau E. et al. Specific contribution of lamin A and lamin C in the development of laminopathies. Exp Cell Res 2008:314:2362-2375.

11 Sylvius N. Bilinska ZT. Veinot JP. et al. In vivo and in vitro examination of the functional significances of novel lamin gene mutations in heart failure patients. J Med Genet 2005:42:639-647.

12 Hubner S. Eam JE. Wagstaff KM. et al. Laminopathy-inducing lamin A mutants can induce redistribution of lamin binding proteins into nuclear aggregates. Exp Cell Res 2006:312:171-183.

13 Muchir A. van Engelen BG. Lammens M. et al. Nuclear envelope alterations in fibroblasts from LGMD1B patients carrying nonsense Y259X heterozygous or homozygous mutation in lamin A/C gene. Exp Cell Res 2003:10:352-362.

14 Panse VG. Kressler D. Pauli A. et al. Formation and nuclear export of preribosomes are functionally linked to the small-ubiquitin-related modifier pathway. Traffic 2006;7:1311-1321.

15 Geiss-Friedlander R. Melchior F. Concepts in sumolyation: a decade on. Nat Rev Mol Cell Biol 2007:8:947-956.

16 Zhong N. Radu G. Ju W. et al. Novel progerin-interactive partner proteins hnRNP E1. EGF. Mel 18. and UBC9 interact with lamin A/C. Biochem Biophys Res Commun 2005:338:855-861.

17 Rodriguez MS. Dargemont C. Hay RT. SUMO-1 conjugation in vivo requires both a consensus modification motif and nuclear targeting. J Biol Chem 2001:276:12654-12659.

18 Zhang YQ. Sarge KD. Sumoylation regulates lamin A function and is lost in lamin A mutants associated with familial cardiomyopathies. J Cell Biol 2008:182:35-39.

19 Makhnevych T. Sydorskyy Y. Xin X. et al. Global map of SUMO function revealed by protein-protein interaction and genetic networks. Mol Cell 2009:33:124-135

20 Arimura T. Helbling-Leclerc A. Massart C. et al. Mouse model carrying H222P-Lmna mutation develops muscular dystrophy and dilated cardiomyopathy similar to human striated muscle laminopathies. Hum Mol Genet 2005:14:155-169.

21 Yasugi T. Howley PM. Identification of the structural and functional human homolog of the yeast ubiquitin conjugating enzyme UBC9. Nucleic Acids Res 1996:24:2005-2010.

22 Rosenblatt JD. Lunt AI. Parry DJ. et al. Culturing satellite cells from living single muscle fiber explants. In Vitro Cell Dev Biol anim 1995;31:773-779.

23 Pichler A. Analysis of sumoylation. Methods Mol Biol 2008:446:131-138.

24 Dechat T. Pfleghaar K. Sengupta K. et al. Nuclear lamins: major factors in the structural organization and function of the nucleus and chromatin. Genes Dev 2008:22:832-853.

25 Lee YJ. Miyake S. Wakita H. et al. Protein SUMOylation is massively increased in hibernation torpor and is critical for the cytoprotection provided by ischemic preconditioning and hypothermia in SHSY5Y cells. J Cereb Blood Flow Metab 2007:27:950-962.

26 Ja Lee Y. Castri P, Bembry J. et al. SUMOylation participates in induction of ischemic tolerance. J Neurochem 2009:109:257-267.

27 Girdwood DW. Tatham MH. Hay RT. SUMO and transcriptional regulation. Semin Cell Dev Biol 2004;15:201-210.

28 Rosenkranz S. TGF-beta1 and angiotensin networking in cardiac remodelling. 2004:63:423-432.

29 Lin X. Liang M. Liang YY. et al. Activation of transforming growth factor-beta signalling by SUMO-1 modification of tumor suppressor Smad4/DPC4. J Biol Chem 2003:278:18714-18719.

30 Kang JS. Saunier EF. Akhurst RJ. et al. The type I TGF-beta receptor is covalently modified and regulated by sumoylation. Nat Cell Biol 2008:10:654-664.

31 Lin X. Liang M. Liang YY. et al. SUMO-1/Ubc9 promotes nuclear accumulation and metabolic stability of tumour suppressor Smad4. J Biol Chem 2003:278:31043-31048.

32 Ohshima T. Shimotohno K. Transforming growth factor-beta-mediated signaling via the p38 MAP kinase pathway activates Smad-dependent transcription through SUMO-1 modification of Smad4. J Biol Chem 2003:278:50833-50842.

33 Liang M. Melchior F. Feng XH. et al. Regulation of Smad4 sumoylation and transforming growth factor-beta signalling by protein inhibitor of activated STAT1. J Biol Chem 2004:279:22857-22865.

34 Shimada K. Suzuki N. Ono Y. et al. Ubc9 promotes the stability of Smad4 and the nuclear accumulation of Smad1 in osteoblast-like Saos-2 cells. Bone 2008:42:886-893.

35 Long J. Wang. He D. et al. Repression of Smad4 transcriptional activity by SUMO modification. Biochem J 2004:379:23-29.

36 Palancade B. Doye V. Sumoylating and desumoylating enzymes at nuclear pores: underpinning their unexpected duties? Trends Cell Biol 2008:18:174-183.

37 Hutchison CJ. Lamins: building blocks or regulators of gene expression? Nat Rev Mol Cell Biol 2002:3:848-858.

38 Zhang H. Saitoh H. Matunis MJ. Enzymes of the SUMO modification pathway localize to filaments of the nuclear pore complex. Mol Cell Biol 2002;22:6498-6508.

39 Hang J. Dasso M. Association of the human SUMO-1 protease SENP2 with the nuclear pore. J Biol Chem 2002:277:19961-19966.

40 Mahajan R. Delphin C. Guan T. et al. A small ubiquitin-related polypeptide involved in targeting RanGAP1 to nuclear pore complex protein RanBP2. Cell 1997:88:97-107.

FIGURE LEGENDS

Figure 1: Lamin A and C are not sumoylated by sumo1. (A-C) Western blots of C2C12 nuclear proteins: (A) Untransfected (UNT) or sumo1-YFP transfected, or triple transfected wild-type lamin A-CFP, lamin C-Red and sumo1-YFP probed for lamin A/C. N-ethylmaleimide (NEM) was included with harvesting of selected samples to stabilize sumo conjugation. (B) Western blot A stripped and reprobed for SP3. (C) UNT or triple transfected wild-type and mutant lamin C-Red, wild-type sumo1-YFP and wild-type Ubc9-HA probed for lamin A/C. (D-E) Immunoprecipitation of endogenous and exogenous lamin A and C. (D) Nuclear extracts of sumo1-HA transfected C2C12 cells were immunoprecipitated using anti-lamin A/C antibody and western blotting was performed for lamin A/C. (E) Nuclear extracts of lamin A-CFP, lamin C-CFP, or empty CFP vector transfected COS7 cells were immunoprecipitated using anti-GFP tag antibody and western blotting was performed for the GFP tags. All protein was harvested in the presence of NEM. Emerin, a known lamin A/C binding partner, was included as a positive control for immunoprecipitation.

Figure 2: Sumo1 localization is disturbed by mutant lamin A/C in a mutation-dependent manner. Confocal microscopy images of nuclei of C2C12 cells expressing wild-type and mutant lamin A-CFP, lamin C-Red and wild-type sumo1-YFP. Lamin A and lamin C images are represented in one panel as they co-localize in all cells. Each picture presented is representative of the most commonly observed phenotype.

Figure 3: Ubc9 co-localizes with wild-type and mutant lamin A/C. Confocal microscopy images of nuclei of C2C12 cells expressing wild-type and mutant lamin A-CFP, lamin C-Red and wild-type sumo1-YFP. Lamin A and lamin C images are represented in one panel as they co-localize in all cells. Each picture presented is representative of the most commonly observed phenotype.

Figure 4: Mutant lamin A/C expression correlates with an increase in levels of sumoylated proteins. Western blot analysis of sumo1 in nuclear protein harvested from C2C12 cells transfected with wild-type and mutant lamin C-CFP and sumo1-YFP harvested with NEM. Blot was re-probed for β-actin as a loading control. Blot is representative of increased sumoylation observed in both lamin C, ubc9 and sumo1 transfections (n=2) as well as lamin A, lamin C, and sumo1 transfections (n=6).

Figure 5: Sumo1 localization and sumoylation of an unknown protein is disturbed by endogenous p.*His222Pro* mutant lamin A/C in primary mouse myoblasts. (A-B) Fluorescent microscopy images of non-transfected and sumo1-YFP transfected $Lmna^{+/+}$ (WT) and $Lmna^{H222P/H222P}$ primary myoblast nuclei. (A) Untransfected myoblasts immunostained for endogenous sumo-1 (green). (B) Sumo1-YFP transfected myoblasts expressing YFP-tagged sumo1 (green). All myoblasts were counterstained for DAPI (blue). Each picture presented is representative of the most commonly observed phenotype. (C) Western blot analysis of sumo1 in whole cell extracts from $Lmna^{+/+}$ and $Lmna^{H222P/H222P}$ myoblasts transfected with wild-type sumo1-YFP harvested with NEM. Bottom Blot was reprobed for vinculin as a loading control. The asterisk (*) marks an unknown sumoylated protein whose sumoylation is increased in the $Lmna^{H222P/H222P}$ myoblasts. The blot is representative of two independent experiments.

Figure 6: Sumo1 localization disrupted in soleus muscle sections from $Lmna^{H222P}$ mice. Fluorescent microscopy images of soleus muscle cross sections from $Lmna^{-/+}$ and $Lmna^{H222P/H222P}$ mice. Top row sections were stained for sumo1 (green). Bottom row sections

were stained with only secondary antibody to show background signal of anti-mouse-568nm antibody (green). All sections were counterstained for DAPI (blue). Each picture presented is representative of the most commonly observed phenotype. Scale bar represents 10μm. Red arrow highlights one cell with nuclear envelope localization of sumo1. Yellow arrow highlights one cell with intranuclear aggregation of sumo1.

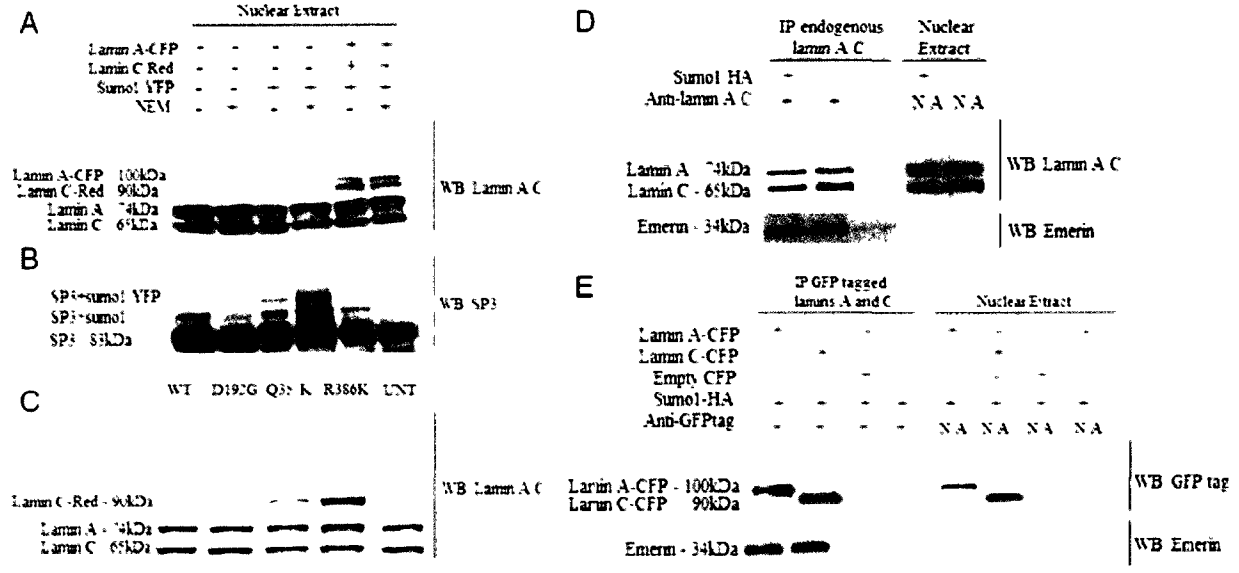

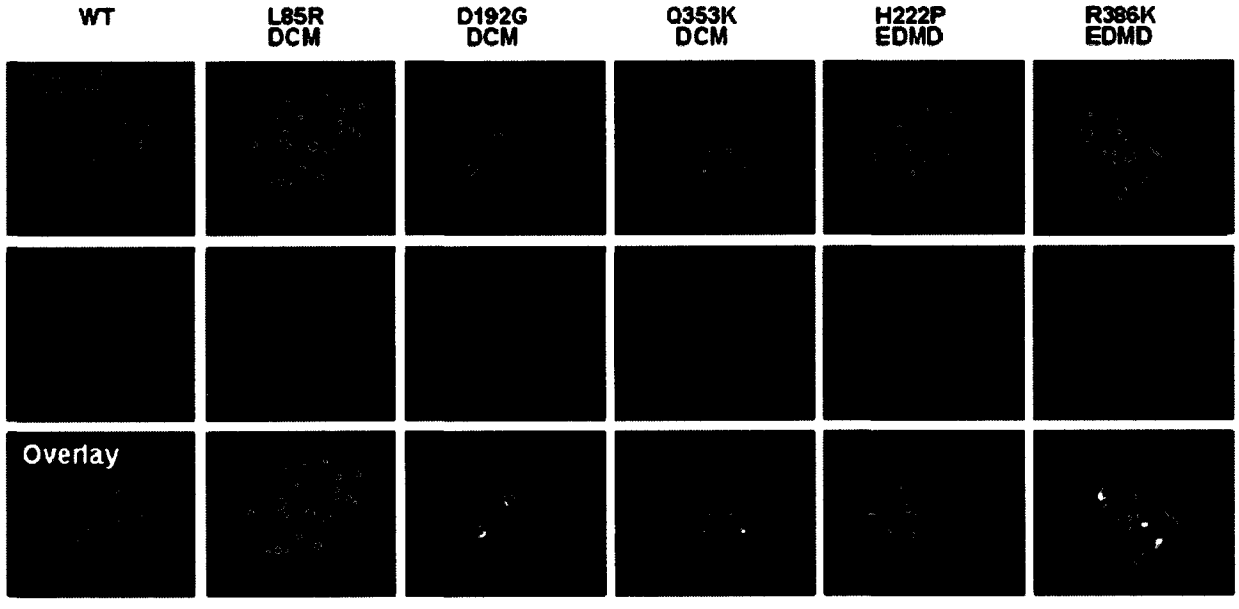

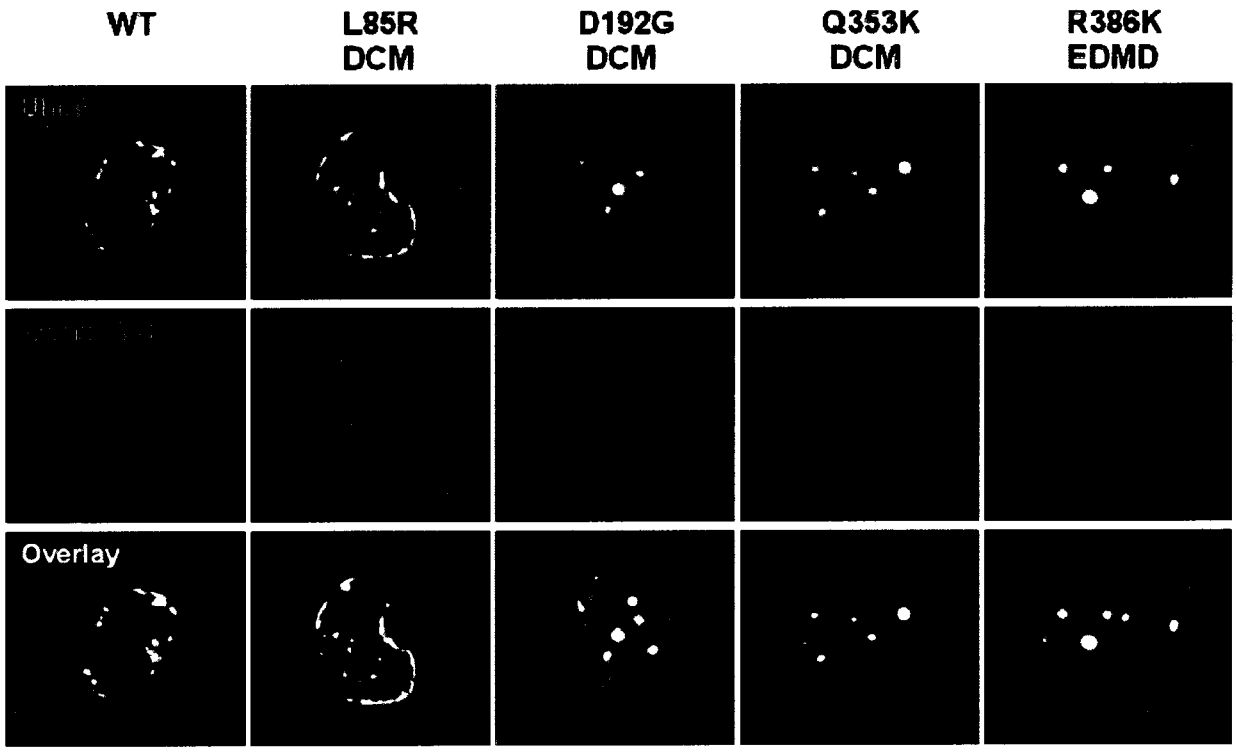
WT
L85R
DCM
D192G
DCM
Q353K
DCM
R386K
EDMD
Overlay

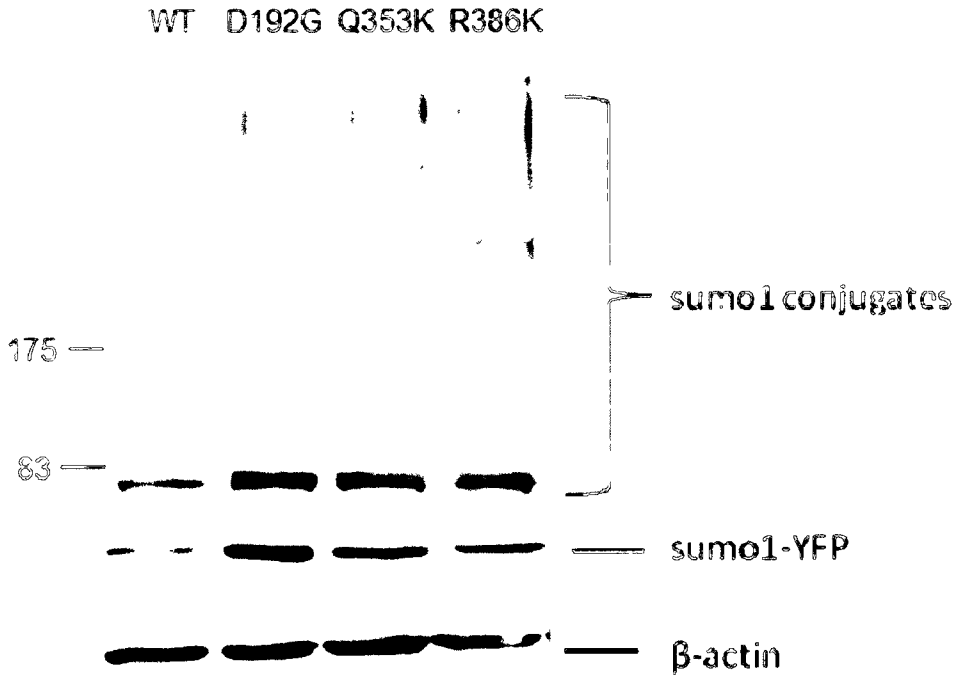
WT D192G Q353K R386K
sumo1 conjugates
175
83
sumo1-YFP
β-actin

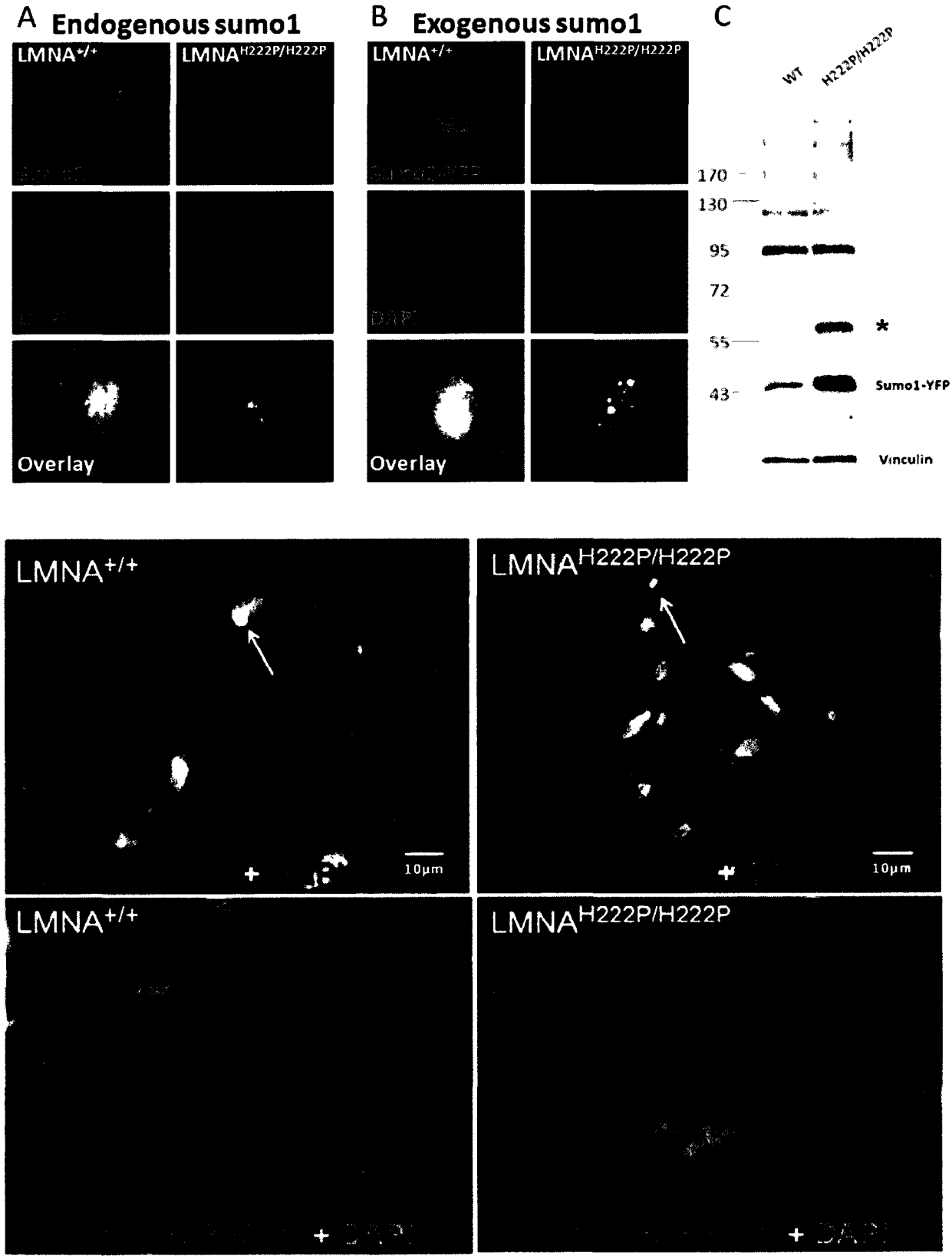
A Endogenous sumo1
LMNA+/+
LMNAH222P/H222P
Overlay
B Exogenous sumo1
LMNA+/+
LMNAH222P/H222P
Overlay
C
WT
H222P/H222P
170
130
95
72
55
43
*
Sumo1-YFP
Vinculin
LMNA+/+
10μm
LMNAH222P/H222P
10μm
LMNA+/+
LMNAH222P/H222P